

JAERI-M

88-034

BENCHMARK EXPERIMENTS ON A 60 CM-THICK  
GRAPHITE CYLINDRICAL ASSEMBLY

February 1988

Hiroshi MAEKAWA, Yujiro IKEDA, Yukio OYAMA  
Seiya YAMAGUCHI, Koichi TSUDA, Tooru FUKUMOTO\*  
Kazuaki KOSAKO, Michio YOSHIZAWA\*\*and Tomoo NAKAMURA

日本原子力研究所  
Japan Atomic Energy Research Institute

JAERI-M レポートは、日本原子力研究所が不定期に公刊している研究報告書です。

入手の問合せは、日本原子力研究所技術情報部情報資料課（〒319-11茨城県那珂郡東海村）  
あて、お申しこしください。なお、このほかに財団法人原子力弘済会資料センター（〒319-11茨城  
県那珂郡東海村日本原子力研究所内）で複写による実費頒布をおこなっております。

JAERI-M reports are issued irregularly.

Inquiries about availability of the reports should be addressed to Information Division, Department  
of Technical Information, Japan Atomic Energy Research Institute, Tokai-mura, Naka-gun,  
Ibaraki-ken 319-11, Japan.

© Japan Atomic Energy Research Institute, 1988

---

編集兼発行 日本原子力研究所  
印 刷 日立高速印刷株式会社

Benchmark Experiments on a 60 cm-thick  
Graphite Cylindrical Assembly

Hiroshi MAEKAWA, Yujiro IKEDA, Yukio OYAMA, Seiya YAMAGUCHI  
Koichi TSUDA, Tooru FUKUMOTO\*, Kazuaki KOSAKO  
Michio YOSHIZAWA\*\* and Tomoo NAKAMURA

Department of Reactor Engineering  
Tokai Research Establishment  
Japan Atomic Energy Research Institute  
Tokai-mura, Naka-gun, Ibaraki-ken

(Received January 29, 1988)

Integral experiments on a graphite cylindrical assembly have been carried out, using the FNS facility to provide benchmark data for verification of methods and data used in fusion neutronics research. The size of assembly was 63 cm (diameter) by 61 cm (length). Measurements included  $^{235}\text{U}$ ,  $^{238}\text{U}$ ,  $^{237}\text{Np}$  and  $^{232}\text{Th}$  fission rates ;  $^{27}\text{Al}(\text{n},\alpha)^{24}\text{Na}$ ,  $^{58}\text{Ni}(\text{n},2\text{n})^{57}\text{Ni}$ ,  $^{58}\text{Ni}(\text{n},\text{p})^{58}\text{Co}$ ,  $^{90}\text{Zr}(\text{n},2\text{n})^{89}\text{Zr}$ ,  $^{93}\text{Nb}(\text{n},2\text{n})^{92m}\text{Nb}$ ,  $^{115}\text{In}(\text{n},\text{n}')^{115m}\text{In}$  and  $^{197}\text{Au}(\text{n},\gamma)^{198}\text{Au}$  reaction rates. Neutron energy spectra in the assembly, as well as response rates of TLDs and PIN diodes, were also measured. Measured data are presented in tabular form together with estimated errors. A sample calculation using the DOT3.5 code is provided to facilitate the reader understanding of the experiments. Although several different measuring techniques are used in the experiment, the data are mutually consistent. This fact support that present experimental data can be applied to the benchmark verification of methods and data.

KEYWORDS: Fusion Neutronics, Benchmark Experiment, Graphite, FNS, Neutron Spectrum, Foil Activation, Fission Rate, TLD, PIN Diode, DOT3.5, JENDL-3

---

\* Present address, Century Research Center Corporation Ltd.

\*\* Hokkaido University; Present address, Dep. Health Physics, JAERI.

黒鉛 60 cm 厚円筒体系によるベンチマーク実験

日本原子力研究所東海研究所原子炉工学部

前川 洋・池田裕二郎・大山 幸夫・山口 誠哉  
津田 孝一・福本 亮\*・小迫 和明\*・吉沢 道夫\*\*  
中村 知夫

(1988年1月29日受理)

核融合炉の研究で用いられている計算手法およびデータベースを検証するベンチマークデータを提供する目的で、黒鉛円筒体系での積分実験をFNSを用いて実施した。実験体系は直径 63 cm, 長さ 61 cm である。 $^{235}\text{U}$ ,  $^{238}\text{U}$ ,  $^{237}\text{Np}$  と  $^{232}\text{Th}$  の核分裂率分布および  $^{27}\text{Al}(\text{n}, \alpha) ^{24}\text{Na}$ ,  $^{58}\text{Ni}(\text{n}, 2\text{n}) ^{57}\text{Ni}$ ,  $^{58}\text{Ni}(\text{n}, \text{p}) ^{58}\text{Co}$ ,  $^{90}\text{Zr}(\text{n}, 2\text{n}) ^{89}\text{Zr}$ ,  $^{93}\text{Nb}(\text{n}, 2\text{n}) ^{92m}\text{Nb}$ ,  $^{115}\text{In}(\text{n}, \text{n}') ^{115m}\text{In}$  と  $^{197}\text{Au}(\text{n}, \text{r}) ^{198}\text{Au}$  の反応率分布を測定した。また、体系内の中性子エネルギースペクトルや TLD と PIN ダイオードのレスポンス分布も測定した。測定データは誤差と共に、表で示されている。読者が実験を良く理解できるように、DOT 3.5 による計算例を示した。種々の測定法を用いたにもかかわらず、実験値同志の整合性は良かった。この事実は今回測定した実験データが計算手法やデータベースの評価に利用できることを示している。

---

東海研究所：〒319-11 茨城県那珂郡東海村白方字白根 2-4

\* センチュリ・リサーチ・センター㈱

\*\* 北海道大学

## Contents

1.	Introduction .....	1
2.	Experimental Assembly, Arrangement and Neutron Source .....	3
3.	Fission-Rate Distributions Measured by Micro-Fission Chambers .....	10
4.	Reaction-Rate Distributions Measured by Activation Foils .....	15
5.	In-System Neutron Spectra Measured by a Small Spherical NE213 Spectrometer .....	20
6.	Response Distribution of Thermoluminescence Dosimeters .....	43
7.	Discussion and Concluding Remarks .....	50
	Acknowledgement .....	51
	References .....	51
	Appendix 1 Fission-Rate Distributions Measured by Fission Track Recorders (FTD) .....	54
	Appendix 2 Response Distribution of PIN Diode .....	58
	Appendix 3 Sample Calculation .....	60

## 目 次

1.	緒 言 .....	1
2.	実験体系, 配置および中性子源 .....	3
3.	小型核分裂計数管で測定した核分裂率分布 .....	10
4.	放射化箔で測定した反応率分布 .....	15
5.	小型球型 N E 213 で測定した体系内中性子スペクトル .....	20
6.	熱蛍光線量計 (T L D) のレスポンス分布 .....	43
7.	検討および結語 .....	50
	謝 辞 .....	51
	参考文献 .....	51
	付録 1 核分裂片検出器 (F T D) で測定した核分裂率分布 .....	54
	付録 2 P I N ダイオードのレスポンス分布 .....	58
	付録 3 計 算 例 .....	60

## 1. Introduction

Experimental studies are required to verify the accuracy of both calculational methods and nuclear data which are used in nuclear design and analysis of a fusion reactor. The most suitable experiments for this type of method and data verification are clean benchmark experiments on a simple geometry with simple material compositions. A series of clean benchmark experiments was planned to provide useful benchmark data considering following items:

- 1) The experimental assembly and layout will be arranged to make a calculational model easily and accurately.
- 2) The data will be measured as absolute values in order to compare the measured and calculated results directly.
- 3) The conditions, which are necessary for analysis, will be given as many and accurate as possible (e.g., source spectrum, atom density and so on).
- 4) Various types of measured data will be obtained by the use of different methods in order to supply the information as much as possible and also to make crosscheck between observed data.
- 5) The measured data will be obtained in not only one media but in several mediae having various characteristics.

As the first experiment of this series, the integral experiment on a lithium-oxide cylindrical assembly was carried out at FNS. The experiment in detail and numerical results have been published in JAERI-M report.<sup>1)</sup> As the second clean benchmark experiment, integral experiment on a graphite cylindrical slab assembly was planned and have been carried out.

The graphite assembly was chosen because of following reasons:

- 1) The nuclear data of carbon in evaluated nuclear data files are rather good comparing the other elements.
- 2) Since the slowing-down power of graphite is large, neutron spectrum in the graphite assembly is softer than that in the lithium-oxide assembly.
- 3) The assembly can be consist of only one element including a

experimental channel, in which detectors are to be inserted.

Measured quantities and methods used in this work are summarized as follows:

- (a) Fission-rate distributions of  $^{235}\text{U}$ ,  $^{238}\text{U}$ ,  $^{237}\text{Np}$  and  $^{232}\text{Th}$ 
  - \* on-line micro-fission chambers containing  $^{235}\text{U}$ ,  $^{238}\text{U}$ ,  $^{237}\text{Np}$  and  $^{232}\text{Th}$
- (b) Reaction-rate distributions of  $^{27}\text{Al}(\text{n},\alpha)^{24}\text{Na}$ ,  $^{58}\text{Ni}(\text{n},2\text{n})$   
 $^{57}\text{Ni}$ ,  $^{58}\text{Ni}(\text{n},\text{p})^{58}\text{Co}$ ,  $^{90}\text{Zr}(\text{n},2\text{n})^{89}\text{Zr}$ ,  $^{93}\text{Nb}(\text{n},2\text{n})^{92m}\text{Nb}$ ,  
 $^{115}\text{In}(\text{n},\text{n}')^{115m}\text{In}$  and  $^{197}\text{Au}(\text{n},\gamma)^{198}\text{Au}$ 
  - \* offline gamma-ray spectroscopy of irradiated Al, Ni, Zr, Nb, In and Au foils
- (c) Neutron spectra within the assembly
  - \* online pulse-height spectrum recording and unfolding of a small sphere NE213 spectrometer
  - \* offline evaluation of threshold reactions induced in foils (MFA)<sup>†</sup>
- (d) Response distributions of thermoluminescence dosimeters (TLD)
  - \* offline reading of thermoluminescence from irradiated TLDs of LiF, CaSO<sub>4</sub>, LiF & CaSO<sub>4</sub>, Mg<sub>2</sub>SiO<sub>4</sub>, Sr<sub>2</sub>SiO<sub>4</sub> and Ba<sub>2</sub>SiO<sub>4</sub>

In addition to these measurements, the response distribution of PIN diodes was measured as well as fission-rate distributions by offline scanning of solid-state track recorders packed with  $^{235}\text{U}$ ,  $^{238}\text{U}$  and  $^{232}\text{Th}$  foils, in an effort to develop new techniques. They are presented in Appendix. To give the reader a better understanding of the use of the experimental data for purposes of comparison with theoretical predictions, a sample calculation based on DOT3.5<sup>2)</sup> is provided in Appendix A.3.

---

<sup>†</sup> The result of the MFA measurements is omitted from this report and will be published elsewhere.

## 2. Experimental Assembly, Arrangement and Neutron Source

Reactor-grade graphite blocks were stacked in thin wall (2 mm) aluminum tubes to form a cylindrical slab in the same manner as the lithium-oxide assembly.<sup>1)</sup> The size of graphite assembly was 31.4 cm in equivalent radius and 61.0 cm in thickness. The blocks used in this assembly were four types except near the central region where there was an experimental channel. A sectional view of the assembly is shown in Fig. 2.1. The graphite blocks used were selected from the inventory so as to have the density with the deviation within  $\pm 2\%$ . The data of blocks are summarized in Table 2.1. The average density was  $(1.641 \pm 0.015)$  g/cm<sup>3</sup>.

The experimental channel — a set of sheath and drawer — was made of the same grade graphite [ $100 \times 100 \times 1000$  mm<sup>3</sup>,  $(1.654 \pm 0.002)$  g/cm<sup>3</sup>] in order to save the changing time of detector position and for minimizing the personnel exposure for experimentists. Photographs of graphite blocks and the set of sheath and drawer are shown in Figs. 2.2 and 2.3, respectively. A sectional view of the sheath, drawer and spacers are also shown in Fig. 2.4. The experimental channel was placed at the central axis of the assembly. Therefore, this experimental assembly consisted of a single element, i.e., carbon, except the aluminum framework. Graphite blocks with experimental hole of 21 mm dia. were made to allow insertion of a detector. They are shown in Fig. 2.5. Appendix A.3 describes a two-dimentional model for a experimental analysis. Homogenized nuclide densities in each region are tableted in Table 2.2.

The 80-degree beam line in the first target room of the FNS facility was used for the present experiment. The experimental layout is shown in Fig. 2.6. A high speed water-cooled target<sup>3)</sup> was set at the end of the beam line. A  $7.4 \times 10^{11}$  Bq (20 Ci) Ti-T target was mounted on the target assembly. Neutrons were generated at the distance of 20 cm from the assembly surface on its central axis. The setting accuracy is estimated to be within  $\pm 1$  mm. A view of the experimental arrangement is shown in Fig. 2.7. The layout in the first target room of 15 m  $\times$  15 m is illastrated in Fig. 2.8. The distances from the target to the west and south walls are 5.5 m, and those to

the ceiling, the grating floor and the basement floor are 7.9, 1.8 and 3.8 m, respectively.

Neutron yields were determined by means of the associated  $\alpha$ -particle detection method.<sup>4)</sup> A small silicon surface-barrier detector with a aperture of about 1 mm dia. was mounted inside the beam line to detect the  $\alpha$ -particle of  $^3\text{T}(\text{d},\text{n})^4\text{He}$  reaction. Source characteristics<sup>5)</sup> — neutron yield, angular distribution and spectra of the target assembly were measured by the time-of-flight technique,<sup>6)</sup> foil activation and an NE213 spectrometer<sup>7)</sup>.

A good agreement was obtained between neutron yields measured by different methods within the experimental error. An analysis by Monte Carlo computation<sup>8)</sup> also showed fairly good agreement with measured neutron energy spectra as well as angular distributions, the latter obtained by foil activation. Thus, the caluclated source spectrum and other characteristics were essentially confirmed and can be used as input information in the benchmark calculations.

Table 2.1 Data of graphite blocks used in the experiments.

Size [ mm ]	Quantity	Total weight [ kg ]	Density [ g / cm <sup>3</sup> ]
25.3 × 50.6 × 50.6	43	4.56	1.638 ± 0.011
50.6 × 50.6 × 50.6	50	10.66	1.637 ± 0.010
50.6 × 50.6 × 101.6	64	27.32	1.648 ± 0.016
25.3 × 50.6 × 203.2	332	141.57	1.639 ± 0.017
50.6 × 50.6 × 203.2	222	189.34	1.639 ± 0.017
100 × 100 × 1000*	4	65.99	1.654 ± 0.002
Weighted average			1.642 ± 0.015

\*The sheath, drawer and spacer, i.e., A, B, C and D show in Fig. 2.4, were made from these blocks.

Table 2.2 Homogenized nuclide density for each region of graphite assembly.

Nuclei	Air	Graphite	Al-frame
O	1.040 -5*	----	----
N	3.881 -5	----	----
C	----	8.232 <sub>2</sub> -2	----
Al	----	----	1.067 -2
Mg	----	----	6.000 -5
Si	----	----	4.354 -5
Fe	----	----	1.145 -5

\* Read as  $1.040 \times 10^{-5}$  [  $10^{24}$  atoms /  $\text{cm}^3$  ].

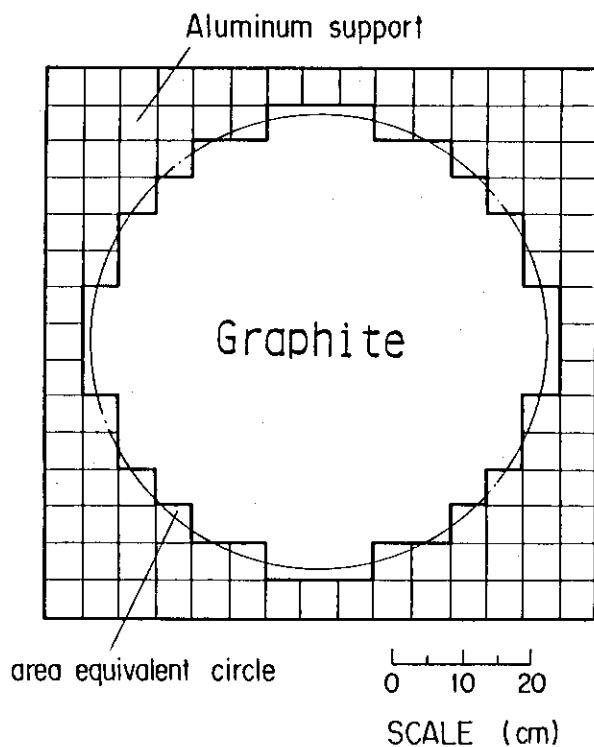


Fig. 2.1 Sectional view of the cylindrical assembly.

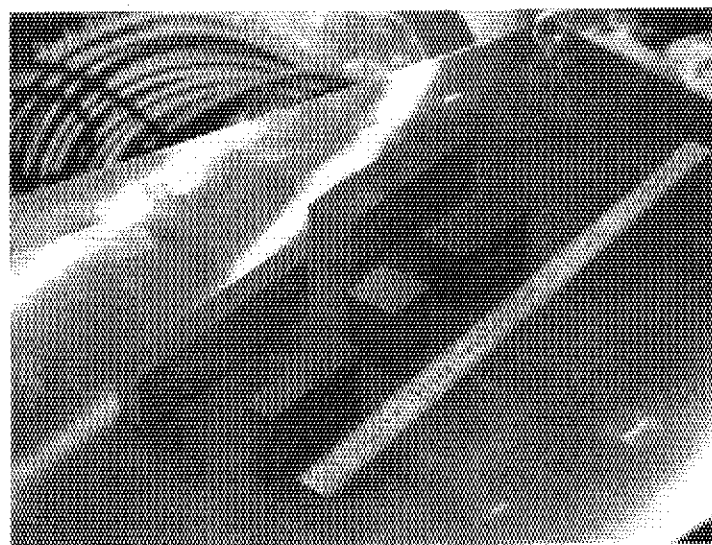


Fig. 2.2 Graphite blocks.

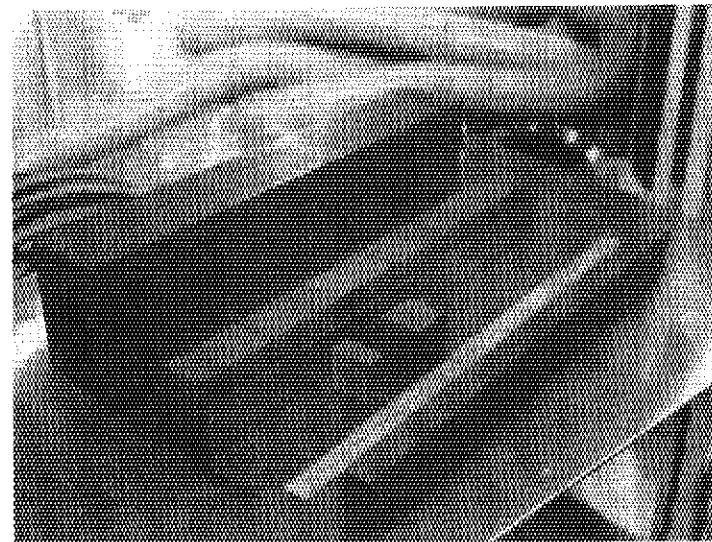
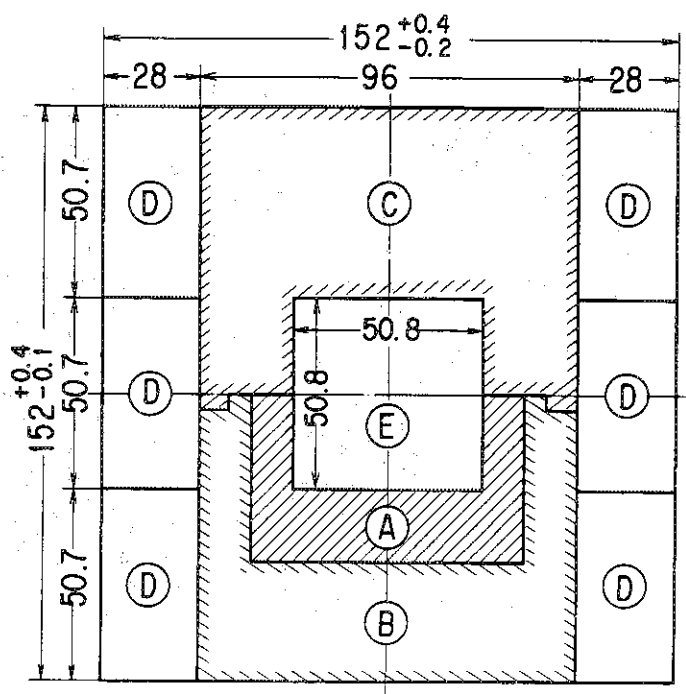


Fig. 2.3 Graphite seath, drawer and spacer for experimental channel.



- A : Boat ( Drawer )
- B & C : Guide Rail ( Sheath )
- D : Spacer
- E : Void for Special-Sized Blocks

Fig. 2.4 A sectional view of the graphite sheath and drawer.

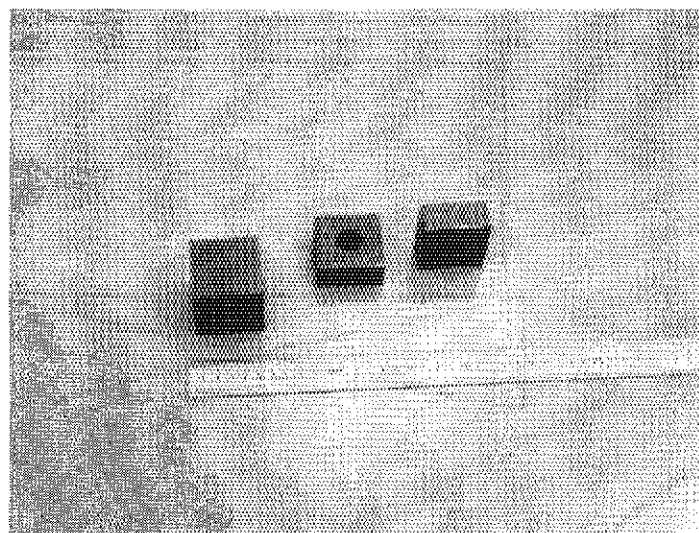


Fig. 2.5 Graphite blocks with experimental hole.

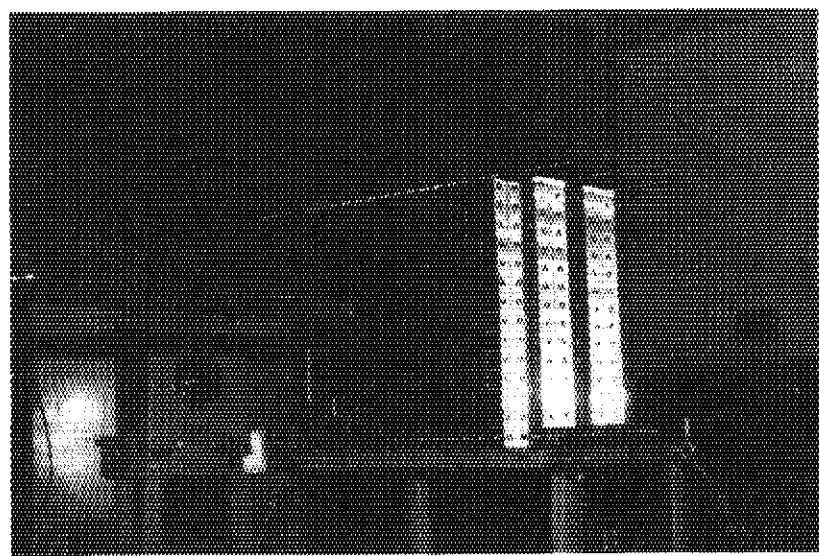


Fig. 2.6 A view of experimental arrangement.

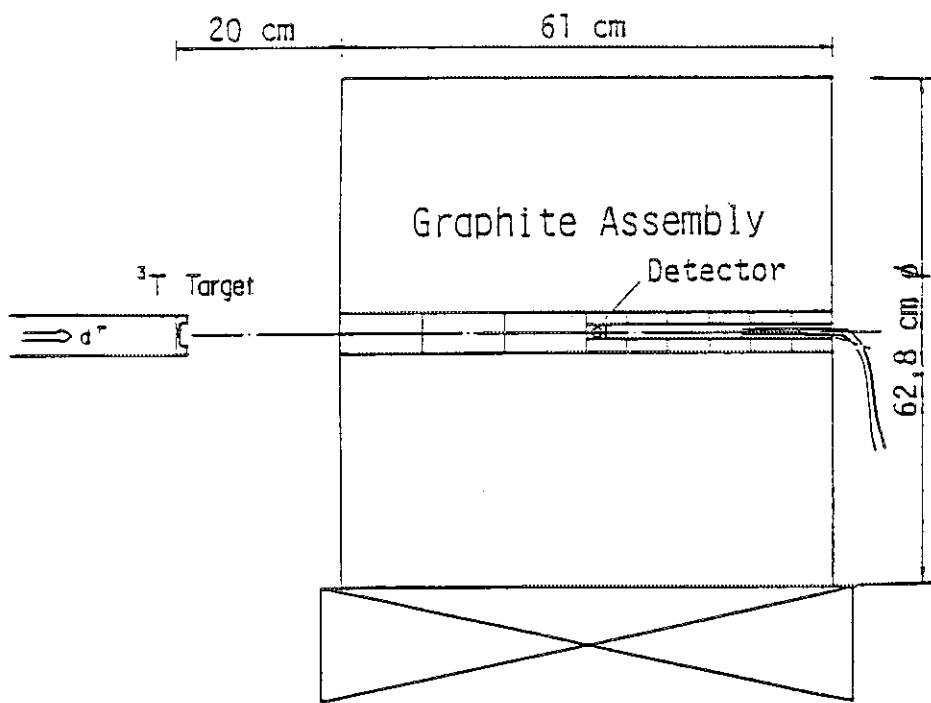


Fig. 2.7 Experimental layout.

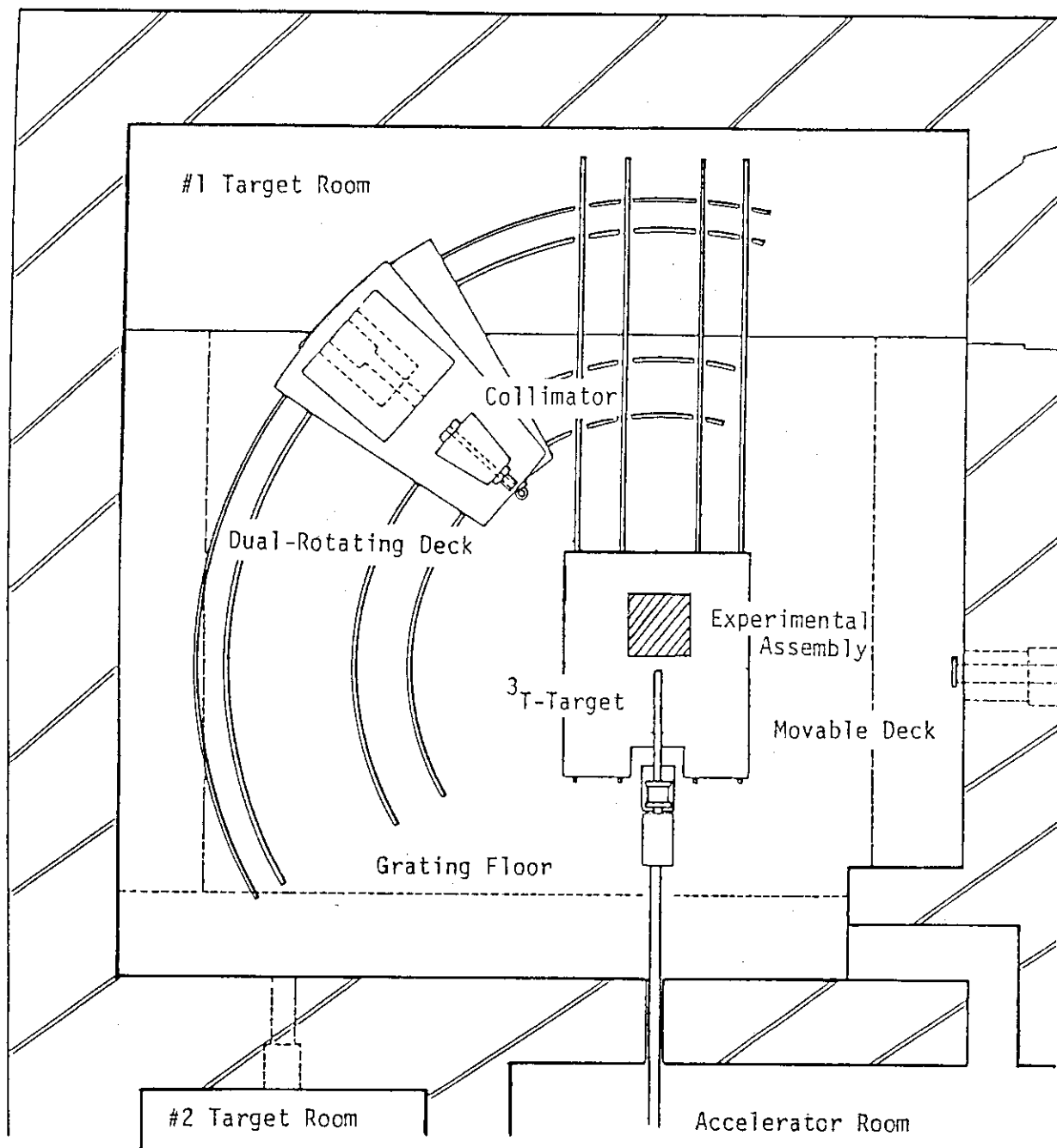


Fig. 2.8 Layout of the FNS first target room.

### 3. Fission-Rate Distributions Measured by Micro-Fission Chambers

Fission-rate distributions were measured with three micro-fission chambers coated respectively with about 4 mg of the oxides of  $^{235}\text{U}$ ,  $^{238}\text{U}$  and  $^{232}\text{Th}$ ; a fourth chamber was coated with about 1.6 mg of the oxide of  $^{237}\text{Np}$ . The chamber were Type FC4A manufactured by T.C. Centronic Ltd, had 6.25 mm O.D. and 25.4 mm active length. The four chambers were just the same as those used in the experiment on the  $\text{Li}_2\text{O}$  assembly.<sup>1)</sup>

All the counter traverse experiments were made in the central experimental hole of 21 mm dia. Fission rates in the  $^{235}\text{U}$  and  $^{238}\text{U}$  chambers were measured simultaneously, side by side, in the same hole. Similar measurements were carried out with the  $^{237}\text{Np}$  and  $^{232}\text{Th}$  chambers. As the detector was successively withdrawn along the axis, the graphite blocks with experimental hole were replaced by solid blocks, i.e., the graphie blocks without hole, to minimize neutron streaming. The remaining channel toward the rear of the assembly served to pass the signal cable.

The deuteron beam energy during the counter traverse was 330 keV and the beam current was varied from 100  $\mu\text{A}$  to 2 mA with the count rate.

The four fission chambers were calibrated by a scheme very similar to that used in a previous experiment.<sup>9)</sup> A chamber was placed in front of the water-cooled target at distances of 20, 30 and 40 cm to count the neutrons emitted in the forward direction. The chamber was positioned with its axis at 0°, 45° and 90° to the incident  $d^+$  beam. To correct for the effect of room-return neutrons, the fission chamber was placed at a distance of 2 m from the target. The background effect was found to be 9.3 and 1.6 % for the  $^{235}\text{U}$  and  $^{237}\text{Np}$  chambers respectively, and effect was negligible for the other chambers. The room-returned background was subtracted from the data.

The number of effective atoms present in the chamber coating is calculated by the equation ;

$$N = \frac{C_0}{P \bar{\sigma}_f Y}, \quad [\text{fissile atoms/chamber}] \quad (3.1)$$

where  $N$  is the effective number of atoms in the micro-fission chamber,  $Y$  the neutron yield at the target obtained by  $\alpha$ -monitoring,  $C_0$  the total count of fissions during the measuring time,  $P$  a geometrical factor determined by the configuration of target and chamber,  $\bar{\sigma}_f$  the fission cross section averaged over the source spectrum and the atomic composition ;

$$\bar{\sigma}_f = \sum_i \sigma_f^i N_i , \quad (3.2)$$

where  $\sigma_f^i$  the average fission cross section, is given by,

$$\sigma_f^i = \int \sigma(E) \phi_f(E) dE , \quad (3.3)$$

where

$N_i$  : isotopic abundance of i-th fissile material,  
 $\sigma(E)$  : fission cross section,  
 $\phi_f(E)$  : forward source neutron spectrum.

The fission cross-section data were taken from the ENDF/B-IV data file and the result of a Monte Carlo calculation<sup>8)</sup> was used as the source spectrum. It is noted that the integral of the forward source neutron spectrum is not unity. The value of  $P$  was calculated by numerical integration.<sup>9)</sup>

The effect of the structural material of the chamber was included in the effective atom number. The effective numbers of fissile atoms present in the chambers were calculated by Eq. (3.1) and are summarized in Table 3.1. The data at 45° were very close to those of 90 degree, while the data of 0 degree were a little differed from those of the others. Therefore the data for 0° to the axis (parallel) were calculated by averaging over three positions and the data of non-parallel over the other positions. The calibration errors were estimated to be 2.8 % for  $^{235}\text{U}$ ,  $^{238}\text{U}$  and  $^{232}\text{Th}$ , and 3.8 % for  $^{237}\text{Np}$  chambers. Major sources of error were uncertainties in the neutron yield ( $Y$ ) and positioning ( $P$ ) ; the latter error was 1 %.

The absolute fission rate  $R(z)$ , for each chamber at the position  $z$  is given by the equation;

$$R(z) = \frac{F_0(z)}{N(z) Y_t}, \quad [\text{fissions/source neutron/atom}] \quad (3.4)$$

where  $F_0(z)$  is the total fission count at  $z$ ,  $N(z)$  the number of effective fissile atoms present in the chamber, and  $Y_t$  the total neutron yield at the target during the measurement. The  $N(z)$  was estimated by assist of a pre-experimental analysis. An energy integrated angular flux within 6.72 degree was assumed as the forward (parallel) component. The  $N(z)$  was obtained by averaging over the calculated fluxes of parallel and non-parallel components.

The uranium in the  $^{235}\text{U}$  micro-fission chamber contained 7 %  $^{236}\text{U}$ , and inversely that in the  $^{238}\text{U}$  chamber 0.044 %  $^{235}\text{U}$ , for which appropriate corrections were made in the observed fission rates. In the  $^{237}\text{Np}$  chamber, the neptunium contained 0.1 % plutonium, mostly  $^{239}\text{Pu}$ . Fissions contributed by this plutonium fraction were accounted for estimating its fission rate from that of  $^{235}\text{U}$ , assuming an average ratio of 1.26 between the fission cross sections of  $^{239}\text{Pu}$  and  $^{235}\text{U}$ . The error due to this assumption should be small. The corresponding amount of impurity for  $^{232}\text{Th}$  chamber was unknown, hence, the results obtained with  $^{232}\text{Th}$  were not corrected.

The absolute fission rates thus determined are summarized in Table 3.2. The error estimates given in the table were determined in the following manner. The error was mainly caused by the errors of total neutron yield (2.1 %) and effective fissile atom numbers (3.2 ~ 4.6 %). The latter error included the angular-dependency of chambers. The absolute fission-rate distributions are shown in Fig. 3.1.

Table 3.1 Measured effective fissile atom numbers  
in micro-fission chambers.

Chamber	Effective fissile atom number [ $\times 10^{18}$ atoms/chamber ]			
	$^{238}\text{U}$	$^{235}\text{U}$	$^{237}\text{Np}$	$^{232}\text{Th}$
Parallel	7.32 <sub>8</sub>	6.73 <sub>4</sub>	2.20 <sub>5</sub>	6.78 <sub>6</sub>
Non-parallel	7.77 <sub>8</sub>	7.33 <sub>2</sub>	2.43 <sub>2</sub>	7.61 <sub>3</sub>

Table 3.2 Fission-rates in the graphite assembly  
measured by micro-fission chambers.

Position*1 [cm]	Fission rate [fission/atom/source neutron]			
	U-235	U-238	N <sub>p</sub> -237	Th-232
24.1	3.88 -27(4.1%)	1.82 <sub>3</sub> -28(3.9%)	4.65 -28(5.1%)	5.79 -29(4.7%)
26.6	5.04 -27(4.1%)	1.37 <sub>9</sub> -28(3.9%)	3.67 -28(5.1%)	4.42 -29(4.7%)
31.7	6.93 -27(4.1%)	8.40 -29(3.9%)	2.34 -28(5.1%)	2.71 -29(4.7%)
36.8	8.23 -27(4.1%)	5.13 -29(3.9%)	1.50 <sub>9</sub> -28(5.1%)	1.77 <sub>5</sub> -29(4.7%)
41.8	8.82 -27(4.1%)	3.34 -29(3.9%)	9.58 -29(5.1%)	1.17 <sub>6</sub> -29(4.8%)
46.9	8.84 -27(4.1%)	2.16 -29(3.9%)	6.14 -29(5.1%)	8.47 -30(4.8%)
51.9	8.30 -27(4.1%)	1.43 <sub>8</sub> -29(3.9%)	3.88 -29(5.1%)	6.04 -30(4.8%)
57.0	7.39 -27(4.1%)	9.40 -30(3.9%)	2.47 -29(5.1%)	4.44 -30(4.8%)
62.1	6.18 -27(4.1%)	6.07 -30(3.9%)	1.52 <sub>2</sub> -29(5.2%)	3.13 -30(4.8%)
67.1	4.79 -27(4.1%)	4.12 -30(3.9%)	9.65 -30(5.2%)	2.28 -30(4.8%)
72.2	3.30 -27(4.1%)	2.65 -30(3.9%)	5.80 -30(5.3%)	1.52 <sub>9</sub> -30(5.0%)
77.2	1.74 <sub>2</sub> -27(4.1%)	1.67 <sub>2</sub> -30(4.0%)	3.89 -30(5.2%)	8.88 -31(5.0%)

\*1 Distance from the target and along the central axis.

\*2 Read as  $3.88 \times 10^{-28}$ .

\*3 Estimated experimental error.

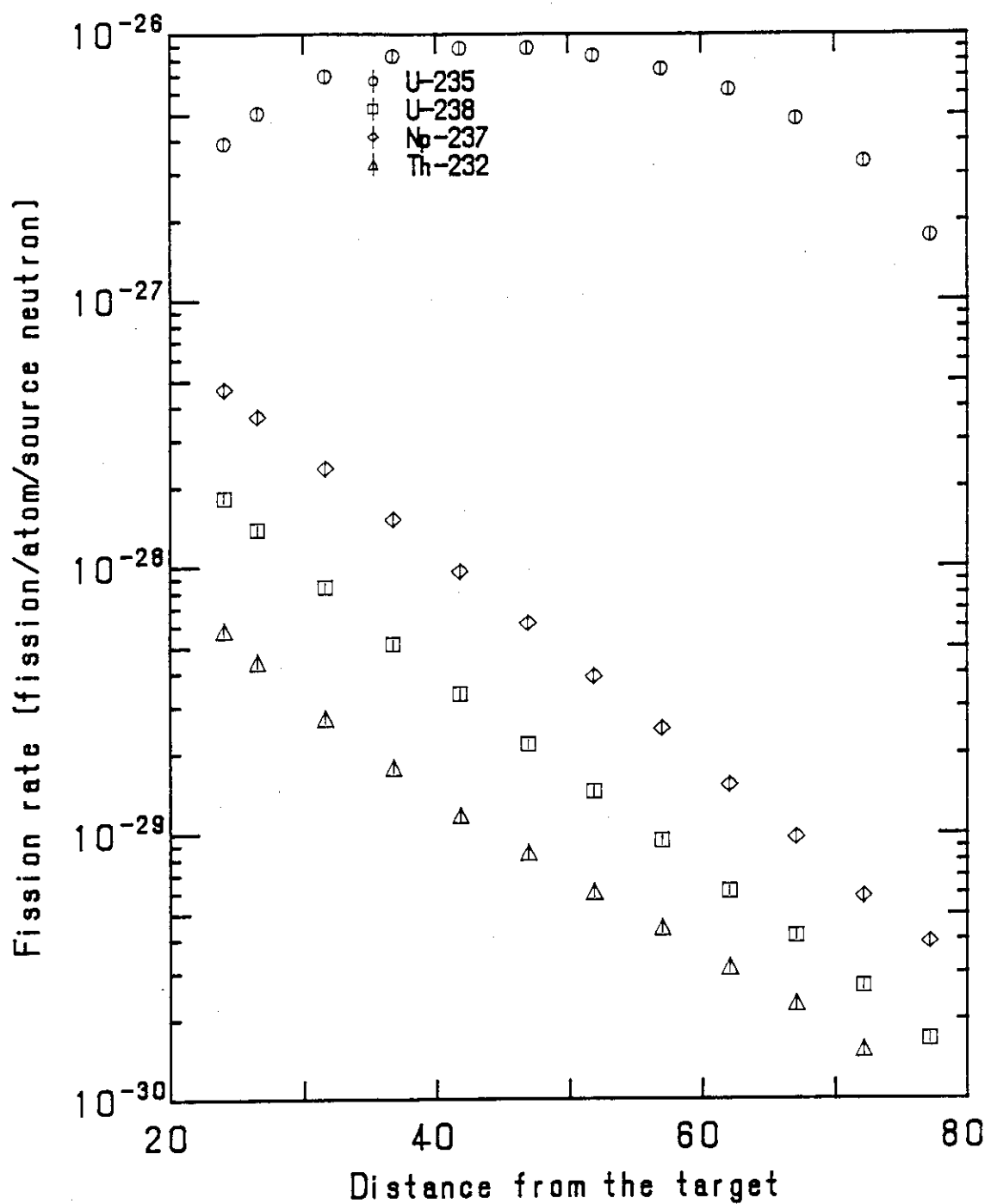


Fig. 3.1 Fission-rate distributions in the graphite assembly measured by micro-fission chambers.

#### 4. Reaction-Rate Distributions Measured by Activation Foils

Reaction-rate distributions of  $^{27}\text{Al}(n,\alpha)^{24}\text{Na}$ ,  $^{58}\text{Ni}(n,2n)^{57}\text{Ni}$ ,  $^{58}\text{Ni}(n,p)^{58}\text{Co}$ ,  $^{90}\text{Zr}(n,2n)^{89}\text{Zr}$ ,  $^{93}\text{Nb}(n,2n)^{92m}\text{Nb}$ ,  $^{115}\text{In}(n,n')^{115m}\text{In}$  and  $^{197}\text{Au}(n,\gamma)^{198}\text{Au}$  were measured along the central axis of the assembly by the foil activation technique. The seven reactions were selected for their different energy responses, covering the whole energy range from thermal to 15 MeV.

Foils of Al, Ni, Zr, Nb, In and Au were inserted into the small spaces between graphite blocks. The Al, Ni, Zr and Nb foils were 10 mm in diameter and 0.5 mm in thickness; the In foils were 10 mm square and 0.1 mm in thickness; the Au foils were 10 mm square and 0.001 mm in thickness. Foils were irradiated for about 12 hours by D-T neutrons. Energy and average current of  $d^+$  beam were 330 keV and 1.7 mA, respectively. Total neutron yield and rate were  $4.799 \times 10^{15}$  and  $1.351 \times 10^{11}$  n/s at the target, respectively. After irradiation, spectra of gamma-rays emitted from the foils were measured with a 60  $\text{cm}^3$  Ge(Li) detector. The  $\gamma$ -ray spectra were analyzed by the code BOB75,<sup>10)</sup> to compute peak areas. Reaction rates were deduced from the measured gamma-ray peak counts, detector efficiency and decay data, with corrections for self-absorption, sum peak and saturation factor during the irradiation. The reaction-rate, R, is given by

$$R = \frac{\lambda \cdot C}{N \cdot X \cdot Y \cdot Y_n} ,$$

$$N = \frac{W \cdot N_0 \cdot a}{A} ,$$

$$X = e_f \cdot b \cdot s ,$$

$$Y = [1 - e^{-\lambda \cdot t_b}] \cdot e^{-\lambda t_c} \cdot [1 - e^{-\lambda \cdot t_m}] ,$$

where

$\lambda$  : decay constant,

C : measured gamma-ray counts,

W : weight of foil,

$N_0$  : Avogadro constant,

$Y_n$  : source neutron yield,  
 $a$  : abundance,  
 $A$  : atomic number,  
 $e_f$  : detector efficiency,  
 $b$  : gamma-ray branching ratio,  
 $P$  : gamma-ray self-absorption coefficient for each foil,  
 $s$  : saturation correction coefficient,  
 $t_b$  : irradiation time,  
 $t_c$  : cooling time,  
 $t_m$  : measuring time.

The neutron yield,  $Y_n$ , was monitored by the associated  $\alpha$ -particle counting method.<sup>4)</sup> Decay data of the reaction products, taken from Ref.(11), are summarized in Table 4.1.

The measured reaction rates at various positions are listed in Table 4.2. Counting statistics errors were in the range of  $\pm 0.5$  to 9 % ; that of uncertainty detector efficiency was about 2.5 %. Other error sources were in the decay data, the source neutron yield and corrections for self-absorption, sum peak and saturation factors. The error assessment is given in Table 4.3. These reaction-rate distributions are shown in Figs. 4.1 and 4.2.

Table 4.1 Decay data needed for reaction-rate calculation.

Reaction	Half life	Detected $\gamma$ -ray energy [keV]	$\gamma$ -ray branching ratio [%]
$^{27}\text{Al}(n,\alpha)^{24}\text{Na}$	15.02 h	1368.6	100
$^{58}\text{Ni}(n,2n)^{57}\text{Ni}$	36.0 h	1377.6	77.6
$^{58}\text{Ni}(n,p)^{58}\text{Co}$	70.78 d	810.76	99.44
$^{90}\text{Zr}(n,2n)^{89}\text{Zr}$	78.43 h	909.2	99.01
$^{93}\text{Nb}(n,2n)^{92m}\text{Nb}$	10.14 d	934.5	99.2
$^{115}\text{In}(n,n')^{115m}\text{In}$	4.49 h	336.2	45.9
$^{197}\text{Au}(n,\gamma)^{198}\text{Au}$	2.696 d	411.8	95.40

Table 4.2 Reaction-rate distribution in the graphite assembly.

(a)  $^{27}\text{Al}(n,\alpha)^{24}\text{Na}$ ,  $^{58}\text{Ni}(n,2n)^{57}\text{Ni}$ ,  $^{58}\text{Ni}(n,p)^{58}\text{Co}$  and  $^{90}\text{Zr}(n,2n)^{89}\text{Zr}$ .

Position*1 [cm]	Reaction rate [reaction/atom/source neutron]			
	$^{27}\text{Al}(n,\alpha)^{24}\text{Na}$	$^{58}\text{Ni}(n,2n)^{57}\text{Ni}$	$^{58}\text{Ni}(n,p)^{58}\text{Co}$	$^{90}\text{Zr}(n,2n)^{89}\text{Zr}$
19.9	2.33 *2 -29(3.1%)	8.12 -30(5.0%)	7.98 -29(3.1%)	1.48 <sub>6</sub> -28(3.1%)
29.9	7.42 -30(3.2%)	1.96 <sub>3</sub> -30(3.2%)	3.71 -29(5.0%)	3.59 -29(3.2%)
40.2	2.60 -30(3.2%)	5.50 -31(5.0%)	1.53 <sub>0</sub> -29(5.2%)	1.07 <sub>2</sub> -29(3.4%)
50.3	9.61 -31(3.8%)	1.64 <sub>4</sub> -31(5.8%)	6.72 -30(5.2%)	3.44 -30(3.7%)
60.5	3.69 -31(3.7%)	5.40 -32(11.1%)	2.94 -30(5.5%)	1.23 <sub>0</sub> -30(4.5%)
70.7	1.41 <sub>3</sub> -31(6.0%)	1.98 <sub>3</sub> -32(5.1%)	1.28 <sub>8</sub> -30(5.0%)	4.27 -31(3.7%)
80.9	5.00 -32(8.8%)	————	————	————

\*1 Distance from the target and along the central axis.

\*2 Read as  $2.33 \times 10^{-29}$ .

\*3 The error of neutron yield (2.2%) is excluded.

(b)  $^{93}\text{Nb}(n,2n)^{92m}\text{Nb}$ ,  $^{115}\text{In}(n,n')^{115m}\text{In}$  and  $^{197}\text{Au}(n,\gamma)^{198}\text{Au}$ .

Position [cm]	Reaction rate [ reaction/atom/source neutron ]		
	$^{93}\text{Nb}(n,2n)^{92m}\text{Nb}$	$^{115}\text{In}(n,n')^{115m}\text{In}$	$^{197}\text{Au}(n,\gamma)^{198}\text{Au}$ *4
19.9	8.78 -29(3.2%)	3.13 -29(3.3%)	2.77 -28(3.0%)
29.9	2.44 -29(3.2%)	1.99 <sub>1</sub> -29(3.2%)	1.70 <sub>7</sub> -27(3.1%)
40.2	8.13 -30(3.1%)	9.80 -30(3.6%)	————
50.3	2.78 -30(3.1%)	4.57 -30(4.1%)	2.13 -27(3.1%)
60.5	1.05 <sub>3</sub> -30(3.7%)	2.17 -30(5.2%)	1.54 <sub>6</sub> -27(3.1%)
70.7	3.87 -31(3.6%)	9.26 -31(7.4%)	8.54 -28(3.0%)
80.9	1.46 <sub>8</sub> -31(3.2%)	————	1.39 <sub>4</sub> -28(3.1%)

\*4 Not corrected for self-shielding effect because the foil was very thin (0.001 mm).

Table 4.3 Error analysis for the reaction-rate measurement.  
 The measured data are presented in Table 4.2.

Item	Error [ $\pm$ %]
Counting statistics	0.5 ~ 9
Detector efficiency	2.5
Natural abundance	< 0.2
Foil weight	< 0.1
Sum peak	0.5 (only for $^{24}\text{Na}$ )
Saturation factor	0.5
Source neutron yield	3.0
Times for irradiation, cooling and measuring	~ negligible
Decay data	< 0.5

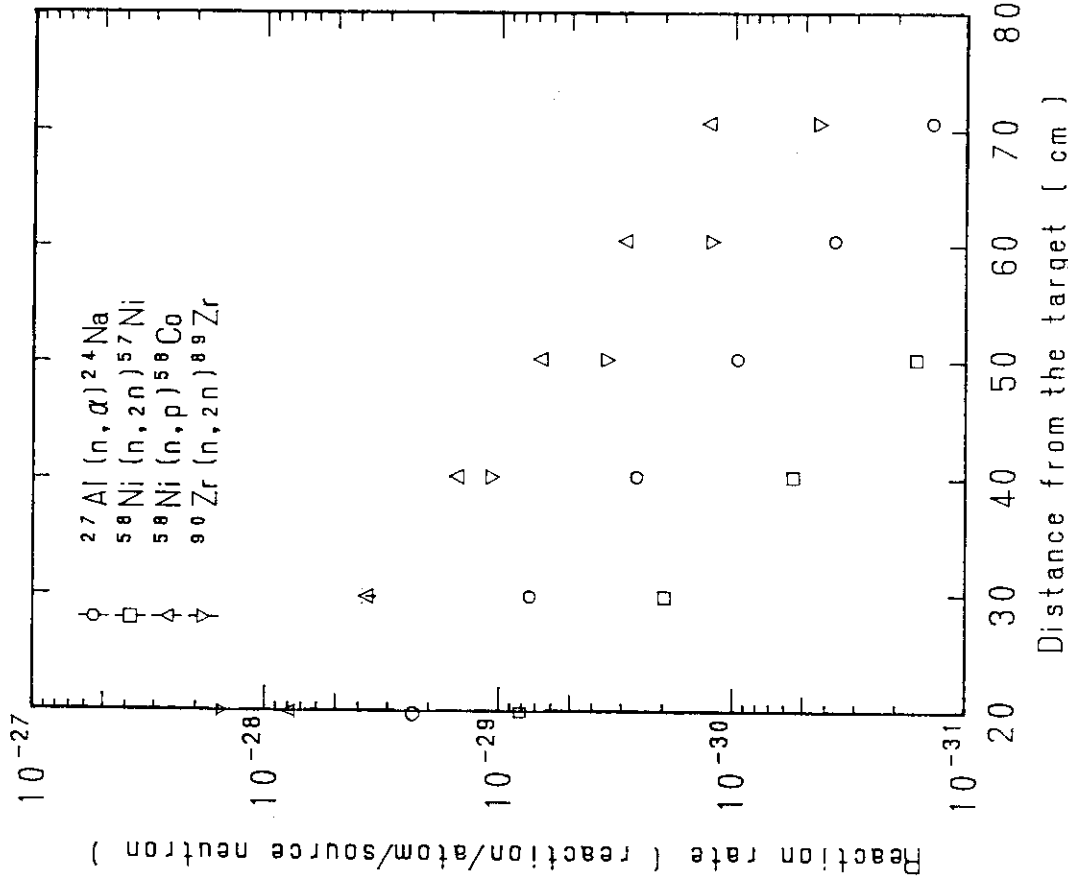


Fig. 4.1

Reaction-rate distributions of  $^{27}\text{Al}(n,\alpha)^{24}\text{Na}$ ,  $^{58}\text{Ni}(n,2n)^{57}\text{Ni}$ ,  $^{58}\text{Ni}(n,p)^{58}\text{Co}$  and  $^{90}\text{Zr}(n,2n)^{89}\text{Zr}$  in the graphite assembly.

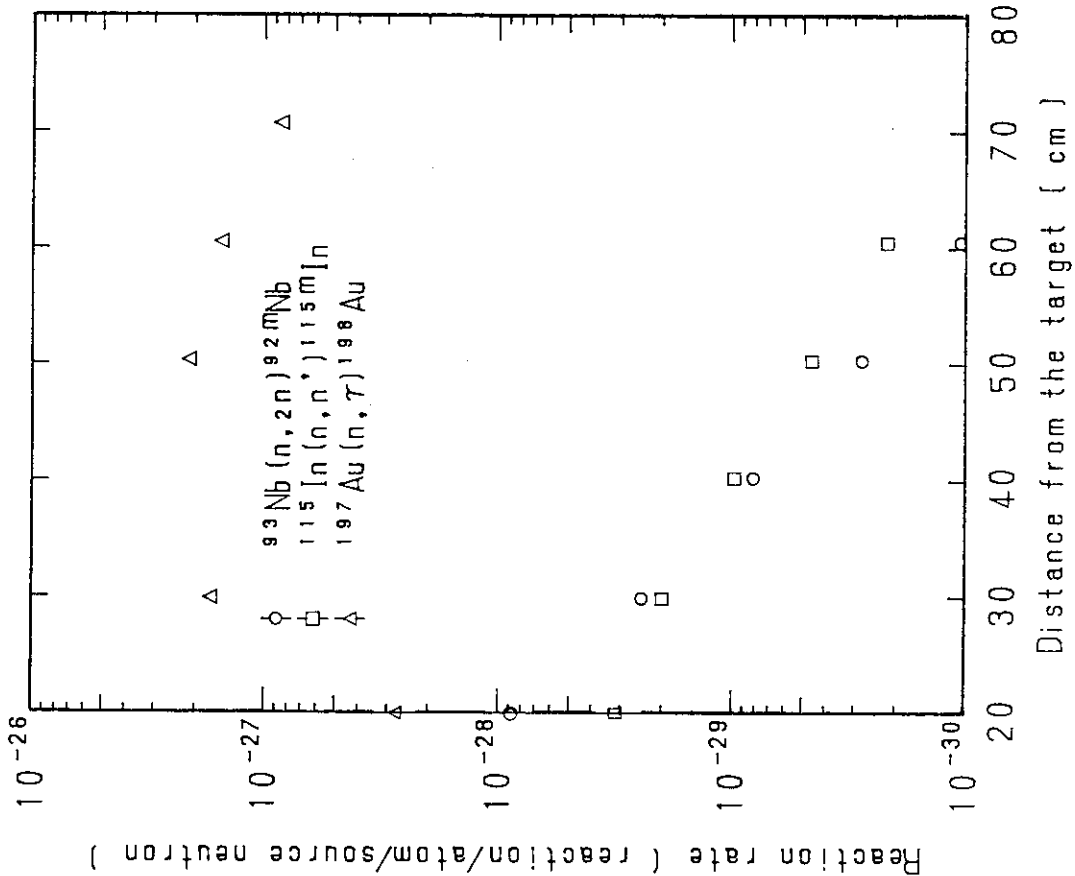


Fig. 4.2

Reaction-rate distributions of  $^{93}\text{Nb}(n,2n)^{92}\text{Nb}$ ,  $^{115}\text{In}(n,n')^{115m}\text{In}$  and  $^{197}\text{Au}(n,\gamma)^{198}\text{Au}$ .

## 5. In-System Neutron Spectra Measured by a Small Spherical NE213 Spectrometer

A 14 mm-diameter spherical NE213 neutron spectrometer<sup>7)</sup> was used for in-system neutron spectrum measurements. The measurements were carried out at eight points along the central axis. The detector was inserted into the special graphite blocks equipped with an experimental hole of 21 mm dia. Positions of the detector center are summarized in Table 5.1. The table also shows the  $\alpha$ -particle counts detected by the source neutron monitor. The deuteron energy was 330 keV ; the conversion factor from alpha counts to the total neutron yield is  $5.530 \times 10^7$  [neutrons/alpha count] for that energy. The measuring time was 2000 sec each position at an average count rate of about 1 kcps for the sum of neutrons and gamma-rays. The anode signal from the photomultiplier was split into two signal lines after the pre-amplifier and analyzed by two independent pulse height analyzers, with different amplifier gain and with pulse shape discrimination system (JAERI model 154A).<sup>12)</sup> This scheme provided a linear response over the wide dynamic range that must be covered.

Data were stored on a floppy diskette and later processed by the use of a VAX-11/780 computer system. The two pulse height spectra obtained were joined at an appropriate energy point. This combined recoil-proton spectrum was unfolded by the FORIST code<sup>13)</sup> and normalized to the total neutron yield.

The FORIST code determines the appropriate resolution function by internal iteration, hence, the given resolution function somewhat differs from the actual detector resolution. The resolution function [ window function  $W(E)$  ] is given together with the unfolded spectrum for each case. The spectrum obtained by FORIST corresponds to the calculated spectrum with following relation :

$$\Phi_{\text{obs}}(E) = \int_0^{\infty} \frac{1}{2\pi\sigma} \exp \left[ -\frac{(E-E')^2}{2\sigma^2(E')} \right] \cdot \Phi_{\text{cal}}(E') dE' ,$$

where

$$\sigma(E') = \frac{W(E') \cdot E'}{235} .$$

and the denominator 235 is the conversion factor<sup>13)</sup>.

The unfolded results obtained by this measurement are summarized in Tables 5.3 ~ 5.10. These tables indicate the upper and lower limits of the confidence interval given by the FORIST code, which means the true spectrum exists in this range with 67 % probability. The tables also include the window functions related to the detector resolution mentioned above. All spectra presented in the tables have been smeared by these resolution functions and have been normalized to scalar fluxes per unit  $4\pi$  source neutron produced at the target. Figures 5.1 ~ 5.8 show midpoints of the upper and lower fluxes with uncertainty band (confidence interval).

The probable errors of the results include two contributions. One of these, the statistical error, is included in the results as the confidence interval. The other error is related to the response matrices which are used in the unfolding procedure. This is included in the systematic errors summarized in Table 5.2. The systematic errors also include the error in the  $\alpha$ -monitor, as described in Ref. (4). The response matrix error is difficult to evaluate because there is no good way to determine the covariance matrix of response matrix terms. Thus we just give the efficiency error as the error of the integrated spectrum. The efficiency was calibrated through comparison of response with a standard neutron field determined by  $\alpha$ -monitor and a Monte Carlo calculation.

Table 5.1 Detector location and alpha count of  
in-system neutron spectral measurement.

Data No.	Position*1 [ cm ]	Alpha count : $C_\alpha$ [ counts ]
1	$24.1 \pm 0.1$	1,050 (3.9%)*2
2	$26.7 \pm 0.1$	1,604 (3.4%)
3	$31.7 \pm 0.1$	2,379 (3.1%)
4	$41.8 \pm 0.1$	4,887 (2.7%)
5	$52.0 \pm 0.1$	9,848 (2.5%)
6	$62.1 \pm 0.1$	17,383 (2.5%)
7	$72.1 \pm 0.1$	35,977 (2.3%)
8	$77.2 \pm 0.1$	65,925 (2.4%)

\*1 Distance from the target.

\*2 Experimental error for source intensity.

(See Table 5.2.)

Table 5.2 Systematic errors in the unfolded spectra\*1.

Item	Error [ % ]	Comment
Source intensity	$\pm \sqrt{(2.34)^2 + (10^4/C_\alpha)}$	Alpha monitor
Efficiency	$\pm 2.0\%$	Calibration error*2

\*1 Except the error related to the unfolding process.

\*2 The calibration was performed by using the same D-T neutron source and  $\alpha$ -monitor.

Therefore, the systematic error (2.34 %) is excluded in the value.

Table 5.3 In-system neutron spectrum in the graphite assembly ( $z = 24.1$  cm). (a) Scalar spectrum.

GRAPHITE 60-CM ASSEMBLY < IN-SYSTEM SPECTRUM >						
J	ENERGY(EV)	PWID	ERR	JIND	J	ENERGY(EV)
1	2.1020E+05	-3.9948E-07	1.0000E+00	3.1630E+01	4.6	1.9950E+06
2	2.2100E+05	-4.7515E-07	1.0000E+00	8.C510E-01	4.7	2.0970E+06
3	2.3230E+05	-5.6242E-07	1.0000E+00	7.9340E+01	4.8	2.2040E+06
4	2.4420E+05	-6.5338E-07	1.0000E+00	7.8150E+01	4.9	2.3170E+06
5	2.5680E+05	-7.5110E-07	1.0000E+00	7.7000E+01	5.0	2.4360E+06
6	2.6990E+05	-8.4639E-07	1.0000E+00	7.5820E+01	5.1	2.5610E+06
7	2.8330E+05	-9.3041E-07	1.0000E+00	7.4660E+01	5.2	2.6920E+06
8	2.9830E+05	-9.8751E-07	1.0000E+00	7.3490E+01	5.3	2.8300E+06
9	3.1360E+05	-9.9824E-07	1.0000E+00	7.2300E+01	5.4	2.9750E+06
10	3.2970E+05	-9.9900E-07	1.0000E+00	7.1140E+01	5.5	3.1280E+06
11	3.4660E+05	-7.7240E-07	1.0000E+00	6.9780E+01	5.6	3.2880E+06
12	3.6440E+05	-4.7128E-07	1.0000E+00	6.8800E+01	5.7	3.4570E+06
13	3.8300E+05	-4.0864E-10	1.0000E+00	6.7630E+01	5.8	3.6340E+06
14	4.0200E+05	-6.6483E-07	6.2482E-01	6.6000E+01	5.9	3.8210E+06
15	4.2350E+05	1.5374E-06	2.1.6095E-06	6.5630E+01	6.0	4.0160E+06
16	4.4500E+05	2.6005E+05	1.4516E-01	6.4690E+01	6.1	4.2220E+06
17	4.6780E+05	3.8541E-05	1.0813E-01	6.3830E+01	6.2	4.4390E+06
18	4.9180E+05	5.2264E-06	8.9566E-02	6.2950E+01	6.3	4.6660E+06
19	5.1700E+05	6.6750E-06	7.6614E-02	6.2100E+01	6.4	4.9060E+06
20	5.4360E+05	8.1676E-05	6.7154E-02	6.1200E+01	6.5	5.1570E+06
21	5.7140E+05	9.6931E-05	6.1096E-02	6.3000E+01	6.6	5.4220E+06
22	6.0070E+05	1.1270E+05	5.7677E-02	5.9360E+01	6.7	5.7000E+06
23	6.3150E+05	1.2941E+05	5.5411E-02	5.8430E+01	6.8	5.9920E+06
24	6.6390E+05	1.4733E+05	5.2198E-02	5.7490E+01	6.9	6.2990E+06
25	6.9790E+05	1.6679E+05	4.9264E-02	5.6560E+01	7.0	6.6220E+06
26	7.3370E+05	1.8546E+05	4.7332E-02	5.5620E+01	7.1	6.9610E+06
27	7.7130E+05	2.0390E+05	4.6441E-02	5.4720E+01	7.2	7.3180E+06
28	8.1090E+05	2.2056E+05	4.6792E-02	5.3860E+01	7.3	7.6940E+06
29	8.5250E+05	2.3492E+05	4.7566E-02	5.2990E+01	7.4	8.0880E+06
30	8.9260E+05	2.4920E+05	4.9264E-02	5.2160E+01	7.5	8.5030E+06
31	9.4210E+05	2.5695E+05	4.5530E-02	5.1340E+01	7.6	8.9390E+06
32	9.9040E+05	2.6560E+05	4.4615E-02	5.0470E+01	7.7	9.3970E+06
33	1.0410E+06	2.7329E+05	4.4993E-02	4.9570E+01	7.8	9.8790E+06
34	1.0950E+06	2.8122E+05	4.5697E-02	4.8640E+01	7.9	1.0390E+07
35	1.1510E+06	2.9070E+05	4.7303E-02	4.7590E+01	8.0	1.0920E+07
36	1.2100E+06	3.0166E+05	4.5510E+01	4.6510E+01	8.1	1.1480E+07
37	1.2720E+06	3.1417E+05	4.4739E-02	4.5400E+01	8.2	1.2070E+07
38	1.3370E+06	3.2859E+05	4.3721E-02	4.4210E+01	8.3	1.2680E+07
39	1.4060E+06	3.4276E+05	4.4076E-02	4.2950E+01	8.4	1.3340E+07
40	1.4780E+06	3.5412E-05	4.5165E-02	4.1720E+01	8.5	1.4020E+07
41	1.5530E+06	3.6143E-05	4.5842E-02	4.0570E+01	8.6	1.4740E+07
42	1.6330E+06	3.6500E-05	4.5346E-02	3.9520E+01	8.7	1.5490E+07
43	1.7170E+06	3.6572E-05	4.4723E-02	3.8560E+01	8.8	1.6290E+07
44	1.8050E+06	3.6465E-05	4.4889E-02	3.7690E+01	8.9	1.7120E+07
45	1.8970E+06	3.6227E-05	4.6289E-02	3.6860E+01	9.0	1.8000E+07

```

    * ERR X 100 = %
    ** WIND = % [FWHM]
    *** EN/CM**2/[ETHARGY/SOURCE]

```

Table 5.3 (b) Integral spectrum.

GRAPHITE 60-CM ASSEMBLY ---< RUNNING INTEGRAL >---											
J	ENERGY(eV)	FLP	PLO	J	ENERGY(eV)	PLO	J	ENERGY(eV)	PLO	PUP	
1	1.7556E+07	2.6804E-07	1.6049E-07	4.6	1.8502E-06	1.7209E-04	1.4739E-04	1.4739E-04	1.4963E-04	1.4963E-04	
2	1.6697E+07	1.9954E-06	1.3801E-06	4.7	1.7604E+06	1.7399E-04	1.4963E-04	1.4963E-04	1.5138E-04	1.5138E-04	
3	1.5888E+07	1.0212E-05	8.7552E-06	4.8	1.6746E+06	1.7590E-04	1.5312E-04	1.5312E-04	1.5781E-04	1.5781E-04	
4	1.5088E+07	5.0906E-05	2.3481E-05	4.9	1.5927E+06	1.7781E-04	1.5970E-04	1.5970E-04	1.5485E-04	1.5485E-04	
5	1.4376E+07	6.1785E-05	5.7540E-05	5.0	1.5147E+06	1.7970E-04	1.5485E-04	1.5485E-04	1.5654E-04	1.5654E-04	
6	1.3674E+07	8.3495E-05	8.2541E-05	5.1	1.4415E+06	1.8155E-04	1.5818E-04	1.5818E-04	1.5834E-04	1.5834E-04	
7	1.3011E+07	1.0184E-04	9.4227E-05	5.2	1.3713E+06	1.8334E-04	1.5850E-04	1.5850E-04	1.5975E-04	1.5975E-04	
8	1.2367E+07	1.0778E-04	9.9013E-05	5.3	1.3040E+06	1.8506E-04	1.5975E-04	1.5975E-04	1.6125E-04	1.6125E-04	
9	1.1772E+07	1.1155E-04	1.0161E-04	5.4	1.2406E+06	1.8670E-04	1.6125E-04	1.6125E-04	1.6268E-04	1.6268E-04	
10	1.1197E+07	1.1422E-04	1.0328E-04	5.5	1.1801E+06	1.8827E-04	1.6268E-04	1.6268E-04	1.6407E-04	1.6407E-04	
11	1.0650E+07	1.1690E-04	1.0494E-04	5.6	1.1226E+06	1.8979E-04	1.6407E-04	1.6407E-04	1.6541E-04	1.6541E-04	
12	1.0133E+07	1.1965E-04	1.0666E-04	5.7	1.0680E+06	1.9126E-04	1.6541E-04	1.6541E-04	1.6671E-04	1.6671E-04	
13	9.6335E+06	1.2213E-04	1.0823E-04	5.8	1.0153E+06	1.9269E-04	1.6671E-04	1.6671E-04	1.6798E-04	1.6798E-04	
14	9.1650E+06	1.2439E-04	1.0960E-04	5.9	9.6592E+05	1.9407E-04	1.6798E-04	1.6798E-04	1.6921E-04	1.6921E-04	
15	8.7183E+06	1.2630E-04	1.1069E-04	6.0	9.1884E+05	1.9542E-04	1.6921E-04	1.6921E-04	1.7039E-04	1.7039E-04	
16	8.2931E+06	1.2786E-04	1.1161E-04	6.1	8.7407E+05	1.9671E-04	1.7039E-04	1.7039E-04	1.7150E-04	1.7150E-04	
17	7.8383E+06	1.2943E-04	1.1250E-04	6.2	8.3145E+05	1.9794E-04	1.7150E-04	1.7150E-04	1.9910E-04	1.9910E-04	
18	7.5040E+06	1.3111E-04	1.1375E-04	6.3	7.9088E+05	1.9910E-04	1.7256E-04	1.7256E-04	2.0016E-04	1.7256E-04	
19	7.1373E+06	1.3281E-04	1.1619E-04	6.4	7.5226E+05	1.9910E-04	1.7353E-04	1.7353E-04	1.7441E-04	1.7441E-04	
20	6.7891E+06	1.3443E-04	1.1619E-04	6.5	7.1558E+05	2.0113E-04	1.7520E-04	1.7520E-04	1.7520E-04	1.7520E-04	
21	6.4585E+06	1.3600E-04	1.1735E-04	6.6	6.8067E+05	2.0201E-04	1.7520E-04	1.7520E-04	1.7590E-04	1.7590E-04	
22	6.1435E+06	1.3751E-04	1.1849E-04	6.7	6.4751E+05	2.0278E-04	1.7590E-04	1.7590E-04	1.7651E-04	1.7651E-04	
23	5.8441E+06	1.3883E-04	1.1957E-04	6.8	6.1591E+05	2.0346E-04	1.7651E-04	1.7651E-04	1.7704E-04	1.7704E-04	
24	5.5593E+06	1.4023E-04	1.2058E-04	6.9	5.8587E+05	2.0457E-04	1.7750E-04	1.7750E-04	1.7818E-04	1.7818E-04	
25	5.2881E+06	1.4147E-04	1.2148E-04	7.0	5.5729E+05	2.0501E-04	1.7818E-04	1.7818E-04	1.7878E-04	1.7878E-04	
26	5.0297E+06	1.4270E-04	1.2244E-04	7.1	5.3018E+05	2.0537E-04	1.7878E-04	1.7878E-04	1.7842E-04	1.7842E-04	
27	4.7849E+06	1.4394E-04	1.2341E-04	7.2	5.0424E+05	2.0565E-04	1.7842E-04	1.7842E-04	1.7860E-04	1.7860E-04	
28	4.5508E+06	1.4509E-04	1.2431E-04	7.3	4.7966E+05	2.0617E-04	1.7860E-04	1.7860E-04	1.7871E-04	1.7871E-04	
29	4.3294E+06	1.4609E-04	1.2508E-04	7.4	4.5625E+05	2.0658E-04	1.7877E-04	1.7877E-04	1.7885E-04	1.7885E-04	
30	4.1178E+06	1.4698E-04	1.2575E-04	7.5	4.3401E+05	2.0692E-04	1.7885E-04	1.7885E-04	1.7911E-04	1.7911E-04	
31	3.9168E+06	1.4788E-04	1.2644E-04	7.6	4.1285E+05	2.0717E-04	1.7885E-04	1.7885E-04	1.7917E-04	1.7917E-04	
32	3.7267E+06	1.4829E-04	1.2728E-04	7.7	3.9276E+05	2.0742E-04	1.7885E-04	1.7885E-04	1.7933E-04	1.7933E-04	
33	3.5443E+06	1.5013E-04	1.2829E-04	7.8	3.7354E+05	2.0767E-04	1.7933E-04	1.7933E-04	1.7972E-04	1.7972E-04	
34	3.3716E+06	1.5149E-04	1.2944E-04	7.9	3.5540E+05	2.0802E-04	1.7973E-04	1.7973E-04	1.8017E-04	1.8017E-04	
35	3.2068E+06	1.5291E-04	1.3064E-04	8.0	3.3804E+05	2.0837E-04	1.7973E-04	1.7973E-04	1.8061E-04	1.8061E-04	
36	3.0508E+06	1.5437E-04	1.3188E-04	8.1	3.2156E+05	2.0861E-04	1.7973E-04	1.7973E-04	1.8117E-04	1.8117E-04	
37	2.9015E+06	1.5587E-04	1.3320E-04	8.2	3.0586E+05	2.0891E-04	1.7973E-04	1.7973E-04	1.8161E-04	1.8161E-04	
38	2.7601E+06	1.5747E-04	1.3463E-04	8.3	2.9093E+05	2.0927E-04	1.7973E-04	1.7973E-04	1.8204E-04	1.8204E-04	
39	2.6255E+06	1.5919E-04	1.3618E-04	8.4	2.7679E+05	2.0961E-04	1.7973E-04	1.7973E-04	1.8247E-04	1.8247E-04	
40	2.4978E+06	1.6097E-04	1.3779E-04	8.5	2.6324E+05	2.0987E-04	1.7973E-04	1.7973E-04	1.8284E-04	1.8284E-04	
41	2.3759E+06	1.6279E-04	1.3944E-04	8.6	2.5046E+05	2.1013E-04	1.7973E-04	1.7973E-04	1.8321E-04	1.8321E-04	
42	2.2598E+06	1.6462E-04	1.4110E-04	8.7	2.3817E+05	2.1039E-04	1.7973E-04	1.7973E-04	1.8358E-04	1.8358E-04	
43	2.1496E+06	1.6644E-04	1.4277E-04	8.8	2.2656E+05	2.0617E-04	1.7973E-04	1.7973E-04	1.7799E-04	1.7799E-04	
44	2.0452E+06	1.6831E-04	1.4445E-04	8.9	2.1554E+05	2.0617E-04	1.7973E-04	1.7973E-04	1.7794E-04	1.7794E-04	
45	1.9457E+06	1.7019E-04	1.4616E-04	9.0	2.0501E+05	2.0617E-04	1.7973E-04	1.7973E-04	1.7790E-04	1.7790E-04	

\* ENERGY = LOWER BOUNDARY

Table 5.4

In-system neutron spectrum in the graphite assembly  
( $z = 26.7$  cm). (a) Scalar spectrum.

GRAPHITE 60-CM ASSEMBLY		< IN-SYSTEM SPECTRUM >						
J	ENERGY (EV)	PMID	ERR	WIND	J ENERGY (EV)	PMID	ERR	WIND
1	2.020E+05	-3.3415E-07	1.0000E+00	3.1680E+01	4.6	1.9350E+06	3.6495E-05	4.2814E-02
2	2.2100E+05	-3.9720E-07	1.0000E+00	8.0510E+01	4.7	2.0970E+06	3.6394E-05	4.2828E-02
3	2.3230E+05	-4.6794E-07	1.0000E+00	7.9340E+01	4.8	2.2040E+06	3.6173E-05	4.3161E-02
4	2.4420E+05	-5.4516E-07	1.0000E+00	7.8160E+01	4.9	2.3170E+06	3.5820E-05	4.3562E-02
5	2.5680E+05	-6.2568E-07	1.0000E+00	7.7000E+01	5.0	2.4360E+06	3.5132E-05	4.4621E-02
6	2.6990E+05	-7.0350E-07	1.0000E+00	7.5820E+01	5.1	2.5610E+06	3.3767E-05	4.6538E-02
7	2.8380E+05	-7.8147E-07	1.0000E+00	7.4660E+01	5.2	2.6920E+06	3.1559E-05	4.9362E-02
8	2.9830E+05	-8.6474E-07	1.0000E+00	7.3480E+01	5.3	2.8300E+06	2.8892E-05	5.4483E-02
9	3.1360E+05	-8.1788E-07	1.0000E+00	7.2320E+01	5.4	2.9750E+06	2.6663E-05	6.3231E-02
10	3.2970E+05	-7.5823E-07	1.0000E+00	7.1140E+01	5.5	3.1280E+06	2.5752E-05	7.1926E-02
11	3.46660E+05	-6.0920E-07	1.0000E+00	6.9980E+01	5.6	3.2880E+06	2.5982E-05	7.4242E-02
12	3.6440E+05	-3.4176E-07	1.0000E+00	6.8800E+01	5.7	3.4570E+06	2.6103E-05	7.2542E-02
13	3.8300E+05	-7.2575E-08	5.82277E+00	6.7630E+01	5.8	3.6340E+06	2.4861E-05	2.6820E+01
14	4.0270E+05	6.5585E-07	5.7748E-01	6.6690E+01	5.9	3.8210E+06	2.2344E-05	8.2239E-02
15	4.2330E+05	1.4197E-06	2.4349E-01	6.5630E+01	6.0	4.0160E+06	1.9919E-05	2.6060E+01
16	4.4500E+05	2.3591E-06	1.4821E-01	6.4690E+01	6.1	4.2220E+06	1.8977E-05	9.3744E-02
17	4.6780E+05	3.4522E-06	1.1188E-01	6.2835E+01	6.2	4.4390E+06	1.9831E-05	1.0508E-01
18	4.9180E+05	4.6615E-06	9.2632E-02	6.2950E+01	6.3	4.6660E+06	2.1592E-05	1.0371E-01
19	5.1700E+05	5.9500E-06	7.9324E-02	6.2100E+01	6.4	4.9060E+06	2.2847E-05	1.0487E-01
20	5.4360E+05	7.2867E-06	6.8850E-02	6.1200E+01	6.5	5.1570E+06	2.2822E-05	2.2720E+01
21	5.7140E+05	8.6655E-06	6.2500E-02	6.0300E+01	6.6	5.4220E+06	2.2244E-05	2.2180E+01
22	6.0070E+05	1.0105E-05	5.8719E-02	5.9360E+01	6.7	5.7000E+06	2.2284E-05	1.1670E+01
23	6.3150E+05	1.1646E-05	5.5991E-02	5.8436E+01	6.8	5.9920E+06	2.3127E-05	2.3330E+01
24	6.6390E+05	1.3303E-05	5.2763E-02	5.7490E+01	6.9	6.2990E+06	2.4441E-05	1.3060E+01
25	6.9790E+05	1.5069E-05	4.9445E-02	5.6566E+01	7.0	6.6220E+06	2.6375E-05	1.3020E+01
26	7.3370E+05	1.6863E-05	4.7102E-02	5.5620E+01	7.1	6.9610E+06	2.8653E-05	1.2661E-01
27	7.7130E+05	1.8596E-05	4.6141E-02	5.4720E+01	7.2	7.3180E+06	3.0345E-05	1.3306E-01
28	8.1090E+05	2.0410E-05	4.5530E-02	5.3866E+01	7.3	7.6940E+06	3.0721E-05	1.4918E-01
29	8.5250E+05	2.1532E-05	4.7205E-02	5.2990E+01	7.4	8.0880E+06	2.9135E-05	1.6715E-01
30	8.9620E+05	2.2680E-05	4.6718E-02	5.2160E+01	7.5	8.5030E+06	2.7559E-05	1.3277E-01
31	9.4210E+05	2.3640E-05	4.5328E-02	5.1340E+01	7.6	8.9390E+06	3.0131E-05	1.9809E-01
32	9.9040E+05	2.4476E-05	4.4005E-02	5.0470E+01	7.7	9.3970E+06	3.2070E+07	2.2362E-01
33	1.0410E+06	2.5524E-05	4.4211E-02	4.9570E+01	7.8	9.8790E+06	4.0791E-05	1.7963E-01
34	1.0950E+06	2.6078E-05	4.5245E-02	4.8640E+01	7.9	1.0390E+07	1.00666E-04	9.6462E-01
35	1.1510E+06	2.7004E-05	4.5716E-02	4.7590E+01	8.0	1.0920E+07	4.2839E-05	1.9245E-01
36	1.2100E+06	2.8117E-05	4.5084E-02	4.6510E+01	8.1	1.1480E+07	3.0131E-05	1.5070E+01
37	1.2720E+06	2.9412E-05	4.3797E-02	4.5400E+01	8.2	1.2070E+07	5.3800E-05	2.1029E-01
38	1.3370E+06	3.0808E-05	4.3083E-02	4.4210E+01	8.3	1.2680E+07	1.00666E-04	1.4540E+01
39	1.4060E+06	3.2202E-05	4.2910E-02	4.2950E+01	8.4	1.3340E+07	2.3671E-04	1.4120E+01
40	1.4780E+06	3.3445E-05	4.3651E-02	4.1720E+01	8.5	1.4020E+07	4.3656E-04	1.3160E+01
41	1.5530E+06	3.4483E-05	4.3810E-02	4.0570E+01	8.6	1.4740E+07	4.4884E-04	2.9489E-02
42	1.6330E+06	3.5322E-05	4.3358E-02	3.9530E+01	8.7	1.5490E+07	2.3939E-04	1.3160E+01
43	1.7170E+06	3.5923E-05	4.2442E-02	3.8560E+01	8.8	1.6290E+07	1.1800E-04	3.3030E-02
44	1.8050E+06	3.6306E-05	4.1667E-02	3.7690E+01	8.9	1.7120E+07	2.4067E-05	1.5046E-01
45	1.8970E+06	3.6482E-05	4.2283E-02	3.6860E+01	9.0	1.8000E+07	3.7840E-06	1.9222E-01

\* ERR X 100 = %  
\*\* WIND = % [FWHM]  
\*\*\* [CN/CM\*\*2/LETARGY/SOURCE]

Table 5.4 (b) Integral spectrum.

GRAPHITE 60-CM ASSEMBLY -----< RUNNING INTEGRAL >		J ENERGY (EV)	PUP	PLO	J ENERGY (EV)	PUP	PLO
1	1.7556E+07	2.2557E-07	1.5283E-07	4.6	1.8502E+06	1.4988E-04	1.2990E-04
2	1.6697E+07	1.6100E-06	1.1751E-06	4.7	1.7604E+06	1.5177E-04	1.3164E-04
3	1.5888E+07	7.8229E-06	6.7622E-06	4.8	1.6746E+06	1.5365E-04	1.3336E-04
4	1.5108E+07	2.2644E-05	2.0880E-05	4.9	1.5927E+06	1.5549E-04	1.3505E-04
5	1.4376E+07	4.5748E-05	4.2660E-05	5.0	1.5147E+06	1.5729E-04	1.3670E-04
6	1.3674E+07	6.8268E-05	6.3796E-05	5.1	1.4415E+06	1.5903E-04	1.3830E-04
7	1.3011E+07	8.0766E-05	7.4969E-05	5.2	1.3713E+06	1.6071E-04	1.3984E-04
8	1.2367E+07	8.6284E-05	7.9571E-05	5.3	1.3040E+06	1.6232E-04	1.4131E-04
9	1.1772E+07	8.9457E-05	8.1724E-05	5.4	1.2406E+06	1.6385E-04	1.4272E-04
10	1.1197E+07	9.1801E-05	8.3253E-05	5.5	1.1801E+06	1.6532E-04	1.4406E-04
11	1.0650E+07	9.4358E-05	8.4980E-05	5.6	1.1226E+06	1.6674E-04	1.4535E-04
12	1.0133E+07	9.6593E-05	8.6764E-05	5.7	1.0680E+06	1.6810E-04	1.4660E-04
13	9.6351E+06	9.9413E-05	8.8424E-05	5.8	1.0153E+06	1.6942E-04	1.4780E-04
14	9.1650E+06	1.0153E-04	8.9860E-05	5.9	9.6595E+05	1.7069E-04	1.4897E-04
15	8.7183E+06	1.0343E-04	9.1030E-05	6.0	9.1884E+05	1.7193E-04	1.5010E-04
16	8.2931E+06	1.0503E-04	9.2135E-05	6.1	8.7407E+05	1.7312E-04	1.5118E-04
17	7.3383E+06	1.0678E-04	9.3348E-05	6.2	8.3145E+05	1.7424E-04	1.5221E-04
18	7.5040E+06	1.0854E-04	9.4655E-05	6.3	7.9088E+05	1.7530E-04	1.5317E-04
19	7.1373E+06	1.1026E-04	9.5971E-05	6.4	7.5226E+05	1.7627E-04	1.5406E-04
20	6.7891E+06	1.1183E-04	9.7222E-05	6.5	7.1558E+05	1.7716E-04	1.5486E-04
21	6.4585E+06	1.1337E-04	9.8366E-05	6.6	6.3067E+05	1.7795E-04	1.5558E-04
22	6.1435E+06	1.1475E-04	9.9428E-05	6.7	6.1742E+05	1.7865E-04	1.5621E-04
23	5.8441E+06	1.1606E-04	1.0064E-04	6.8	6.1591E+05	1.7926E-04	1.5676E-04
24	5.5593E+06	1.1731E-04	1.0164E-04	6.9	5.2587E+05	1.7980E-04	1.5723E-04
25	5.2381E+06	1.1856E-04	1.0239E-04	7.0	5.5729E+05	1.8026E-04	1.5764E-04
26	5.0297E+06	1.1982E-04	1.0341E-04	7.1	5.3018E+05	1.8065E-04	1.5798E-04
27	4.7849E+06	1.2108E-04	1.0433E-04	7.2	5.0424E+05	1.8097E-04	1.5825E-04
28	4.5508E+06	1.2228E-04	1.0540E-04	7.3	4.7966E+05	1.8122E-04	1.5846E-04
29	4.3294E+06	1.2337E-04	1.0628E-04	7.4	4.5625E+05	1.8141E-04	1.5862E-04
30	4.1178E+06	1.2442E-04	1.0713E-04	7.5	4.3401E+05	1.8155E-04	1.5872E-04
31	3.9168E+06	1.2551E-04	1.0804E-04	7.6	4.1282E+05	1.8164E-04	1.5877E-04
32	3.7267E+06	1.2672E-04	1.0906E-04	7.7	3.9276E+05	1.8169E-04	1.5878E-04
33	3.5443E+06	1.2805E-04	1.1021E-04	7.8	3.7354E+05	1.8171E-04	1.5877E-04
34	3.3716E+06	1.2945E-04	1.1142E-04	7.9	3.5554E+05	1.8171E-04	1.5873E-04
35	3.2068E+06	1.3085E-04	1.1263E-04	8.0	3.3804E+05	1.8171E-04	1.5867E-04
36	3.0508E+06	1.3223E-04	1.1382E-04	8.1	3.2156E+05	1.8171E-04	1.5860E-04
37	2.9015E+06	1.3364E-04	1.1507E-04	8.2	3.0586E+05	1.8171E-04	1.5851E-04
38	2.7601E+06	1.3517E-04	1.1644E-04	8.3	2.9093E+05	1.8171E-04	1.5843E-04
39	2.6255E+06	1.3682E-04	1.1794E-04	8.4	2.7679E+05	1.8171E-04	1.5836E-04
40	2.4978E+06	1.3859E-04	1.1955E-04	8.5	2.6324E+05	1.8171E-04	1.5829E-04
41	2.3759E+06	1.4042E-04	1.2122E-04	8.6	2.5046E+05	1.8171E-04	1.5822E-04
42	2.2598E+06	1.4229E-04	1.2294E-04	8.7	2.3817E+05	1.8171E-04	1.5817E-04
43	2.1466E+06	1.4418E-04	1.2467E-04	8.8	2.2656E+05	1.8171E-04	1.5812E-04
44	2.0452E+06	1.4608E-04	1.2641E-04	8.9	2.1554E+05	1.8171E-04	1.5808E-04
45	1.9457E+06	1.4798E-04	1.2816E-04	9.0	2.0501E+05	1.8171E-04	1.5805E-04

\* ENERGY = LOWER BOUNDARY

Table 5.5 In-system neutron spectrum in the graphite assembly

GRAPHITE 60-CM ASSEMBLY		< IN-SYSTEM SPECTRUM >		J	ENERGY (EV)	PWID	ERR	WIND	J	ENERGY (EV)	PWID	ERR	WIND
1	2.1020E+05	-1.0337E-07	1.0000E+00	3.1680E+01	4.6	1.9950E+06	2.5586E-05	3.8552E-02	3.6000E+01	2.5321E-05	3.8997E-02	3.5140E+01	
2	2.2100E+05	-1.2061E-07	1.0000E+00	3.0510E+01	4.7	2.0970E+06	2.5321E-05	3.8997E-02	3.5140E+01	2.5042E-05	3.9076E-02	3.4310E+01	
3	2.3230E+05	-1.3856E-07	1.0000E+00	7.9340E+01	4.8	2.2040E+06	2.3170E+06	2.4728E-05	3.9395E-02	3.3550E+01	2.4330E+01		
4	2.4420E+05	-1.5605E-07	1.0000E+00	7.8150E+01	4.9	2.3170E+06	2.4360E+06	2.4236E-05	3.9692E-02	3.2800E+01	2.3040E+01		
5	2.5680E+05	-1.7105E-07	1.0000E+00	7.7000E+01	5.0	2.4360E+06	2.4360E+06	2.3387E-05	4.1621E-02	3.2040E+01	2.1250E+01		
6	2.6990E+05	-1.8011E-07	1.0000E+00	7.5820E+01	5.1	2.5610E+06	2.5610E+06	2.2003E-05	4.4444E-02	3.1250E+01	2.0490E+01		
7	2.8380E+05	-1.7872E-07	1.0000E+00	7.4660E+01	5.2	2.6920E+06	2.8300E+06	2.0285E-05	4.8334E-02	3.0490E+01	1.9740E+01		
8	2.9830E+05	-1.5995E-07	1.0000E+00	7.3480E+01	5.3	2.8300E+06	2.9750E+06	1.8678E-05	5.4645E-02	2.9740E+01	1.9740E+01		
9	3.1360E+05	-1.1517E-07	1.0000E+00	7.2320E+01	5.4	2.9750E+06	3.1280E+06	1.7647E-05	6.1349E-02	2.9020E+01	2.9020E+01		
10	3.2970E+05	-3.3157E-08	1.0000E+00	7.1140E+01	5.5	3.1280E+06	3.2380E+06	1.7191E-05	6.5423E-02	2.8300E+01	2.7580E+01		
11	3.4660E+05	9.9082E-03	2.9923E+00	6.9930E+01	5.6	3.2380E+06	3.4570E+06	1.6925E-05	7.8768E-02	2.6820E+01	2.6060E+01		
12	3.6440E+05	2.9572E-07	1.0590E+00	6.8800E+01	5.7	3.4570E+06	1.6535E-05	8.4511E-02	7.1087E-02	2.5270E+01	2.5270E+01		
13	3.8300E+05	5.7068E-07	5.0429E-01	6.7680E+01	5.8	3.6340E+06	1.6127E-05	8.4762E-02	7.1087E-02	2.6060E+01	2.6060E+01		
14	4.0270E+05	9.3525E-07	2.7531E-01	6.6600E+01	5.9	3.8210E+06	1.5961E-05	7.3460E-02	8.9431E-02	2.2180E+01	2.2180E+01		
15	4.2330E+05	1.3961E-06	1.6969E-01	6.5630E+01	6.0	4.0160E+06	1.5961E-05	8.9431E-02	2.4550E+01	2.3940E+01	2.3940E+01		
16	4.4500E+05	1.2392E-06	1.2392E-01	6.4690E+01	6.1	4.2220E+06	1.6105E-05	7.5919E-02	2.4550E+01	2.3940E+01	2.3940E+01		
17	4.6780E+05	2.5987E-06	1.0329E-01	6.3830E+01	6.2	4.4390E+06	1.6434E-05	7.8768E-02	2.3330E+01	2.3330E+01	2.3330E+01		
18	4.9180E+05	3.3198E-06	9.02339E-02	6.2960E+01	6.3	4.6660E+06	1.6815E-05	3.1575E-02	2.2720E+01	2.0560E+01	2.0560E+01		
19	5.1700E+05	4.1044E-06	7.8830E-02	6.2100E+01	6.4	4.9060E+06	1.7052E-05	8.4762E-02	2.0020E+01	1.9035E-01	1.9035E-01		
20	5.4360E+05	4.9330E-06	6.8940E-02	6.1200E+01	6.5	5.1570E+06	1.6854E-05	8.9431E-02	2.2180E+01	1.9480E+01	1.9480E+01		
21	5.7140E+05	5.8195E-06	6.2087E-02	6.0300E+01	6.6	5.4220E+06	1.6264E-05	9.8004E-02	2.1670E+01	1.8970E-01	1.8970E-01		
22	6.0700E+05	6.7667E-06	5.3226E-02	5.9360E+01	6.7	5.7000E+06	1.5827E-05	1.0721E-01	2.1150E+01	1.0920E-01	1.0920E-01		
23	6.3150E+05	7.7911E-06	5.5616E-02	5.8430E+01	6.8	5.9920E+06	1.6079E-05	1.0920E-01	2.0560E+01	1.8040E+01	1.8040E+01		
24	6.6390E+05	8.9011E-06	5.2183E-02	5.7490E+01	6.9	6.2990E+06	1.7066E-05	1.0935E-01	2.0020E+01	1.7620E+01	1.7620E+01		
25	6.9790E+05	1.0075E-05	4.8928E-02	5.6560E+01	7.0	6.6220E+06	1.8435E-05	1.1055E-01	1.9480E+01	1.5822E-01	1.5822E-01		
26	7.3370E+05	1.1248E-05	4.5398E-02	5.5620E+01	7.1	6.9610E+06	1.9522E-05	1.0770E-01	1.8970E+01	1.7739E-01	1.7739E-01		
27	7.7130E+05	1.2458E-05	4.2960E-02	5.4720E+01	7.2	7.3180E+06	2.1490E-05	1.2490E+01	1.776E-01	1.6182E-01	1.6182E-01		
28	8.1090E+05	1.3561E-05	4.5455E-02	5.3860E+01	7.3	7.6940E+06	1.9419E-05	1.3406E-01	1.8040E+01	1.3218E-01	1.3218E-01		
29	8.5250E+05	1.4554E-05	4.6099E-02	5.2990E+01	7.4	8.0880E+06	1.9111E-05	1.4391E-01	1.7620E+01	1.4280E-01	1.4280E-01		
30	8.9620E+05	1.5428E-05	4.5330E-02	5.2160E+01	7.5	8.5030E+06	1.9251E-05	1.5822E-01	1.7220E+01	1.3373E-01	1.3373E-01		
31	9.4210E+05	1.6205E-05	4.3410E-02	5.1340E+01	7.6	8.9390E+06	2.0848E-05	1.7739E-01	1.6780E+01	1.4760E-01	1.4760E-01		
32	9.9040E+05	1.6919E-05	4.1937E-02	5.0470E+01	7.7	9.3970E+06	2.4903E-05	1.6360E+01	1.4540E+01	1.3218E-01	1.3218E-01		
33	1.0410E+06	1.7615E-05	4.1940E-02	4.9570E+01	7.8	9.3790E+06	2.9842E-05	1.0109E-01	1.3200E+01	1.5470E+01	1.5470E+01		
34	1.0950E+06	1.8363E-05	4.2519E-02	4.8640E+01	7.9	1.0390E+07	3.2402E-05	1.4012E-01	5.1553E-02	1.2530E+01	1.5070E+01		
35	1.1510E+06	1.9202E-05	4.2742E-02	4.7590E+01	8.0	1.0920E+07	3.2766E-05	1.5507E-01	2.5698E-02	1.4870E+01	1.4870E+01		
36	1.2100E+06	2.0174E-05	4.3759E-02	4.6510E+01	8.1	1.1480E+07	3.2095E-05	1.3402E-01	2.3460E-02	1.2530E+01	1.4760E+01		
37	1.2720E+06	2.1281E-05	4.0209E-02	4.5400E+01	8.2	1.2070E+07	3.1260E-05	1.6182E-01	2.6468E-02	1.4540E+01	1.6182E-01		
38	1.3370E+06	2.2445E-05	3.8670E-02	4.4210E+01	8.3	1.2680E+07	4.9827E-05	1.0109E-01	1.3690E+01	1.3270E+01	1.3270E+01		
39	1.4060E+06	2.3594E-05	3.8284E-02	4.2950E+01	8.4	1.3340E+07	1.4012E-04	5.1553E-02	1.3200E+01	1.2530E+01	1.2530E+01		
40	1.4780E+06	2.4592E-05	3.8609E-02	4.1720E+01	8.5	1.4020E+07	2.5507E-04	2.5698E-02	1.4870E+01	1.4870E+01	1.4870E+01		
41	1.5530E+06	2.5345E-05	3.8747E-02	4.0570E+01	8.6	1.4740E+07	2.3460E-04	2.8749E-02	1.2530E+01	1.2530E+01	1.2530E+01		
42	1.6330E+06	2.5832E-05	3.8486E-02	3.9530E+01	8.7	1.5490E+07	1.2598E-04	1.4540E+01	2.6468E-02	1.4540E+01	2.6468E-02		
43	1.7170E+06	2.6034E-05	3.7711E-02	3.8560E+01	8.8	1.6290E+07	3.6497E-05	1.0109E-01	8.2120E-02	1.3270E+01	1.3270E+01		
44	1.8050E+06	2.6025E-05	3.7590E-02	3.7690E+01	8.9	1.7120E+07	2.2490E-06	6.4482E-02	1.4070E+01	1.4070E+01	1.4070E+01		
45	1.8970E+06	2.5815E-05	3.8062E-02	3.6860E+01	9.0	1.8000E+07	3.1882E-07	1.0000E+00	1.4870E+01	1.4870E+01	1.4870E+01		

\* ERR X 100 = %

\*\* WIND = % [FWHM]

\*\*\* [N/CM\*\*2/LETARGY/SOURCE]

Table 5.5 (b) Integral spectrum.

GRAPHITE 60-CM ASSEMBLY -----< RUNNING INTEGRAL >		J ENERGY (EV)	P LP	P LD	J ENERGY (EV)	P UP	P LD
1	1.7556E+07	0.0000E+00	-3.1835E-08	4.6	1.8502E+06	8.7831E-05	7.6928E-05
2	1.6697E+07	1.8496E-07	8.0550E-09	4.7	1.7604E+06	8.9180E-05	7.8179E-05
3	1.5388E+07	2.1597E-06	1.0830E-06	4.8	1.6746E+06	9.0531E-05	7.9432E-05
4	1.5108E+07	8.6254E-06	7.8153E-06	4.9	1.5927E+06	9.1872E-05	8.0674E-05
5	1.4376E+07	3.3774E-05	1.9208E-05	5.0	1.5147E+06	9.3188E-05	8.1892E-05
6	1.3674E+07	4.1141E-05	3.1613E-05	5.1	1.4415E+06	9.4466E-05	8.3074E-05
7	1.3011E+07	5.1229E-05	3.8279E-05	5.2	1.3713E+06	9.5690E-05	8.4209E-05
8	1.2367E+07	4.3884E-05	4.0518E-05	5.3	1.3040E+06	9.6856E-05	8.5288E-05
9	1.1772E+07	4.5700E-05	4.1828E-05	5.4	1.2406E+06	9.7963E-05	8.6309E-05
10	1.1197E+07	4.7520E-05	4.3218E-05	5.5	1.1801E+06	9.9014E-05	8.7275E-05
11	1.0650E+07	4.9377E-05	4.4637E-05	5.6	1.1226E+06	1.0001E-04	8.8195E-05
12	1.0133E+07	5.1229E-05	4.6026E-05	5.7	1.0680E+06	1.0097E-04	8.9074E-05
13	9.6351E+06	5.2927E-05	4.7312E-05	5.8	1.0153E+06	1.0189E-04	8.9917E-05
14	9.1650E+06	5.4369E-05	4.8360E-05	5.9	9.6595E+05	1.0277E-04	9.0728E-05
15	8.7183E+06	5.5597E-05	4.9217E-05	6.0	9.1884E+05	1.0362E-04	9.1503E-05
16	8.2931E+06	5.6711E-05	5.0028E-05	6.1	8.7407E+05	1.0442E-04	9.2239E-05
17	7.8383E+06	5.7804E-05	5.0846E-05	6.2	8.3145E+05	1.0518E-04	9.2934E-05
18	7.5040E+06	5.8906E-05	5.1687E-05	6.3	7.9088E+05	1.0589E-04	9.3581E-05
19	7.1373E+06	6.0009E-05	5.2558E-05	6.4	7.5226E+05	1.0654E-04	9.4175E-05
20	6.7391E+06	6.1091E-05	5.3429E-05	6.5	7.1558E+05	1.0713E-04	9.4713E-05
21	6.4585E+06	6.2114E-05	5.4249E-05	6.6	6.2067E+05	1.0766E-04	9.5192E-05
22	6.1435E+06	6.3061E-05	5.5029E-05	6.7	6.4751E+05	1.0813E-04	9.5614E-05
23	5.8441E+06	6.3953E-05	5.5725E-05	6.8	6.1591E+05	1.0854E-04	9.5982E-05
24	5.5593E+06	6.4829E-05	5.6431E-05	6.9	5.3587E+05	1.0890E-04	9.6301E-05
25	5.2881E+06	6.5722E-05	5.7165E-05	7.0	5.5729E+05	1.0921E-04	9.6574E-05
26	5.0297E+06	6.6640E-05	5.7932E-05	7.1	5.3018E+05	1.0947E-04	9.6803E-05
27	4.7849E+06	6.7565E-05	5.8712E-05	7.2	5.0424E+05	1.0969E-04	9.6992E-05
28	4.5508E+06	6.8474E-05	5.9485E-05	7.3	4.7966E+05	1.0988E-04	9.7143E-05
29	4.3294E+06	6.9361E-05	6.0242E-05	7.4	4.5625E+05	1.1002E-04	9.7260E-05
30	4.1178E+06	7.0227E-05	6.0986E-05	7.5	4.3401E+05	1.1013E-04	9.7345E-05
31	3.9168E+06	7.1084E-05	6.1725E-05	7.6	4.1285E+05	1.1021E-04	9.7403E-05
32	3.7227E+06	7.2474E-05	6.2474E-05	7.7	3.9276E+05	1.1027E-04	9.7437E-05
33	3.5443E+06	7.2831E-05	6.3244E-05	7.8	3.7354E+05	1.1031E-04	9.7451E-05
34	3.3716E+06	7.3733E-05	6.4034E-05	7.9	3.5564E+05	1.1034E-04	9.7450E-05
35	3.2068E+06	7.4649E-05	6.4837E-05	8.0	3.3804E+05	1.1036E-04	9.7439E-05
36	3.0508E+06	7.5586E-05	6.5666E-05	8.1	3.2156E+05	1.1036E-04	9.7436E-05
37	2.9015E+06	7.6571E-05	6.6548E-05	8.2	3.0586E+05	1.1036E-04	9.7424E-05
38	2.7601E+06	7.7634E-05	6.7514E-05	8.3	2.9093E+05	1.1036E-04	9.7408E-05
39	2.6255E+06	7.8783E-05	6.8565E-05	8.4	2.7679E+05	1.1036E-04	9.7390E-05
40	2.4978E+06	8.001C1E-05	6.9866E-05	8.5	2.6324E+05	1.1036E-04	9.7372E-05
41	2.3759E+06	8.1261E-05	7.0849E-05	8.6	2.5046E+05	1.1036E-04	9.7355E-05
42	2.2598E+06	8.2546E-05	7.2037E-05	8.7	2.3817E+05	1.1036E-04	9.7339E-05
43	2.1496E+06	8.3847E-05	7.3240E-05	8.8	2.2656E+05	1.1036E-04	9.7326E-05
44	2.0452E+06	8.5163E-05	7.4457E-05	8.9	2.1554E+05	1.1036E-04	9.7314E-05
45	1.9457E+06	8.6491E-05	7.5687E-05	9.0	2.0501E+05	1.1036E-04	9.7303E-05

\* ENERGY = LOWER BOUNDARY

Table 5.6 In-system neutron spectrum in the graphite assembly  
 GRAPHITE 60-CM ASSEMBLY  
 -----< IN-SYSTEM SPECTRUM >-----

J	ENERGY (EV)	PWID	ERR	WIND	J	ENERGY (EV)	PWID	ERR	WIND
1	2.1020E+05	-4.1212E-08	1.00000E+00	8.1680E+01	46	1.9950E+06	1.3804E-05	3.4075E-02	3.6000E+01
2	2.2100E+05	-4.7359E-08	1.00000E+00	3.0510E+01	47	2.0970E+06	1.3643E-05	3.3962E-02	3.5140E+01
3	2.3230E+05	-5.3302E-08	1.00000E+00	7.9340E+01	48	2.2040E+06	1.3457E-05	3.4057E-02	3.4310E+01
4	2.4420E+05	-5.8336E-08	1.00000E+00	7.8160E+01	49	2.3170E+06	1.3198E-05	3.4780E-02	3.3550E+01
5	2.5680E+05	-6.1319E-08	1.00000E+00	7.7000E+01	50	2.4360E+06	1.2811E-05	3.5492E-02	3.2800E+01
6	2.6990E+05	-6.0386E-08	1.00000E+00	7.5820E+01	51	2.5610E+06	1.2190E-05	3.7496E-02	3.2040E+01
7	2.8338E+05	-5.3135E-08	1.00000E+00	7.4660E+01	52	2.6920E+06	1.1315E-05	4.0125E-02	3.1250E+01
8	2.9830E+05	-3.6045E-08	1.00000E+00	7.3480E+01	53	2.8300E+06	1.0287E-05	4.4144E-02	3.0490E+01
9	3.1360E+05	-4.7241E-09	1.00000E+00	7.2320E+01	54	2.9750E+06	9.3473E-06	4.9560E-02	2.9740E+01
10	3.2970E+05	4.6472E-08	3.6620E+00	7.1140E+01	55	3.1280E+06	8.6943E-06	5.5372E-02	2.9020E+01
11	3.4660E+05	1.2388E-07	1.3767E+00	6.9980E+01	56	3.2880E+06	8.2557E-06	5.9392E-02	2.8300E+01
12	3.6440E+05	2.3461E-07	6.9782E-01	6.8800E+01	57	3.4570E+06	8.2222E-06	6.1407E-02	2.7580E+01
13	3.8300E+05	3.8524E-07	3.9053E-01	6.7630E+01	58	3.6340E+06	8.1887E-06	6.2636E-02	2.6820E+01
14	4.0270E+05	5.8116E-07	2.3118E-01	6.6600E+01	59	3.8210E+06	8.2889E-06	6.3175E-02	2.6060E+01
15	4.2330E+05	8.2549E-07	1.5029E-01	6.5630E+01	60	4.0160E+06	8.5766E-06	6.2486E-02	2.5527E+01
16	4.4500E+05	1.1180E-05	1.1353E-01	6.4690E+01	61	4.2220E+06	9.0339E-06	6.5939E-02	2.4550E+01
17	4.6780E+05	1.4553E-06	9.6842E-02	6.3830E+01	62	4.4390E+06	9.5913E-06	6.0473E-02	2.3940E+01
18	4.9180E+05	1.8311E-06	8.5312E-02	6.2950E+01	63	4.6660E+06	1.0109E-05	6.0157E-02	2.3330E+01
19	5.1700E+05	2.2399E-06	7.4830E-02	6.2100E+01	64	4.9060E+06	1.0281E-05	6.2114E-02	2.2720E+01
20	5.4360E+05	2.6791E-06	6.5781E-02	6.1200E+01	65	5.1570E+06	9.8482E-06	6.6564E-02	2.2180E+01
21	5.7140E+05	3.1515E-05	5.9382E-02	6.0300E+01	66	5.4220E+06	9.9934E-06	8.21315E-02	2.1670E+01
22	6.0070E+05	3.66118E-06	5.56000E-02	5.9360E+01	67	5.7000E+06	8.4248E-06	8.4746E-02	2.1100E+01
23	6.3150E+05	4.2217E-06	5.2657E-02	5.8430E+01	68	5.9920E+06	8.4333E-06	8.6785E-02	2.0560E+01
24	6.6390E+05	4.8318E-06	4.9269E-02	5.7490E+01	69	6.2990E+06	9.0205E-06	8.4839E-02	2.0020E+01
25	6.9790E+05	5.4228E-06	4.6269E-02	5.6560E+01	70	6.6220E+06	9.9934E-06	8.21315E-02	1.9480E+01
26	7.3370E+05	6.1545E-05	4.3529E-02	5.5620E+01	71	6.9820E+06	9.0889E-05	1.8970E+01	1.8970E+01
27	7.7130E+05	6.8183E-06	4.2415E-02	5.4720E+01	72	7.3180E+06	1.0954E-05	8.4008E-02	1.8490E+01
28	8.1090E+05	7.4499E-06	4.2238E-02	5.3860E+01	73	7.6940E+06	1.0127E-05	9.9639E-02	1.8040E+01
29	8.5250E+05	8.0289E-06	4.2420E-02	5.2990E+01	74	8.0880E+06	9.5824E-06	1.0918E-01	1.7620E+01
30	8.9620E+05	8.5506E-06	4.1702E-02	5.2160E+01	75	8.5030E+06	1.0598E-05	1.0720E-01	1.7220E+01
31	9.4210E+05	9.0146E-06	3.9699E-02	5.1340E+01	76	8.9390E+06	1.03190E-05	1.0787E-01	1.5070E+01
32	9.9040E+05	9.4347E-06	3.8157E-02	5.0470E+01	77	9.3970E+06	1.5872E-05	8.9182E-02	1.6360E+01
33	1.0410E+06	9.8248E-06	3.7821E-02	4.9570E+01	78	9.8790E+06	1.6885E-05	8.6311E-02	1.5930E+01
34	1.0950E+06	1.0230E-05	3.8205E-02	4.8640E+01	79	1.0390E+07	1.5886E-05	9.9807E-02	1.5470E+01
35	1.1510E+06	1.0671E-05	3.8149E-02	4.7590E+01	80	1.0920E+07	1.3592E-05	1.0787E-01	1.5070E+01
36	1.2100E+06	1.1184E-05	3.7378E-02	4.6510E+01	81	1.1480E+07	1.2043E-05	1.1534E-01	1.4760E+01
37	1.2720E+06	1.1761E-05	3.5948E-02	4.5400E+01	82	1.2070E+07	1.5459E-05	1.0253E-01	1.4540E+01
38	1.3370E+06	1.2355E-05	3.4727E-02	4.4210E+01	83	1.2680E+07	2.6064E-05	6.0698E-02	1.4100E+01
39	1.4060E+06	1.2910E-05	3.4237E-02	4.2950E+01	84	1.3340E+07	4.9078E-05	4.1389E-02	1.3890E+01
40	1.4780E+06	1.3355E-05	3.4422E-02	4.1720E+01	85	1.4020E+07	7.6212E-05	2.9518E-02	1.3810E+01
41	1.5530E+06	1.3665E-05	3.4611E-02	4.0570E+01	86	1.4740E+07	6.7020E-05	2.7728E-02	1.3810E+01
42	1.6330E+06	1.3864E-05	3.4137E-02	3.9530E+01	87	1.5490E+07	3.2332E-05	2.9652E-02	1.2810E+01
43	1.7170E+06	1.3958E-05	3.3635E-02	3.8560E+01	88	1.6290E+07	9.3165E-06	9.5906E-02	1.4140E+01
44	1.8050E+06	1.3967E-05	3.3432E-02	3.7690E+01	89	1.7120E+07	1.0759E-06	5.4135E-01	1.4360E+01
45	1.8970E+06	1.3912E-05	3.3713E-02	3.6860E+01	90	1.8000E+07	4.5034E-08	3.0079E+00	1.4580E+01

\* ERR X 100 = %

\*\* WIND = % [FWHM]

\*\*\* [N/CM]\*2/LETHARGY/SOURCE]

Table 5.6 (b) Integral spectrum.

GRAPHITE 60-CM ASSEMBLY >		RUNNING INTEGRAL >		PLP		PLD		J ENERGY (eV)		J ENERGY (eV)		PUP		PLC	
J	ENERGY (eV)	J	ENERGY (eV)	J	ENERGY (eV)	J	ENERGY (eV)	J	ENERGY (eV)	J	ENERGY (eV)	J	ENERGY (eV)	J	ENERGY (eV)
1	1.7556E+07	9.0246E-09	-4.5212E-09	4.6	1.8502E+06	3.6208E-05	3.2219E-05								
2	1.6697E+07	9.1942E-08	-2.0152E-08	4.7	1.7604E+06	3.6930E-05	3.2894E-05								
3	1.5888E+07	6.0244E-07	4.4150E-07	4.8	1.6746E+06	3.7652E-05	3.3568E-05								
4	1.5108E+07	2.2670E-06	2.0100E-06	4.9	1.5927E+06	3.8368E-05	3.4238E-05								
5	1.4376E+07	5.7109E-06	5.2680E-06	5.0	1.5147E+06	3.9075E-05	3.4897E-05								
6	1.3674E+07	9.6340E-06	8.9662E-06	5.1	1.4415E+06	3.9766E-05	3.5542E-05								
7	1.3011E+07	1.2189E-05	1.1319E-05	5.2	1.3713E+06	4.0434E-05	3.6166E-05								
8	1.2367E+07	1.3572E-05	1.2543E-05	5.3	1.3040E+06	4.1073E-05	3.6762E-05								
9	1.1772E+07	1.4424E-05	1.3236E-05	5.4	1.2406E+06	4.1682E-05	3.7329E-05								
10	1.1197E+07	1.5096E-05	1.3769E-05	5.5	1.1801E+06	4.2262E-05	3.7867E-05								
11	1.0650E+07	1.5848E-05	1.4375E-05	5.6	1.1226E+06	4.2816E-05	3.8380E-05								
12	1.0133E+07	1.6722E-05	1.5090E-05	5.7	1.0680E+06	4.3347E-05	3.8872E-05								
13	9.6351E+06	1.7639E-05	1.5862E-05	5.8	1.0153E+06	4.3857E-05	3.9345E-05								
14	9.1650E+06	1.8504E-05	1.6585E-05	5.9	9.6595E+05	4.4347E-05	3.9799E-05								
15	8.7183E+06	1.9230E-05	1.7177E-05	6.0	9.1884E+05	4.4815E-05	4.0232E-05								
16	8.2931E+06	1.9817E-05	1.7650E-05	6.1	8.7407E+05	4.5261E-05	4.0641E-05								
17	7.8883E+06	2.0348E-05	1.8077E-05	6.2	8.3145E+05	4.5679E-05	4.1026E-05								
18	7.5040E+06	2.0905E-05	1.8532E-05	6.3	7.9088E+05	4.6067E-05	4.1383E-05								
19	7.1373E+06	2.1499E-05	1.9034E-05	6.4	7.5226E+05	4.6423E-05	4.1709E-05								
20	6.7891E+06	2.2086E-05	1.9537E-05	6.5	7.1558E+05	4.6744E-05	4.2003E-05								
21	6.4585E+06	2.2626E-05	1.9995E-05	6.6	6.8067E+05	4.7031E-05	4.2265E-05								
22	6.1435E+06	2.3116E-05	2.0478E-05	6.7	6.4751E+05	4.7518E-05	4.2494E-05								
23	5.8441E+06	2.3574E-05	2.0793E-05	6.8	6.1591E+05	4.7506E-05	4.2694E-05								
24	5.5593E+06	2.4031E-05	2.1179E-05	6.9	5.2581E+05	4.7700E-05	4.2867E-05								
25	5.2881E+06	2.4516E-05	2.1596E-05	7.0	5.5729E+05	4.7867E-05	4.3016E-05								
26	5.0297E+06	2.5041E-05	2.2055E-05	7.1	5.3018E+05	4.8009E-05	4.3141E-05								
27	4.7849E+06	2.5587E-05	2.2467E-05	7.2	5.0425E+05	4.8130E-05	4.3244E-05								
28	4.5508E+06	2.6123E-05	2.3012E-05	7.3	4.7966E+05	4.8229E-05	4.3328E-05								
29	4.3294E+06	2.6631E-05	2.3463E-05	7.4	4.5625E+05	4.8309E-05	4.3394E-05								
30	4.1178E+06	2.7111E-05	2.3887E-05	7.5	4.3401E+05	4.8371E-05	4.3443E-05								
31	3.9168E+06	2.7566E-05	2.4289E-05	7.6	4.1285E+05	4.8419E-05	4.3478E-05								
32	3.7267E+06	2.8007E-05	2.4677E-05	7.7	3.9276E+05	4.8454E-05	4.3501E-05								
33	3.5443E+06	2.8442E-05	2.5061E-05	7.8	3.7354E+05	4.8481E-05	4.3512E-05								
34	3.3716E+06	2.8878E-05	2.5447E-05	7.9	3.5540E+05	4.8501E-05	4.3516E-05								
35	3.2068E+06	2.9321E-05	2.5840E-05	8.0	3.3804E+05	4.8516E-05	4.3514E-05								
36	3.0508E+06	2.9780E-05	2.6251E-05	8.1	3.2156E+05	4.8527E-05	4.3507E-05								
37	2.9015E+06	3.0270E-05	2.6695E-05	8.2	3.0586E+05	4.8552E-05	4.3507E-05								
38	2.7601E+06	3.0807E-05	2.7186E-05	8.3	2.9093E+05	4.8582E-05	4.3503E-05								
39	2.6255E+06	3.1396E-05	2.7730E-05	8.4	2.7679E+05	4.8652E-05	4.3498E-05								
40	2.4978E+06	3.2028E-05	2.8316E-05	8.5	2.6324E+05	4.8752E-05	4.3492E-05								
41	2.3759E+06	3.2691E-05	2.8934E-05	8.6	2.5046E+05	4.8827E-05	4.3486E-05								
42	2.2598E+06	3.3374E-05	2.9571E-05	8.7	2.3817E+05	4.8852E-05	4.3480E-05								
43	2.1496E+06	3.4070E-05	3.0221E-05	8.8	2.2656E+05	4.8882E-05	4.3475E-05								
44	2.0452E+06	3.4776E-05	3.0880E-05	8.9	2.1554E+05	4.8922E-05	4.3470E-05								
45	1.9457E+06	3.5489E-05	3.1547E-05	9.0	2.0501E+05	4.8952E-05	4.3466E-05								

\* ENERGY = LOWER BOUNDARY

Table 5.7 In-system neutron spectrum in the graphite assembly  
 $(z = 52.0 \text{ cm})$ . (a) Scalar spectrum.

GRAPHITE 60-CM ASSEMBLY		< IN-SYSTEM SPECTRUM >		ERR		WIND		ERR		WIND	
J	ENERGY (EV)	PMID	ERR	J	ENERGY (EV)	PMID	ERR	J	ENERGY (EV)	PMID	ERR
1	2.1020E+05	-2.970C-09	1.0000E+00	8.1680E+01	4.6	1.9950E+06	6.36449E-06	3.1405E-02	3.6000E+01	3.5140E+01	3.5140E+01
2	2.2100E+05	-2.5768E-09	1.0000E+00	8.0510E+01	4.7	2.0970E+06	6.7847E-06	3.1642E-02	3.2015E-02	3.4310E+01	3.4310E+01
3	2.3230E+05	-1.5836E-09	1.0000E+00	7.2340E+01	4.8	2.2040E+06	6.6564E-06	3.2015E-02	3.3550E+01	3.4310E+01	3.4310E+01
4	2.4420E+05	3.5715E-10	1.0000E+00	7.2878E+02	4.9	4.4706E-06	6.4706E-06	3.2296E-02	3.3121E-02	3.2800E+01	3.2800E+01
5	2.5680E+05	3.7766E-09	1.4149E+01	7.7000E+01	5.0	2.4360E+06	6.2150E-06	3.3121E-02	3.3121E-02	3.2800E+01	3.2800E+01
6	2.6960E+05	9.4298E-09	6.4884E+00	7.2820E+01	5.1	2.5610E+06	5.8327E-06	3.5019E-02	3.2040E+01	3.2040E+01	3.2040E+01
7	2.8380E+05	1.8262E-08	3.7727E+00	7.4660E+01	5.2	2.6920E+06	5.4618E-06	3.7245E-02	3.1250E+01	3.1250E+01	3.1250E+01
8	2.9830E+05	3.1643E-08	2.3995E+00	7.3480E+01	5.3	2.8300E+06	4.9829E-06	4.1071E-02	3.0490E+01	3.0490E+01	3.0490E+01
9	3.1360E+05	5.1293E-08	5.2320E+00	7.2320E+01	5.4	5.092E+06	4.5383E-06	2.9740E+01	2.9740E+01	2.9740E+01	2.9740E+01
10	3.2970E+05	7.9400E-08	1.0682E+00	7.1140E+01	5.5	3.1280E+06	4.1265E-06	5.1121E-02	2.9020E+01	2.9020E+01	2.9020E+01
11	3.4660E+05	1.1246E-07	7.1742E-01	6.9980E+01	5.6	3.2380E+06	3.8800E-06	5.5567E-02	2.3300E+01	2.3300E+01	2.3300E+01
12	3.6444E+05	1.7138E-07	4.7616E-01	6.8300E+01	5.7	3.4570E+06	3.7755E-06	5.8552E-02	2.1580E+01	2.1580E+01	2.1580E+01
13	3.8330E+05	2.4109E-07	3.1096E-01	6.7680E+01	5.8	3.6340E+06	3.7990E-06	6.0159E-02	2.5820E+01	2.5820E+01	2.5820E+01
14	4.0270E+05	3.3034E-07	2.3025E-01	6.6600E+01	5.9	3.8210E+06	3.9448E-06	5.9657E-02	2.6060E+01	2.6060E+01	2.6060E+01
15	4.2330E+05	4.4144E-07	1.4001E-01	6.5630E+01	6.0	4.0160E+06	3.9448E-06	2.5270E+01	2.5270E+01	2.5270E+01	2.5270E+01
16	4.4500E+05	5.7566E-07	1.0973E-01	6.4690E+01	6.1	4.2220E+06	4.4445E-06	5.6036E-02	2.4550E+01	2.4550E+01	2.4550E+01
17	4.6780E+05	7.3351E-07	9.5450E-02	6.3830E+01	6.2	4.4390E+06	4.7073E-06	5.6092E-02	2.3940E+01	2.3940E+01	2.3940E+01
18	4.9180E+05	9.1388E-07	8.5265E-02	6.2960E+01	6.3	4.6660E+06	4.9619E-06	5.4401E-02	2.3350E+01	2.3350E+01	2.3350E+01
19	5.1770E+05	1.1161E-06	7.4897E-02	6.2100E+01	6.4	4.9060E+06	5.1418E-06	5.4655E-02	2.2720E+01	2.2720E+01	2.2720E+01
20	5.4360E+05	1.3592E-06	6.5303E-02	6.1200E+01	6.5	5.1705E+06	5.1321E-06	5.9097E-02	2.2180E+01	2.2180E+01	2.2180E+01
21	5.7140E+05	1.5813E-06	5.3409E-02	6.0300E+01	6.6	5.4220E+06	4.9351E-06	5.9097E-02	2.1670E+01	2.1670E+01	2.1670E+01
22	6.0070E+05	1.8459E-06	5.4469E-02	5.9360E+01	6.7	5.7000E+06	4.66334E-06	6.5250E-02	2.1100E+01	2.1100E+01	2.1100E+01
23	6.3150E+05	2.1314E-06	5.1517E-02	5.8430E+01	6.8	5.9920E+06	4.4276E-06	6.9716E-02	2.0560E+01	2.0560E+01	2.0560E+01
24	6.6390E+05	2.4394E-06	4.8209E-02	5.7490E+01	6.9	6.2990E+06	4.3352E-06	7.1662E-02	2.0020E+01	2.0020E+01	2.0020E+01
25	6.9790E+05	4.923E-06	4.4923E-02	5.6560E+01	7.0	6.6220E+06	4.6579E-06	7.1272E-02	1.9480E+01	1.9480E+01	1.9480E+01
26	7.3370E+05	3.1012E-06	4.2291E-02	5.5620E+01	7.1	6.9610E+06	5.0089E-06	6.8220E+06	1.8970E+01	1.8970E+01	1.8970E+01
27	7.7130E+05	3.4368E-06	4.1211E-02	5.4720E+01	7.2	7.3180E+06	5.0285E-06	7.2957E-02	1.8490E+01	1.8490E+01	1.8490E+01
28	8.1060E+05	3.7608E-06	4.0995E-02	5.3860E+01	7.3	7.6940E+06	4.7112E-06	8.4660E-02	1.8040E+01	1.8040E+01	1.8040E+01
29	8.5250E+05	4.0599E-06	4.1119E-02	5.2990E+01	7.4	8.0880E+06	4.5102E-06	9.1359E-02	1.7620E+01	1.7620E+01	1.7620E+01
30	8.9620E+05	4.215E-06	5.2160E-02	5.1605E+01	7.5	8.5030E+06	4.9730E-06	8.7802E-02	1.7220E+01	1.7220E+01	1.7220E+01
31	9.4210E+05	4.5638E-06	5.3242E-02	5.1340E-01	7.6	8.9390E+06	6.2622E-06	8.0720E-02	1.6780E+01	1.6780E+01	1.6780E+01
32	9.9040E+05	4.7785E-06	5.3376E-02	5.0470E+01	7.7	9.3970E+06	7.4551E-06	7.0285E-02	1.6360E+01	1.6360E+01	1.6360E+01
33	1.0410E+06	4.9861E-06	5.6132E-02	4.9570E+01	7.8	9.8790E+06	7.4764E-06	7.2149E-02	1.5930E+01	1.5930E+01	1.5930E+01
34	1.0950E+06	5.2102E-06	5.6202E-02	4.8640E+01	7.9	1.0390E+07	6.6144E-06	8.7173E-02	1.5470E+01	1.5470E+01	1.5470E+01
35	1.1510E+06	5.4606E-06	5.6136E-02	4.7590E+01	8.0	1.0920E+07	5.2473E-06	1.0044E-01	1.5070E+01	1.5070E+01	1.5070E+01
36	1.2100E+06	5.742E-06	5.5097E-02	4.6510E+01	8.1	1.1480E+07	4.4494E-06	1.043E-01	1.4760E+01	1.4760E+01	1.4760E+01
37	1.2720E+06	6.0431E-06	5.3692E-02	4.5400E+01	8.2	1.2070E+07	6.4316E-06	8.7527E-02	1.4540E+01	1.4540E+01	1.4540E+01
38	1.3370E+06	6.3323E-06	5.2424E-02	4.4210E+01	8.3	1.2680E+07	1.1598E-05	4.6460E-02	1.4130E+01	1.4130E+01	1.4130E+01
39	1.4060E+06	6.5860E-06	5.2090E-02	4.2950E+01	8.4	1.3340E+07	2.0716E-05	3.4220E-02	1.3583E+01	1.3583E+01	1.3583E+01
40	1.4780E+06	6.77732E-06	5.2270E-02	4.1720E+01	8.5	1.4020E+07	2.7317E-05	2.7523E-02	1.3580E+01	1.3580E+01	1.3580E+01
41	1.5530E+06	6.8871E-06	5.2246E-02	4.0570E+01	8.6	1.4470E+07	1.4470E-05	2.5360E-02	1.3580E+01	1.3580E+01	1.3580E+01
42	1.6330E+06	6.9443E-06	5.2098E-02	3.9530E+01	8.7	1.5490E+07	7.9933E-06	3.6687E-02	1.3580E+01	1.3580E+01	1.3580E+01
43	1.7170E+06	6.9588E-06	5.1275E-02	3.8560E+01	8.8	1.6290E+07	2.8157E-06	9.1524E-02	1.3870E+01	1.3870E+01	1.3870E+01
44	1.8050E+06	6.9443E-06	5.1045E-02	3.7690E+01	8.9	1.7120E+07	5.1496E-07	2.9227E-01	1.4400E+01	1.4400E+01	1.4400E+01
45	1.8970E+06	6.9115E-06	5.1222E-02	3.6860E+01	9.0	1.8615E+07	2.8615E-08	1.0444E+00	1.4930E+01	1.4930E+01	1.4930E+01

\* ERR X 100 = %

\*\* WIND = % [FWHM]

\*\*\* [N/CM\*2/LETARGY/SOURCE]

Table 5.7 (b) Integral spectrum.

GRAPHITE 60-CM ASSEMBLY -----< RUNNING INTEGRAL >		J ENERGY (EV)	PUP	PL0	J ENERGY (EV)	PUP	PLC
1	1.7556E+07	2.9250E-09	-6.3525E-11	4.6	1.2502E+06	1.5278E-05	1.3754E-05
2	1.6697E+07	3.6198E-08	1.8159E-08	4.7	1.7604E+06	1.4090E-05	1.4090E-05
3	1.5388E+07	1.8987E-07	1.4606E-07	4.8	1.6746E+06	1.5995E-05	1.4427E-05
4	1.5108E+07	6.0420E-07	5.3106E-07	4.9	1.5927E+06	1.6354E-05	1.4763E-05
5	1.4376E+07	1.5920E-06	1.4700E-06	5.0	1.5147E+06	1.6709E-05	1.5097E-05
6	1.3674E+07	2.9955E-06	2.7983E-06	5.1	1.4415E+06	1.7059E-05	1.5424E-05
7	1.3011E+07	4.0668E-06	3.7986E-06	5.2	1.3713E+06	1.7398E-05	1.5743E-05
8	1.2367E+07	4.6736E-06	4.3515E-06	5.3	1.3040E+06	1.7725E-05	1.6050E-05
9	1.1772E+07	5.0233E-06	4.6450E-06	5.4	1.2406E+06	1.8033E-05	1.6341E-05
10	1.1197E+07	5.2702E-06	4.8431E-06	5.5	1.1801E+06	1.2335E-05	1.6619E-05
11	1.0650E+07	5.5589E-06	5.0791E-06	5.6	1.1225E+06	1.8618E-05	1.6882E-05
12	1.0133E+07	6.9184E-06	5.3810E-06	5.7	1.0680E+06	1.8888E-05	1.7133E-05
13	9.6351E+06	6.3192E-06	5.7279E-06	5.8	1.0153E+06	1.9146E-05	1.7373E-05
14	9.1650E+06	6.7183E-06	6.0743E-06	5.9	9.6595E+05	1.9394E-05	1.7603E-05
15	8.1183E+06	7.0567E-06	6.3621E-06	6.0	9.1884E-05	1.9631E-05	1.7823E-05
16	8.2931E+06	7.3272E-06	6.5889E-06	6.1	8.7407E-05	1.9856E-05	1.8030E-05
17	7.8883E+06	7.5733E-06	6.7938E-06	6.2	8.3145E+05	2.0067E-05	1.8225E-05
18	7.5040E+06	7.8283E-06	7.0935E-06	6.3	7.9088E+05	2.0263E-05	1.8405E-05
19	7.1373E+06	8.0986E-06	7.2425E-06	6.4	7.5226E+05	2.0442E-05	1.8570E-05
20	6.7891E+06	8.3661E-06	7.4759E-06	6.5	7.1558E+05	2.0603E-05	1.8719E-05
21	6.4585E+06	8.6156E-06	7.6922E-06	6.6	6.8067E+05	2.0748E-05	1.8851E-05
22	6.1435E+06	8.8506E-06	7.8957E-06	6.7	6.4751E+05	2.0876E-05	1.8967E-05
23	5.8344E+06	9.0874E-06	8.1017E-06	6.8	6.1591E+05	2.0988E-05	1.9068E-05
24	5.5593E+06	9.3353E-06	8.3196E-06	6.9	5.9587E+05	2.1085E-05	1.9155E-05
25	5.2881E+06	9.5971E-06	8.5518E-06	7.0	5.5729E+05	2.1169E-05	1.9230E-05
26	5.0297E+06	9.8680E-06	8.7941E-06	7.1	5.3018E+05	2.1240E-05	1.9292E-05
27	4.7849E+06	1.0139E-05	9.0372E-06	7.2	5.0424E+05	2.1300E-05	1.9344E-05
28	4.5508E+06	1.0401E-05	9.2718E-06	7.3	4.7966E+05	2.1350E-05	1.9386E-05
29	4.3294E+06	1.0649E-05	9.4942E-06	7.4	4.5625E+05	2.1390E-05	1.9419E-05
30	4.1173E+06	1.0884E-05	9.7039E-06	7.5	4.3401E+05	2.1422E-05	1.9444E-05
31	3.9168E+06	1.1105E-05	9.9009E-06	7.6	4.1285E+05	2.1447E-05	1.9463E-05
32	3.7267E+06	1.1314E-05	1.0086E-05	7.7	3.9276E+05	2.1467E-05	1.9477E-05
33	3.5443E+06	1.1515E-05	1.0265E-05	7.8	3.7354E+05	2.1483E-05	1.9485E-05
34	3.3716E+06	1.1720E-05	1.0443E-05	7.9	3.5540E+05	2.1495E-05	1.9491E-05
35	3.2068E+06	1.1920E-05	1.0626E-05	8.0	3.3804E+05	2.1505E-05	1.9491E-05
36	3.0508E+06	1.2137E-05	1.0822E-05	8.1	3.2156E+05	2.1514E-05	1.9491E-05
37	2.9015E+06	1.2372E-05	1.1037E-05	8.2	3.0586E+05	2.1520E-05	1.9489E-05
38	2.7601E+06	1.2632E-05	1.1276E-05	8.3	2.9093E+05	2.1526E-05	1.9487E-05
39	2.6255E+06	1.2915E-05	1.1539E-05	8.4	2.7679E+05	2.1530E-05	1.9485E-05
40	2.4978E+06	1.3219E-05	1.1822E-05	8.5	2.6324E+05	2.1533E-05	1.9482E-05
41	2.3759E+06	1.3511E-05	1.2123E-05	8.6	2.5046E+05	2.1536E-05	1.9479E-05
42	2.2598E+06	1.3874E-05	1.2436E-05	8.7	2.3817E+05	2.1539E-05	1.9477E-05
43	2.1496E+06	1.4218E-05	1.2758E-05	8.8	2.2656E+05	2.1539E-05	1.9477E-05
44	2.0452E+06	1.4568E-05	1.3087E-05	8.9	2.1554E+05	2.1539E-05	1.9477E-05
45	1.9457E+06	1.4922E-05	1.3419E-05	9.0	2.0501E+05	2.1539E-05	1.9476E-05

\* ENERGY = LOWER BOUNDARY

Table 5.8 In-system neutron spectrum in the graphite assembly  
( $z = 62.1$  cm). (a) Scalar spectrum.

GRAPHITE 50-CM ASSEMBLY		< IN-SYSTEM SPECTRUM >									
J	ENERGY (eV)	PWID		ERR	WIND	J	ENERGY (eV)	PWID	ERR	WIND	
1	2.1020E+05	5.7378E-10	2.3624E+01	3.1630E+01	4.6	1.9950E+06	3.2243E-06	3.1045E-02	3.5970E-02	3.1045E-02	3.5970E-01
2	2.2100E+05	1.2055E-09	1.3419E+01	3.0510E+01	4.7	2.0970E+06	3.1681E-06	3.1979E-02	3.5140E+01	3.1979E-02	3.5140E+01
3	2.3230E+05	2.2146E-09	8.6562E+00	7.5340E+01	4.8	2.2040E+06	3.0984E-06	3.1434E-02	3.4310E+01	3.1434E-02	3.4310E+01
4	2.4420E+05	3.7477E-09	5.1789E-09	7.8160E+01	4.9	2.3170E+06	3.034E-06	3.1960E-02	3.3550E+01	3.1960E-02	3.3550E+01
5	2.5680E+05	6.1789E-09	4.2344E+00	7.7000E+01	5.0	2.4360E+06	2.8683E-06	3.2800E+01	3.2800E+01	3.2800E+01	3.2800E+01
6	2.6990E+05	9.7496E-09	3.0729E+00	7.5820E+01	5.1	2.5610E+06	2.6937E-06	3.4573E-02	3.2040E+01	3.4573E-02	3.2040E+01
7	2.8380E+05	1.4992E-08	2.2503E+00	7.4660E+01	5.2	2.6920E+06	2.4808E-06	3.7962E-02	3.1250E+01	3.7962E-02	3.1250E+01
8	2.9830E+05	2.2514E-08	1.6506E+00	7.3480E+01	5.3	2.8300E+06	2.2538E-06	4.1790E-02	3.0490E+01	4.1790E-02	3.0490E+01
9	3.1360E+05	3.5170E-08	1.2320E+00	7.2320E+01	5.4	2.9750E+06	2.0524E-06	4.5840E-02	2.9740E+01	4.5840E-02	2.9740E+01
10	3.2970E+05	4.7882E-08	8.6694E-01	7.1140E+01	5.5	3.1230E+06	1.9143E-06	4.9868E-02	2.9020E+01	4.9868E-02	2.9020E+01
11	3.4660E+05	6.7835E-08	6.1279E-01	6.9930E+01	5.6	3.2880E+06	1.8466E-06	5.3196E-02	2.3300E+01	5.3196E-02	2.3300E+01
12	3.6440E+05	9.4402E-08	4.289E-01	6.8800E+01	5.7	3.4570E+06	1.8335E-06	5.5546E-02	2.7580E+01	5.5546E-02	2.7580E+01
13	3.8300E+05	1.2879E-07	2.8487E-01	6.7680E+01	5.8	3.6340E+06	1.8615E-06	5.6614E-02	2.6820E+01	5.6614E-02	2.6820E+01
14	4.0270E+05	1.7222E-07	1.9066E-01	6.6600E+01	5.9	3.8210E+06	1.9339E-06	5.5935E-02	2.6060E+01	5.5935E-02	2.6060E+01
15	4.2330E+05	2.2581E-07	1.3401E-01	6.5630E+01	6.0	4.0160E+06	2.0379E-06	5.4245E-02	2.5270E+01	5.4245E-02	2.5270E+01
16	4.4500E+05	2.8999E-07	1.0673E-01	6.4690E+01	6.1	4.2220E+06	2.1390E-06	5.3425E-02	2.4550E+01	5.3425E-02	2.4550E+01
17	4.6780E+05	3.6495E-07	9.3934E-02	6.3830E+01	6.2	4.4390E+06	2.2195E-06	5.3581E-02	2.3940E+01	5.3581E-02	2.3940E+01
18	4.9180E+05	4.5044E-07	8.4586E-02	6.2960E+01	6.3	4.6660E+06	2.3061E-06	5.3367E-02	2.3330E+01	5.3367E-02	2.3330E+01
19	5.1700E+05	5.4959E-07	7.4978E-02	6.2100E+01	6.4	4.9080E+06	2.4139E-06	5.2858E-02	2.2720E+01	5.2858E-02	2.2720E+01
20	5.4360E+05	6.5135E-07	6.5935E-02	6.1200E+01	6.5	5.1570E+06	2.4925E-06	5.2000E-02	2.2180E+01	5.2000E-02	2.2180E+01
21	5.7140E+05	7.6646E-07	5.9025E-02	6.0300E+01	6.6	5.4220E+06	2.4878E-06	5.3170E-02	2.1670E+01	5.3170E-02	2.1670E+01
22	6.0070E+05	8.9176E-07	5.4884E-02	5.9360E+01	6.7	5.7000E+06	2.4053E-06	5.6834E-02	2.1100E+01	5.6834E-02	2.1100E+01
23	6.3150E+05	1.0294E-06	5.2007E-02	5.8430E+01	6.8	5.9920E+06	2.3122E-06	5.9287E-02	2.0560E+01	5.9287E-02	2.0560E+01
24	6.6390E+05	1.1763E-06	4.3584E-02	5.7490E+01	6.9	6.2990E+06	2.3055E-06	5.9489E-02	2.0020E+01	5.9489E-02	2.0020E+01
25	6.9790E+05	1.3335E-06	4.5135E-02	5.6560E+01	7.0	6.6220E+06	2.4313E-06	5.8676E-02	1.9480E+01	5.8676E-02	1.9480E+01
26	7.3370E+05	1.4975E-06	4.2851E-02	5.5620E+01	7.1	6.9160E+06	2.5602E-06	5.6821E-02	1.8900E+01	5.6821E-02	1.8900E+01
27	7.7130E+05	1.6630E-06	4.1418E-02	5.4720E+01	7.2	7.3180E+06	2.5026E-06	6.1584E-02	1.8490E+01	6.1584E-02	1.8490E+01
28	8.1090E+05	1.8224E-06	4.1130E-02	5.3860E+01	7.3	7.6940E+06	2.3053E-06	7.0825E-02	1.8040E+01	7.0825E-02	1.8040E+01
29	8.5250E+05	1.9759E-06	4.1112E-02	5.2990E+01	7.4	8.0880E+06	2.2141E-06	7.5164E-02	1.7620E+01	7.5164E-02	1.7620E+01
30	8.9620E+05	2.1155E-06	4.5351E-02	5.2160E+01	7.5	8.5030E+06	2.3392E-06	7.3067E-02	1.7220E+01	7.3067E-02	1.7220E+01
31	9.4210E+05	2.4333E-06	3.7696E-02	5.1340E+01	7.6	8.9390E+06	2.8503E-06	7.8861E-02	1.6780E+01	7.8861E-02	1.6780E+01
32	9.9040E+05	2.3652E-06	3.5852E-02	5.0470E+01	7.7	9.3970E+06	2.3148E-06	6.1464E-02	1.6350E+01	6.1464E-02	1.6350E+01
33	1.0410E+06	2.4899E-06	2.5027E-02	4.9570E+01	7.8	9.8790E+06	2.2410E-06	6.4122E-02	1.5930E+01	6.4122E-02	1.5930E+01
34	1.0950E+06	2.6302E-06	3.4677E-02	4.8640E+01	7.9	1.0390E+07	2.6334E-06	7.2819E-02	1.5470E+01	7.2819E-02	1.5470E+01
35	1.1510E+06	2.1172E-02	4.3378E-02	4.7590E+01	8.0	1.0920E+07	2.1137E-06	7.2985E-02	1.5070E+01	7.2985E-02	1.5070E+01
36	1.2100E+06	2.9687E-06	3.3021E-02	4.6490E+01	8.1	1.1480E+07	2.0239E-07	7.0226E-02	1.4760E+01	7.0226E-02	1.4760E+01
37	1.2720E+06	3.1531E-06	3.1383E-02	4.5250E+01	8.2	1.2070E+07	2.5296E-06	8.0167E-02	1.4510E+01	8.0167E-02	1.4510E+01
38	1.3370E+06	3.3197E-06	3.0333E-02	4.3990E+01	8.3	1.2680E+07	4.4780E-07	8.6142E-02	1.3960E+01	8.6142E-02	1.3960E+01
39	1.4060E+06	3.4458E-06	2.9677E-02	4.2730E+01	8.4	1.3340E+07	8.3421E-06	9.2923E-02	1.3940E+01	9.2923E-02	1.3940E+01
40	1.4780E+06	3.5147E-06	2.9810E-02	4.1510E+01	8.5	1.4020E+07	1.0434E-05	1.0434E-02	1.3940E+01	1.0434E-02	1.3940E+01
41	1.5530E+06	3.5229E-06	3.032E-02	4.0340E+01	8.6	1.4740E+07	1.4740E+00	1.4740E+00	1.3940E+01	1.4740E+00	1.3940E+01
42	1.6330E+06	3.4871E-06	2.9963E-02	3.9390E+01	8.7	1.5490E+07	2.4357E-06	5.3279E-02	1.3940E+01	5.3279E-02	1.3940E+01
43	1.7170E+06	3.4229E-06	3.0009E-02	3.8490E+01	8.8	1.6290E+07	3.9076E-07	5.0762E-02	1.4400E+01	5.0762E-02	1.4400E+01
44	1.8050E+06	3.3501E-06	3.0253E-02	3.7630E+01	8.9	1.7120E+07	-7.1698E-08	1.0000E+00	1.4400E+01	1.0000E+00	1.4400E+01
45	1.8970E+06	3.2816E-06	3.0335E-02	3.6800E+01	9.0	1.8000E+07	-3.5648E-08	1.0000E+00	1.4400E+01	1.0000E+00	1.4400E+01

\* ERR  $\times 100 = \%$ 

\*\* WIND = % [FWHM]

\*\*\* [N/CM<sup>2</sup>STERE/HOUR/SOURCE]

Table 5.8 (b) Integral spectrum.

GRAPHITE 60-CM ASSEMBLY -----< RUNNING INTEGRAL >-----		J ENERGY (EV)	PLP	PLD	J ENERGY (EV)	PLP	PLD	PUP	PLC
1	1.7556E+07	0.0000E+00	-3.6648E-09	4.0	1.8502E+06	6.6586E-06	6.9152E-06		
2	1.6697E+07	0.0000E+00	-1.0835E-08	4.7	1.7604E+06	6.8311E-06	6.1777E-06		
3	1.5388E+07	2.5548E-08	2.6931E-09	4.3	1.6746E+06	7.0075E-06	6.3438E-06		
4	1.5108E+07	1.5382E-07	1.1791E-07	4.9	1.5927E+06	7.1870E-06	6.5129E-06		
5	1.4376E+07	5.1750E-07	4.5657E-07	5.0	1.5147E+06	7.3685E-06	6.6838E-06		
6	1.3674E+07	1.0532E-06	9.6423E-07	5.1	1.4415E+06	7.5494E-06	6.8543E-06		
7	1.3011E+07	1.4825E-06	1.3691E-06	5.2	1.3713E+06	7.7268E-06	7.0215E-06		
8	1.2367E+07	1.7168E-06	1.5827E-06	5.3	1.3040E+06	7.8978E-06	7.1822E-06		
9	1.1772E+07	2.8534E-06	1.6991E-06	5.4	1.2406E+06	8.0604E-06	7.3352E-06		
10	1.1197E+07	1.9637E-06	1.7911E-06	5.5	1.1801E+06	8.2138E-06	7.4787E-06		
11	1.0650E+07	2.0792E-06	1.8870E-06	5.6	1.1226E+06	8.3580E-06	7.6134E-06		
12	1.0133E+07	2.2218E-06	2.0077E-06	5.7	1.0680E+06	8.4941E-06	7.7403E-06		
13	9.6351E+06	2.3943E-06	2.1594E-06	5.8	1.0153E+06	8.6230E-06	7.8604E-06		
14	9.1650E+06	2.5702E-06	2.1349E-06	5.9	9.6595E+05	8.7455E-06	7.9745E-06		
15	8.7182E+06	2.7225E-06	2.4476E-06	6.0	9.1884E+05	8.8619E-06	8.0824E-06		
16	8.2931E+06	2.8507E-06	2.5584E-06	6.1	8.7407E+05	8.9719E-06	8.1339E-06		
17	7.8823E+06	2.9697E-06	2.6608E-06	6.2	8.3145E+05	9.0748E-06	8.2866E-06		
18	7.5040E+06	3.0932E-06	2.7679E-06	6.3	7.9088E+05	9.1697E-06	8.3661E-06		
19	7.1373E+06	3.2260E-06	2.8832E-06	6.4	7.5226E+05	9.2563E-06	8.4458E-06		
20	6.7391E+06	3.3613E-06	3.0060E-06	6.5	7.1558E+05	9.3344E-06	8.5175E-06		
21	6.4585E+06	3.4900E-06	3.1203E-06	6.6	6.8067E+05	9.4041E-06	8.5311E-06		
22	6.1435E+06	3.6121E-06	3.2239E-06	6.7	6.4751E+05	9.4658E-06	8.6371E-06		
23	5.8441E+06	3.7346E-06	3.3376E-06	6.8	6.1591E+05	9.5119E-06	8.6858E-06		
24	5.5593E+06	3.8617E-06	3.4511E-06	6.9	5.2587E+05	9.5669E-06	8.7280E-06		
25	5.2881E+06	3.9613E-06	3.5688E-06	7.0	5.5729E+05	9.6075E-06	8.7640E-06		
26	5.0297E+06	4.1238E-06	3.6870E-06	7.1	5.3018E+05	9.6422E-06	8.7944E-06		
27	4.7849E+06	4.2508E-06	3.8013E-06	7.2	5.0424E+05	9.6715E-06	8.8197E-06		
28	4.5508E+06	4.3723E-06	3.9105E-06	7.3	4.7966E+05	9.6960E-06	8.8403E-06		
29	4.3294E+06	4.4892E-06	4.01155E-06	7.4	4.5625E+05	9.7159E-06	8.8569E-06		
30	4.1178E+06	4.6019E-06	4.1167E-06	7.5	4.3401E+05	9.7320E-06	8.8698E-06		
31	3.9168E+06	4.7093E-06	4.2131E-06	7.6	4.1285E+05	9.7448E-06	8.8796E-06		
32	3.7267E+06	4.8114E-06	4.3044E-06	7.7	3.9227E+05	9.7550E-06	8.8866E-06		
33	3.5443E+06	4.9098E-06	4.3922E-06	7.8	3.7354E+05	9.7633E-06	8.8912E-06		
34	3.3716E+06	5.00655E-06	4.4738E-06	7.9	3.5540E+05	9.7700E-06	8.8939E-06		
35	3.2068E+06	5.1178E-06	4.5662E-06	8.0	3.3804E+05	9.7755E-06	8.8952E-06		
36	3.0508E+06	5.2043E-06	4.6571E-06	8.1	3.2156E+05	9.7800E-06	8.8955E-06		
37	2.9015E+06	5.3116E-06	4.7550E-06	8.2	3.0586E+05	9.7836E-06	8.8952E-06		
38	2.7601E+06	5.4290E-06	4.3630E-06	8.3	2.9093E+05	9.7866E-06	8.8944E-06		
39	2.6255E+06	5.5577E-06	4.9823E-06	8.4	2.7679E+05	9.7890E-06	8.8935E-06		
40	2.4978E+06	5.6971E-06	5.1124E-06	8.5	2.6324E+05	9.7910E-06	8.8925E-06		
41	2.3759E+06	5.8452E-06	5.2511E-06	8.6	2.5046E+05	9.7926E-06	8.8915E-06		
42	2.2598E+06	6.0002E-06	5.3965E-06	8.7	2.3817E+05	9.7940E-06	8.8906E-06		
43	2.1496E+06	6.1599E-06	5.5465E-06	8.8	2.2656E+05	9.7950E-06	8.8897E-06		
44	2.0452E+06	6.3233E-06	5.7000E-06	8.9	2.1554E+05	9.7959E-06	8.8890E-06		
45	1.9457E+06	6.4895E-06	5.8562E-06	9.0	2.0501E+05	9.7966E-06	8.8883E-06		

\* ENERGY = LOWER BOUNDARY

Table 5.9 In-system neutron spectrum in the graphite assembly  
( $z = 72.1$  cm). (a) Scalar spectrum.

GRAPHITE 60-CM ASSEMBLY		< IN-SYSTEM SPECTRUM >			
J	ENERGY(EV)	FMID	ERR	WIND	ERR
1	2.1020E+05	-4.2544E-11	1.00000E+00	8.1630E+01	4.6
2	2.2100E+05	1.6810E-10	4.28889E+01	3.0510E+01	4.7
3	2.3230E+05	5.3063E-10	1.6100E+01	7.9340E+01	4.8
4	2.4420E+05	1.1226E-09	8.9371E+00	7.8160E+01	4.9
5	2.5680E+05	2.0613E-09	5.6556E+00	7.7000E+01	5.0
6	2.6990E+05	3.5027E-09	3.8123E+00	7.5820E+01	5.1
7	2.8380E+05	5.6555E-09	2.6535E+00	7.4660E+01	5.2
8	2.9330E+05	8.7973E-09	1.3824E+00	7.3480E+01	5.3
9	3.1360E+05	1.3309E-08	1.3364E+00	7.2320E+01	5.4
10	3.2970E+05	1.9619E-08	9.4287E-01	7.1140E+01	5.5
11	3.4660E+05	2.8271E-08	6.5567E-01	6.9930E+01	5.6
12	3.6440E+05	3.9859E-08	4.4652E-01	6.8800E+01	5.7
13	3.8300E+05	5.4985E-08	2.9292E-01	6.7630E+01	5.8
14	4.0270E+05	7.4277E-08	1.9715E-01	6.6600E+01	5.9
15	4.2330E+05	9.8186E-08	1.3744E-01	6.5630E+01	6.0
16	4.4500E+05	1.2704E-07	1.0276E-01	6.4690E+01	6.1
17	4.6780E+05	1.6097E-07	9.5081E-02	6.3830E+01	6.2
18	4.9180E+05	1.9950E-07	8.5089E-02	6.2960E+01	6.3
19	5.1700E+05	2.4353E-07	7.4644E-02	6.2100E+01	6.4
20	5.4360E+05	2.9198E-07	6.5010E-02	6.1200E+01	6.5
21	5.7140E+05	3.4478E-07	5.3607E-02	6.0300E+01	6.6
22	6.0700E+05	4.0241E-07	5.4449E-02	5.9360E+01	6.7
23	6.3150E+05	4.6462E-07	4.0772E-02	5.2430E+01	6.8
24	6.6390E+05	5.3174E-07	4.7042E-02	5.2990E+01	6.9
25	6.9790E+05	6.0256E-07	4.4822E-02	5.6560E+01	7.0
26	7.3370E+05	6.7640E-07	4.2220E-02	5.5620E+01	7.1
27	7.7130E+05	7.5051E-07	4.0914E-02	5.4720E+01	7.2
28	8.1090E+05	8.2279E-07	4.0772E-02	5.3860E+01	7.3
29	8.5250E+05	8.9199E-07	4.0834E-02	5.2990E+01	7.4
30	8.9620E+05	9.5477E-07	3.9666E-02	5.2160E+01	7.5
31	9.4210E+05	1.0131E-06	3.7435E-02	5.1340E+01	7.6
32	9.9040E+05	1.0681E-06	3.5265E-02	5.0470E+01	7.7
33	1.0410E+06	1.12339E-06	3.4611E-02	4.9570E+01	7.8
34	1.0950E+06	1.1860E-06	3.4497E-02	4.8640E+01	7.9
35	1.1510E+06	1.2567E-06	3.4019E-02	4.7590E+01	8.0
36	1.2100E+06	1.3370E-06	3.2609E-02	4.6420E+01	8.1
37	1.2720E+06	1.4202E-06	3.1076E-02	4.5100E+01	8.2
38	1.3370E+06	1.4958E-06	2.9821E-02	4.3780E+01	8.3
39	1.4060E+06	1.5529E-06	2.9400E-02	4.2490E+01	8.4
40	1.4780E+06	1.5822E-06	2.9711E-02	4.1250E+01	8.5
41	1.5530E+06	1.5830E-06	2.9893E-02	4.0110E+01	8.6
42	1.6330E+06	1.5632E-06	2.9740E-02	3.9190E+01	8.7
43	1.7170E+06	1.5314E-06	2.9925E-02	3.8360E+01	8.8
44	1.8050E+06	1.4950E-06	3.0075E-02	3.7520E+01	8.9
45	1.8970E+06	1.4615E-06	3.0600E-02	3.6710E+01	9.0

\* ERR X 100 = %

\*\* WIND = % [FWHM]

\*\*\* [N/CM\*2/LET/HARG/SOURCE]

Table 5.9 (b) Integral spectrum.

GRAPHITE 60-CM ASSEMBLY -----< RUNNING INTEGRAL >-----		J ENERGY (EV)	PUP	PLG	J ENERGY (EV)	PUP	PLC
1	1.7556E+07	0.0000E+00	-1.0332E-09	4.6	1.8502E+06	2.8742E-06	2.6090E-06
2	1.6697E+07	0.0000E+00	-3.2020E-09	4.7	1.7604E+06	2.9512E-06	2.6815E-06
3	1.5388E+07	5.2280E-09	-1.6553E-09	4.8	1.6746E+06	2.7558E-06	2.7558E-06
4	1.5108E+07	3.8408E-08	2.6733E-08	4.9	1.5927E+06	3.1106E-06	2.8316E-06
5	1.4376E+07	1.5981E-07	1.3990E-07	5.0	1.5147E+06	3.1921E-06	2.9084E-06
6	1.3674E+07	3.6121E-07	3.3108E-07	5.1	1.4415E+06	3.2736E-06	2.9852E-06
7	1.3011E+07	5.3392E-07	4.9403E-07	5.2	1.3713E+06	3.3535E-06	3.0605E-06
8	1.2367E+07	6.3449E-07	5.86779E-07	5.3	1.3040E+06	3.4305E-06	3.1331E-06
9	1.1772E+07	6.9258E-07	6.3715E-07	5.4	1.2406E+06	3.5037E-06	3.2019E-06
10	1.1197E+07	7.4020E-07	6.7769E-07	5.5	1.1801E+06	3.5728E-06	3.2666E-06
11	1.0650E+07	7.9672E-07	7.2634E-07	5.6	1.1226E+06	3.6377E-06	3.3273E-06
12	1.0133E+07	8.6641E-07	7.8714E-07	5.7	1.0680E+06	3.6991E-06	3.3845E-06
13	9.6351E+06	9.4367E-07	8.5598E-07	5.8	1.0153E+06	3.7572E-06	3.4388E-06
14	9.1650E+06	1.0185E-06	9.2254E-07	5.9	9.6590E+05	3.8125E-06	3.4903E-06
15	8.7183E+06	1.0829E-06	9.7818E-07	6.0	9.1884E+05	3.8651E-06	3.5391E-06
16	8.2931E+06	1.1372E-06	1.0260E-06	6.1	8.7407E+05	3.9147E-06	3.5849E-06
17	7.8883E+06	1.1894E-06	1.0713E-06	6.2	8.3145E+05	3.9611E-06	3.6277E-06
18	7.5040E+06	1.2478E-06	1.1229E-06	6.3	7.9088E+05	4.0039E-06	3.6671E-06
19	7.1373E+06	1.3139E-06	1.1825E-06	6.4	7.5226E+05	4.0430E-06	3.7031E-06
20	6.7891E+06	1.3812E-06	1.2435E-06	6.5	7.1529E+05	4.0782E-06	3.7355E-06
21	6.4585E+06	1.4435E-06	1.2996E-06	6.6	6.8097E+05	4.1097E-06	3.7643E-06
22	6.1435E+06	1.5007E-06	1.3508E-06	6.7	6.4751E+05	4.1375E-06	3.7896E-06
23	5.8441E+06	1.5559E-06	1.4000E-06	6.8	6.1591E+05	4.1620E-06	3.8116E-06
24	5.5594E+06	1.6114E-06	1.4496E-06	6.9	5.8581E+05	4.1832E-06	3.8307E-06
25	5.2884E+06	1.6684E-06	1.5007E-06	7.0	5.5729E+05	4.2014E-06	3.8469E-06
26	5.0294E+06	1.7264E-06	1.5531E-06	7.1	5.3018E+05	4.2170E-06	3.8605E-06
27	4.7849E+06	1.7846E-06	1.6056E-06	7.2	5.0424E+05	4.2301E-06	3.8718E-06
28	4.5508E+06	1.8418E-06	1.6573E-06	7.3	4.7966E+05	4.2409E-06	3.8809E-06
29	4.3297E+06	1.8973E-06	1.7076E-06	7.4	4.5625E+05	4.2497E-06	3.8882E-06
30	4.1178E+06	1.9503E-06	1.7532E-06	7.5	4.3401E+05	4.2568E-06	3.8939E-06
31	3.9168E+06	1.9999E-06	1.8002E-06	7.6	4.1283E+05	4.2624E-06	3.8981E-06
32	3.7267E+06	2.0458E-06	1.8413E-06	7.7	3.9276E+05	4.2668E-06	3.9011E-06
33	3.5443E+06	2.0889E-06	1.8879E-06	7.8	3.7354E+05	4.2704E-06	3.9030E-06
34	3.3716E+06	2.1308E-06	1.9171E-06	7.9	3.5540E+05	4.2733E-06	3.9041E-06
35	3.2068E+06	2.1732E-06	1.9551E-06	8.0	3.3804E+05	4.2756E-06	3.9046E-06
36	3.0508E+06	2.2180E-06	1.9957E-06	8.1	3.2156E+05	4.2775E-06	3.9047E-06
37	2.9015E+06	2.2669E-06	2.0404E-06	8.2	3.0586E+05	4.2791E-06	3.9045E-06
38	2.7601E+06	2.3211E-06	2.0904E-06	8.3	2.9093E+05	4.2803E-06	3.9041E-06
39	2.6255E+06	2.3805E-06	2.1456E-06	8.4	2.7679E+05	4.2814E-06	3.9036E-06
40	2.4978E+06	2.4444E-06	2.2054E-06	8.5	2.6324E+05	4.2822E-06	3.9031E-06
41	2.3759E+06	2.5117E-06	2.2684E-06	8.6	2.5046E+05	4.2829E-06	3.9026E-06
42	2.2598E+06	2.5813E-06	2.3337E-06	8.7	2.3817E+05	4.2834E-06	3.9022E-06
43	2.1496E+06	2.6525E-06	2.4006E-06	8.8	2.2656E+05	4.2839E-06	3.9018E-06
44	2.0452E+06	2.7251E-06	2.4687E-06	8.9	2.1554E+05	4.2843E-06	3.9014E-06
45	1.9457E+06	2.79989E-06	2.5382E-06	9.0	2.0501E+05	4.2843E-06	3.9014E-06

\* ENERGY = LOWER BOUNDARY

Table 5.10 In-system neutron spectrum in the graphite assembly  
( $z = 77.2$  cm). (a) Scalar spectrum.

GRAPHITE 60-CM ASSEMBLY -----< IN-SYSTEM SPECTRUM >-----									
J	ENERGY (eV)	PWID	ERR	WIND	J	ENERGY (eV)	PWID	ERR	WIND
1	2.1020E+05	-5.7200E-10	1.0000E+00	8.1630E+01	4.6	1.9950E+06	8.4558E-07	3.0928E-02	3.6000E+01
2	2.2100E+05	-5.7457E-10	1.0000E+00	8.0510E+01	4.7	2.0970E+06	8.3458E-07	3.1412E-02	3.5140E+01
3	2.3230E+05	-5.1570E-10	1.0000E+00	7.9340E+01	4.8	2.2040E+06	8.1885E-07	3.1689E-02	3.4310E+01
4	2.4420E+05	-3.5478E-10	1.0000E+00	7.8160E+01	4.9	2.3170E+06	7.2444E-07	3.2212E-02	3.3550E+01
5	2.5680E+05	-3.1169E-11	1.0000E+00	7.7000E+01	5.0	2.4360E+06	7.6047E-07	3.3437E-02	3.2800E+01
6	2.6990E+05	5.4055E-10	1.0055E+01	7.5820E+01	5.1	2.5610E+06	7.1464E-07	3.5233E-02	3.2040E+01
7	2.8380E+05	1.4812E-09	5.7721E+00	7.4560E+01	5.2	2.6920E+06	6.5871E-07	3.8690E-02	3.1250E+01
8	2.9830E+05	2.9487E-09	3.1945E+00	7.3480E+01	5.3	2.8300E+06	5.9754E-07	4.2835E-02	3.0490E+01
9	3.1360E+05	5.1541E-09	1.9614E+00	7.2320E+01	5.4	2.9750E+06	5.4078E-07	4.7276E-02	2.9740E+01
10	3.2970E+05	8.3609E-09	1.2572E+00	7.1140E+01	5.5	3.1280E+06	4.9815E-07	5.2054E-02	2.9020E+01
11	3.4660E+05	1.2886E-08	8.1171E-01	6.9980E+01	5.6	3.2880E+06	4.7495E-07	5.6214E-02	2.8300E+01
12	3.6440E+05	1.9085E-08	5.930E+00	6.9300E+01	5.7	3.4570E+06	4.7570E-07	5.8605E-02	2.7580E+01
13	3.8300E+05	2.7329E-08	3.3968E-01	6.7680E+01	5.8	3.6340E+06	4.9582E-07	5.8803E-02	2.6820E+01
14	4.0270E+05	3.7988E-08	2.4899E-01	6.6600E+01	5.9	3.8210E+06	5.3580E-07	5.6695E-02	2.6060E+01
15	4.2330E+05	5.1359E-08	1.4946E-01	6.5630E+01	6.0	4.0160E+06	5.7938E-07	5.3845E-02	2.5270E+01
16	4.4500E+05	6.7645E-08	1.1626E-01	6.4690E+01	6.1	4.2220E+06	6.1329E-07	5.2473E-02	2.4550E+01
17	4.6780E+05	8.6942E-08	1.0053E-01	6.3830E+01	6.2	4.4390E+06	6.3810E-07	5.2267E-02	2.3940E+01
18	4.9180E+05	1.0920E-07	3.8722E-02	6.2960E+01	6.3	4.6660E+06	6.6393E-07	5.2120E-02	2.3330E+01
19	5.1700E+05	1.3431E-07	7.7471E-02	6.2100E+01	6.4	4.9060E+06	6.9010E-07	5.2032E-02	2.2720E+01
20	5.4360E+05	1.6211E-07	6.7155E-02	6.1200E+01	6.5	5.1570E+06	7.0386E-07	5.1845E-02	2.2180E+01
21	5.7140E+05	1.9253E-07	5.9798E-02	6.0300E+01	6.6	5.4220E+06	7.0515E-07	5.2543E-02	2.1670E+01
22	6.0700E+05	2.2566E-07	4.1704E-02	5.9360E+01	6.7	5.7000E+06	7.0755E-07	5.3877E-02	2.1100E+01
23	6.3150E+05	2.6137E-07	5.2199E-02	5.8430E+01	6.8	5.9920E+06	7.1777E-07	5.3399E-02	2.0560E+01
24	6.6390E+05	2.9961E-07	4.8951E-02	5.7490E+01	6.9	6.2990E+06	7.3773E-07	5.1715E-02	2.0020E+01
25	6.9790E+05	3.3968E-07	4.5387E-02	5.6560E+01	7.0	6.6220E+06	7.7402E-07	5.0467E-02	1.9480E+01
26	7.3370E+05	3.8081E-07	4.3031E-02	5.5620E+01	7.1	6.9610E+06	8.0611E-07	4.8737E-02	1.8970E+01
27	7.7130E+05	4.2203E-07	4.1704E-02	5.4720E+01	7.2	7.3180E+06	7.8662E-07	5.2394E-02	1.8490E+01
28	8.1090E+05	4.6210E-07	4.1534E-02	5.3860E+01	7.3	7.6940E+06	7.1442E-07	5.969E-02	1.8040E+01
29	8.5250E+05	5.0009E-07	4.1589E-02	5.2990E+01	7.4	8.0880E+06	6.6058E-07	6.4943E-02	1.7620E+01
30	8.9620E+05	5.3561E-07	4.0617E-02	5.2160E+01	7.5	8.5030E+06	6.9313E-07	6.3728E-02	1.7220E+01
31	9.4210E+05	5.6899E-07	3.8183E-02	5.1340E+01	7.6	8.9390E+06	8.0407E-07	6.1125E-02	1.6780E+01
32	9.9040E+05	6.0142E-07	3.6178E-02	5.0470E+01	7.7	9.3970E+06	8.9688E-07	5.6080E-02	1.6360E+01
33	1.0410E+06	6.3456E-07	3.5464E-02	4.9570E+01	7.8	9.8790E+06	9.8790E+06	5.6814E-02	1.5930E+01
34	1.0950E+06	6.7153E-07	3.5424E-02	4.8640E+01	7.9	1.0390E+07	7.4443E-07	7.3353E-02	1.5470E+01
35	1.1510E+06	7.1318E-07	3.4672E-02	4.7590E+01	8.0	1.0920E+07	5.9127E-07	8.0475E-02	1.5070E+01
36	1.2100E+06	7.5945E-07	3.3456E-02	4.6510E+01	8.1	1.1480E+07	5.2614E-07	8.7924E-02	1.4760E+01
37	1.2720E+06	8.0684E-07	3.1766E-02	4.5370E+01	8.2	1.2070E+07	6.6820E-07	7.3887E-02	1.3440E+01
38	1.3370E+06	8.5019E-07	3.0349E-02	4.4180E+01	8.3	1.2680E+07	1.2503E-07	4.0374E-02	1.2090E+01
39	1.4060E+06	8.8313E-07	2.9952E-02	4.2920E+01	8.4	1.3340E+07	2.3335E-07	1.5470E-02	1.1820E+01
40	1.4780E+06	9.0163E-07	3.0243E-02	4.1700E+01	8.5	1.4020E+07	2.6405E-07	1.8390E-02	1.1820E+01
41	1.5530E+06	9.0440E-07	3.0429E-02	4.0550E+01	8.6	1.4740E+07	1.0438E-06	3.4282E-02	1.1820E+01
42	1.6330E+06	8.9629E-07	3.0517E-02	3.9530E+01	8.7	1.5490E+07	1.5261E-07	1.6028E-01	1.2920E+01
43	1.7170E+06	8.8238E-07	3.0231E-02	3.8560E+01	8.8	1.6290E+07	1.0782E-07	1.5679E-01	1.4150E+01
44	1.8050E+06	8.6779E-07	3.0548E-02	3.7690E+01	8.9	1.7120E+07	1.6443E-07	4.8647E-01	1.4400E+01
45	1.8970E+06	8.5514E-07	3.0695E-02	3.6860E+01	9.0	1.8000E+07	1.1380E-09	1.0000E+00	1.4650E+01

\* ERR X 100 = %

\*\* WIND = % [FWHM]

\*\*\* CN/CM \* 2 / LETHARGY/SOURCE]

Table 5.10 (b) Integral spectrum.

GRAPHITE 60-CM ASSEMBLY  
-----< RUNNING INTEGRAL >-----

J	ENERGY(EV)	PLP	PLJ	J	ENERGY(EV)	PUP	PLD
1	1.7556E+07	0.0000E+00	-1.1380E-10	4.6	1.8502E+06	1.7663E-06	1.6080E-06
2	1.6697E+07	1.2210E-09	3.0801E-10	4.7	1.7604E+06	1.6501E-06	1.6501E-06
3	1.5888E+07	7.4572E-09	4.3538E-09	4.8	1.6746E+06	1.8565E-06	1.6929E-06
4	1.5108E+07	1.6311E-02	1.1261E-08	4.9	1.5927E+06	1.9027E-06	1.7363E-06
5	1.4376E+07	7.0290E-08	6.1662E-08	5.0	1.5147E+06	1.9493E-06	1.7802E-06
6	1.3614E+07	2.0505E-07	1.9155E-07	5.1	1.4415E+06	1.9957E-06	1.8239E-06
7	1.3011E+07	3.2405E-07	3.0590E-07	5.2	1.3713E+06	2.0412E-06	1.8667E-06
8	1.2367E+07	3.8909E-07	3.6589E-07	5.3	1.3040E+06	2.0850E-06	1.9080E-06
9	1.1772E+07	4.2467E-07	3.9633E-07	5.4	1.2406E+06	2.1266E-06	1.9470E-06
10	1.1197E+07	4.5359E-07	4.0822E-07	5.5	1.1801E+06	2.1658E-06	1.9837E-06
11	1.0650E+07	4.8554E-07	4.4801E-07	5.6	1.1226E+06	2.2027E-06	2.0181E-06
12	1.0133E+07	5.2549E-07	4.3250E-07	5.7	1.0683E+06	2.2375E-06	2.0505E-06
13	9.6351E+06	5.7172E-07	5.2362E-07	5.8	1.0153E+06	2.2704E-06	2.0811E-06
14	9.1650E+06	6.1898E-07	5.6585E-07	5.9	9.6595E+05	2.3015E-06	2.1101E-06
15	8.7183E+06	6.6164E-07	6.0360E-07	6.0	9.1884E+05	2.3311E-06	2.1375E-06
16	8.2931E+06	6.9850E-07	6.3604E-07	6.1	8.7407E+05	2.3589E-06	2.1632E-06
17	7.8883E+06	7.3368E-07	6.6693E-07	6.2	8.3145E+05	2.3850E-06	2.1871E-06
18	7.5040E+06	7.7154E-07	7.0051E-07	6.3	7.9088E+05	2.4010E-06	2.2093E-06
19	7.1375E+06	8.1293E-07	7.3778E-07	6.4	7.5226E+05	2.4310E-06	2.2295E-06
20	6.7891E+06	8.5520E-07	7.7612E-07	6.5	7.1558E+05	2.4509E-06	2.2477E-06
21	6.4585E+06	8.9585E-07	8.1287E-07	6.6	6.8067E+05	2.4686E-06	2.2639E-06
22	6.1435E+06	9.3466E-07	8.4785E-07	6.7	6.4751E+05	2.4843E-06	2.2782E-06
23	5.8441E+06	9.7245E-07	8.8182E-07	6.8	6.1591E+05	2.4981E-06	2.2906E-06
24	5.5593E+06	1.0097E-06	9.1529E-07	6.9	5.8587E+05	2.5100E-06	2.3102E-06
25	5.2881E+06	1.0468E-06	9.4870E-07	7.0	5.5729E+05	2.5202E-06	2.3103E-06
26	5.0297E+06	1.0839E-06	9.8207E-07	7.1	5.3018E+05	2.5288E-06	2.3178E-06
27	4.7849E+06	1.1202E-06	1.0148E-06	7.2	5.0424E+05	2.5361E-06	2.3240E-06
28	4.5508E+06	1.1551E-06	1.0462E-06	7.3	4.7966E+05	2.5420E-06	2.3290E-06
29	4.3294E+06	1.1887E-06	1.0765E-06	7.4	4.5625E+05	2.5468E-06	2.3329E-06
30	4.1178E+06	1.2209E-06	1.1055E-06	7.5	4.3401E+05	2.5506E-06	2.3359E-06
31	3.9168E+06	1.2515E-06	1.1329E-06	7.6	4.1285E+05	2.5535E-06	2.3381E-06
32	3.7267E+06	1.2798E-06	1.15832E-06	7.7	3.9276E+05	2.5559E-06	2.3396E-06
33	3.5443E+06	1.3060E-06	1.1815E-06	7.8	3.7354E+05	2.5577E-06	2.3405E-06
34	3.3716E+06	1.3311E-06	1.2039E-06	7.9	3.5540E+05	2.5591E-06	2.3409E-06
35	3.2068E+06	1.3562E-06	1.2263E-06	8.0	3.3804E+05	2.5603E-06	2.3411E-06
36	3.0508E+06	1.3824E-06	1.2499E-06	8.1	3.2156E+05	2.5613E-06	2.3409E-06
37	2.9015E+06	1.4107E-06	1.2756E-06	8.2	3.0586E+05	2.5620E-06	2.3407E-06
38	2.7601E+06	1.4419E-06	1.3042E-06	8.3	2.9093E+05	2.5626E-06	2.3404E-06
39	2.6255E+06	1.4761E-06	1.3359E-06	8.4	2.7679E+05	2.5631E-06	2.3400E-06
40	2.4978E+06	1.5131E-06	1.3704E-06	8.5	2.6324E+05	2.5635E-06	2.3397E-06
41	2.3759E+06	1.5524E-06	1.4071E-06	8.6	2.5046E+05	2.5635E-06	2.3397E-06
42	2.2598E+06	1.5934E-06	1.4456E-06	8.7	2.3817E+05	2.5635E-06	2.3396E-06
43	2.1496E+06	1.6356E-06	1.4852E-06	8.8	2.2656E+05	2.5635E-06	2.3396E-06
44	2.0452E+06	1.6786E-06	1.5256E-06	8.9	2.1554E+05	2.5635E-06	2.3395E-06
45	1.9457E+06	1.7222E-06	1.5666E-06	9.0	2.0501E+05	2.5635E-06	2.3395E-06

\* ENERGY = LOWER BOUNDARY

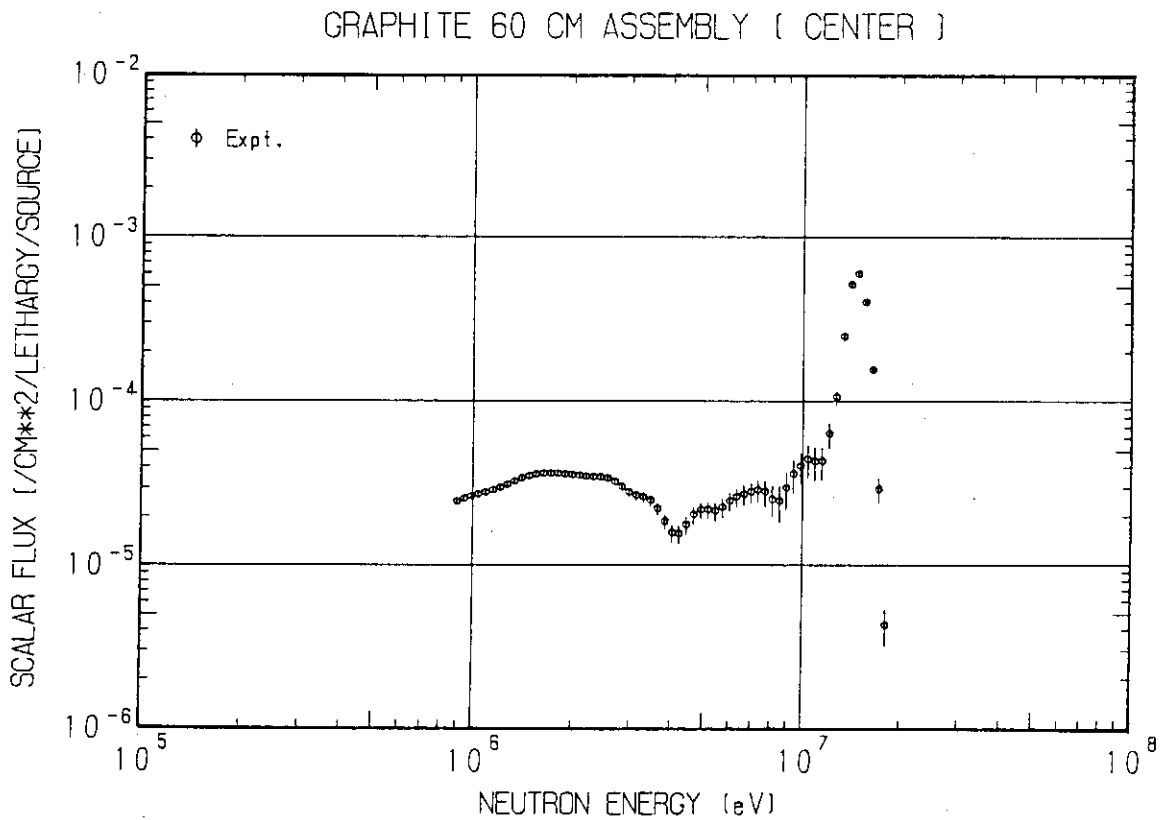


Fig. 5.1      Measured neutron scalar spectrum in the graphite assembly ( $z = 24.1$  cm).

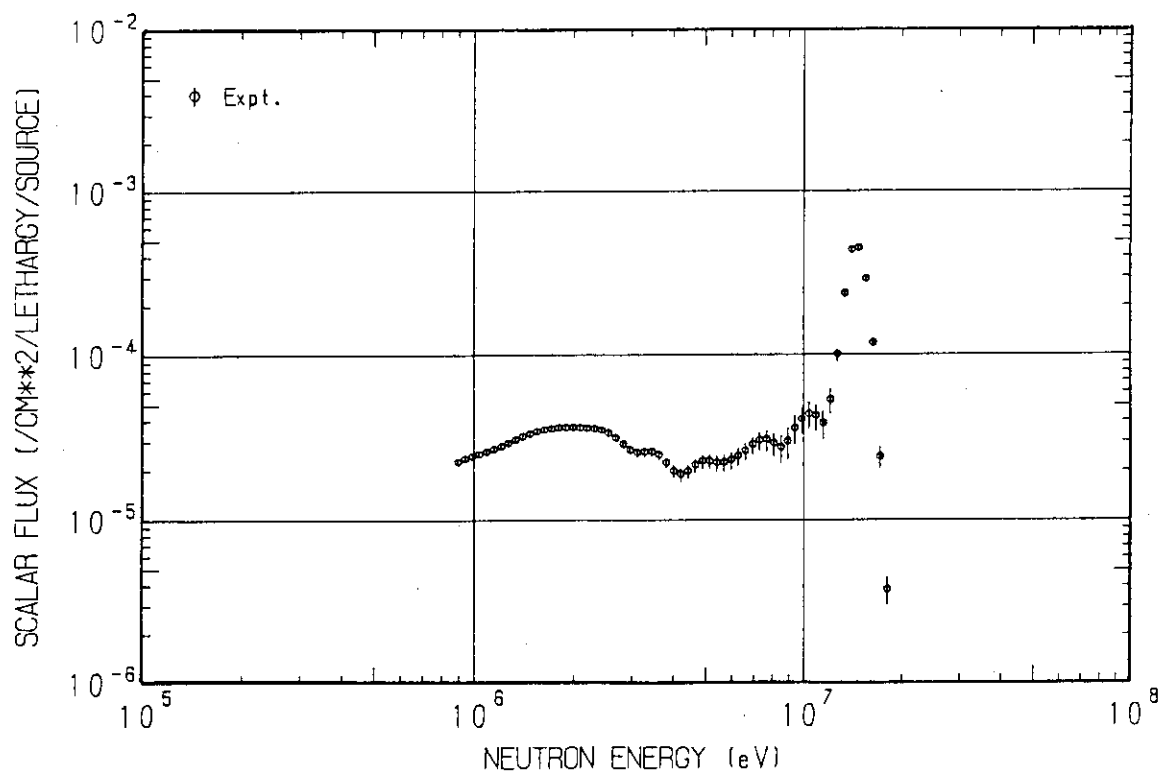


Fig. 5.2      Measured neutron scalar spectrum in the graphite assembly ( $z = 26.7$  cm).

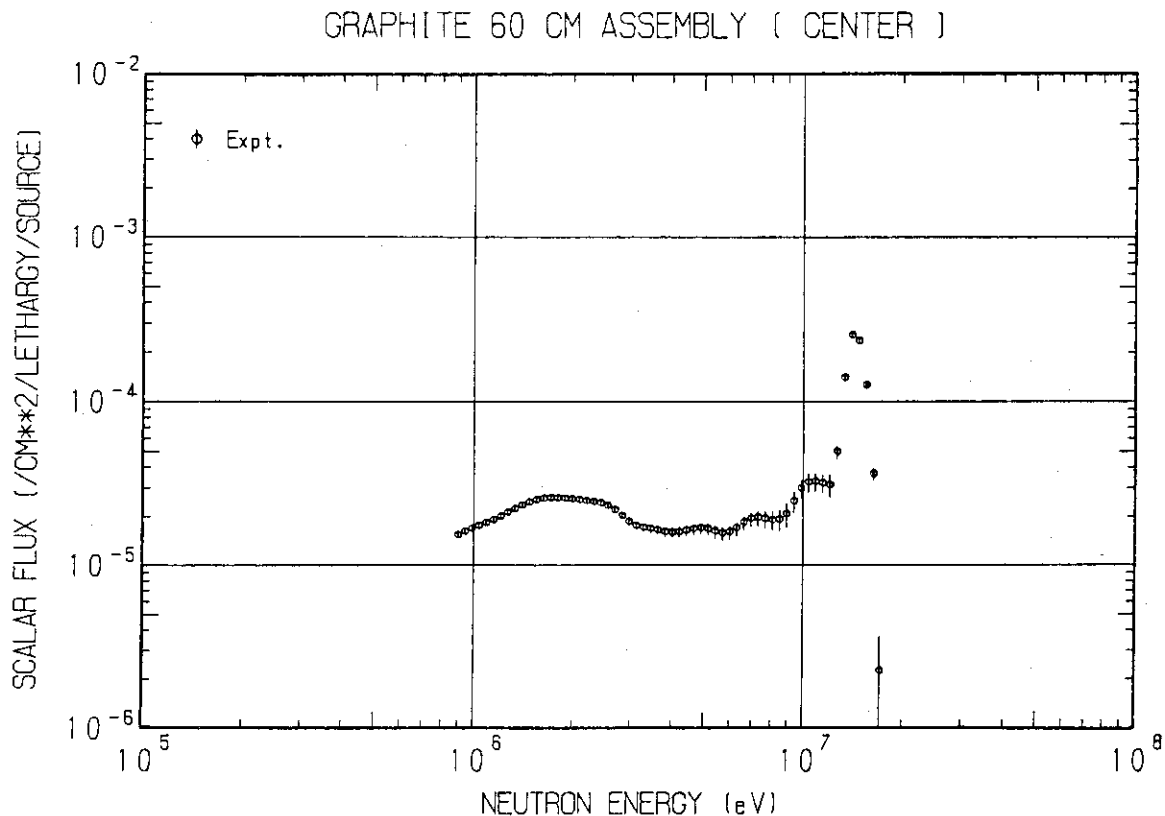


Fig. 5.3      Measured neutron scalar spectrum in the graphite assembly ( $z = 31.7$  cm).

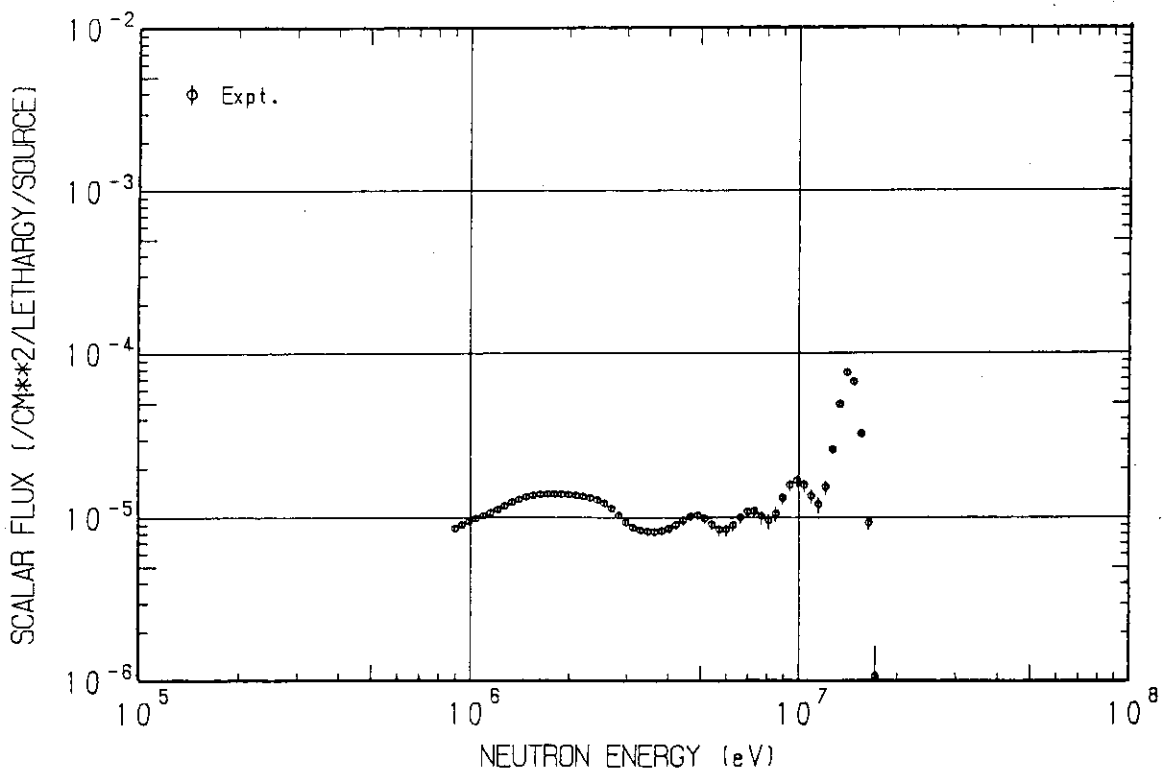


Fig. 5.4      Measured neutron scalar spectrum in the graphite assembly ( $z = 41.8$  cm).

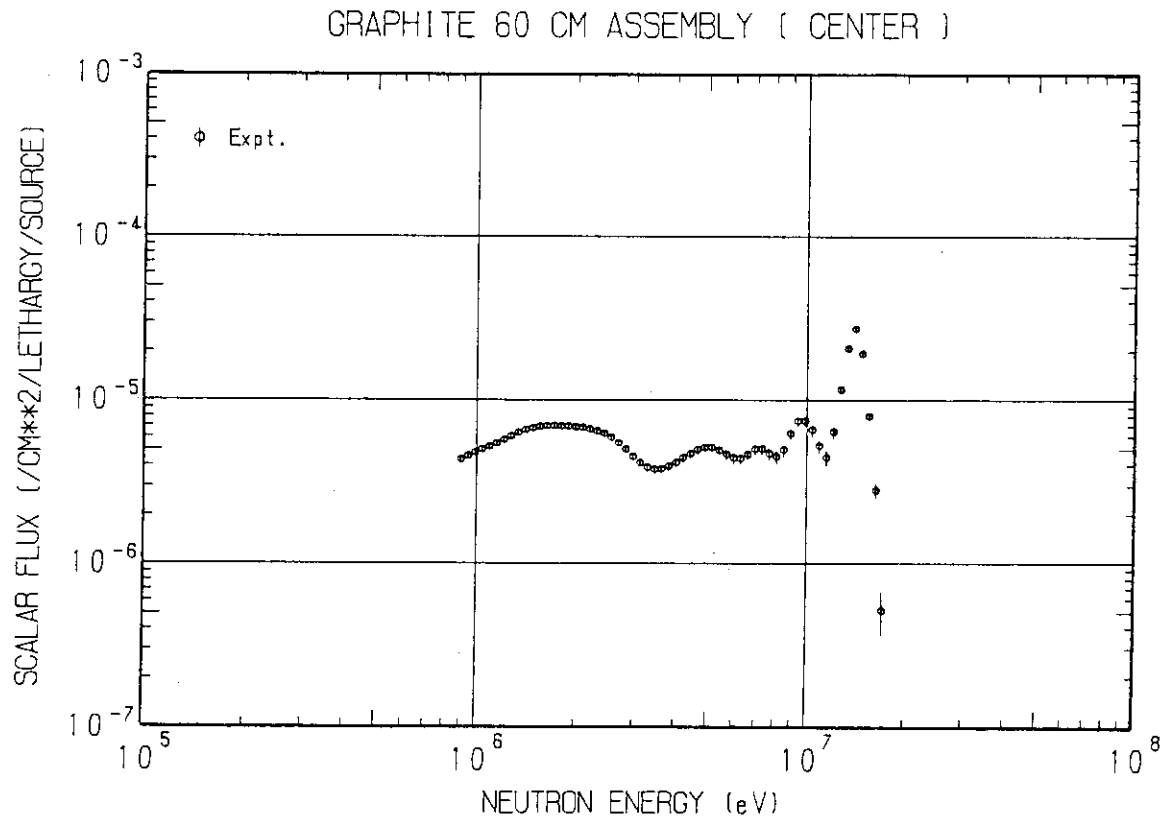


Fig. 5.5      Measured neutron scalar spectrum in the graphite assembly ( $z = 52.0$  cm).

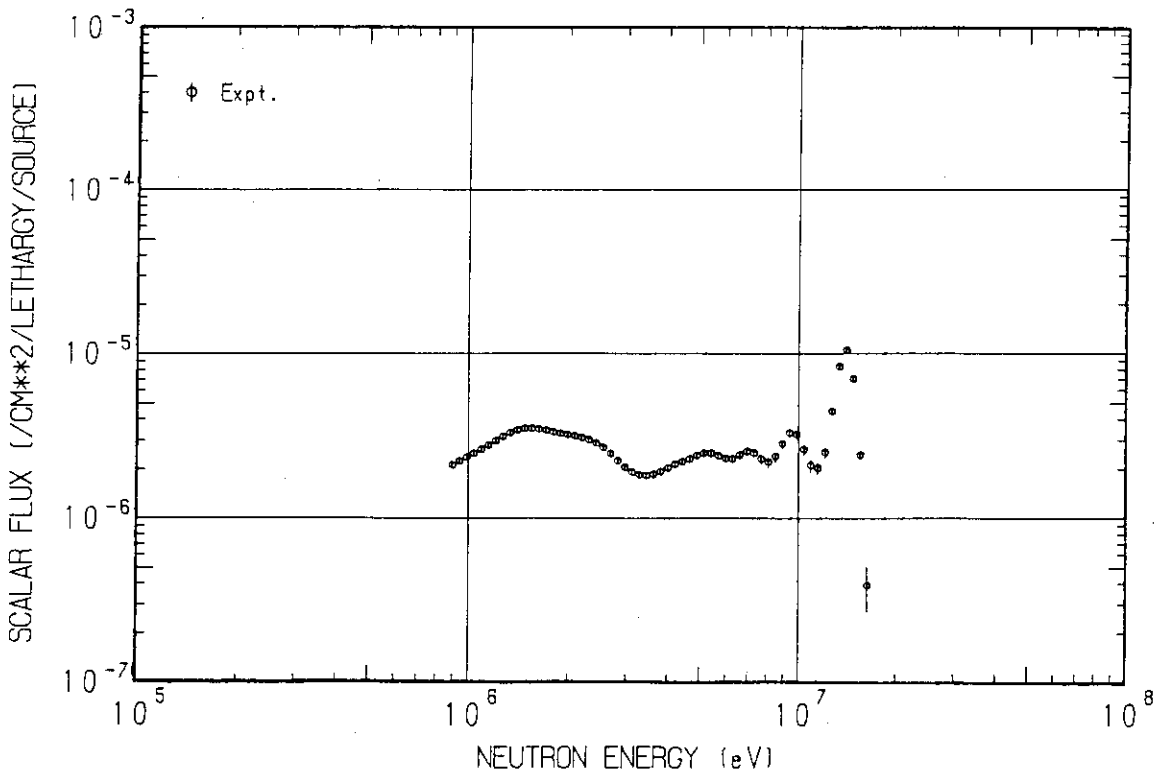


Fig. 5.6      Measured neutron scalar spectrum in the graphite assembly ( $z = 62.1$  cm).

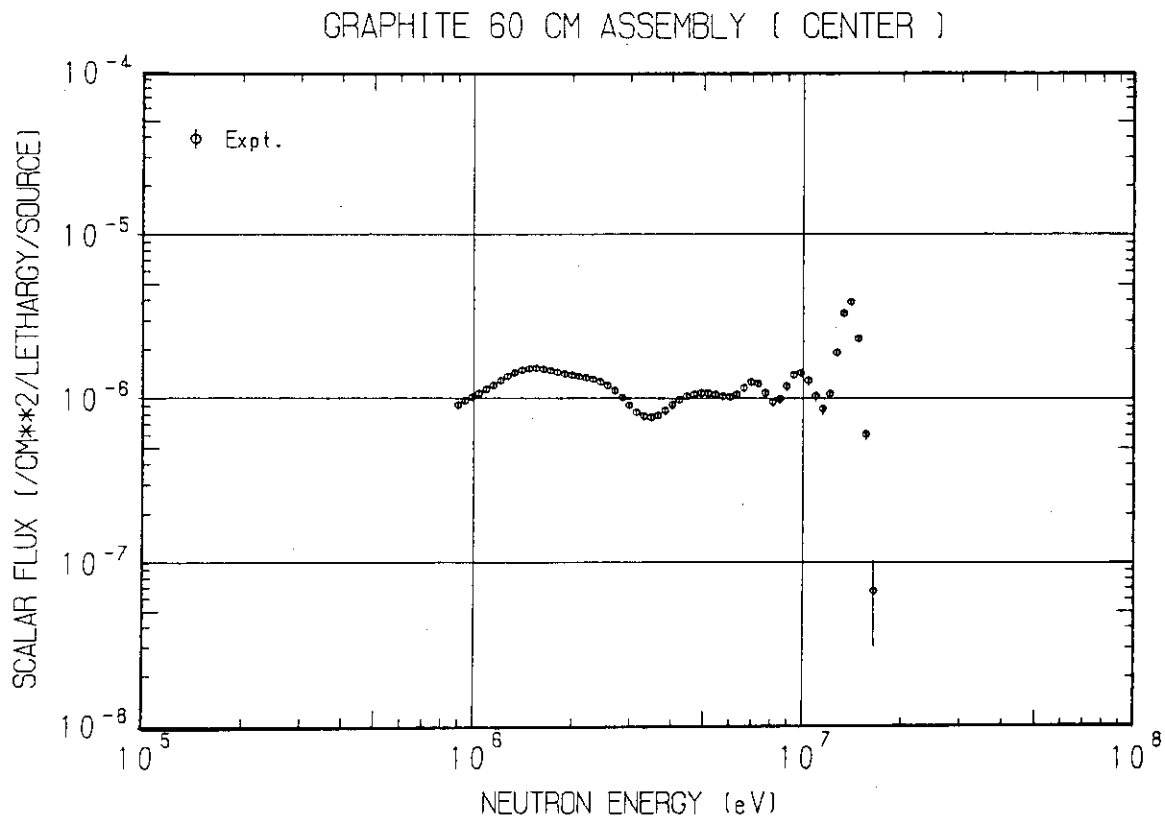


Fig. 5.7      Measured neutron scalar spectrum in the graphite assembly ( $z = 72.1$  cm).

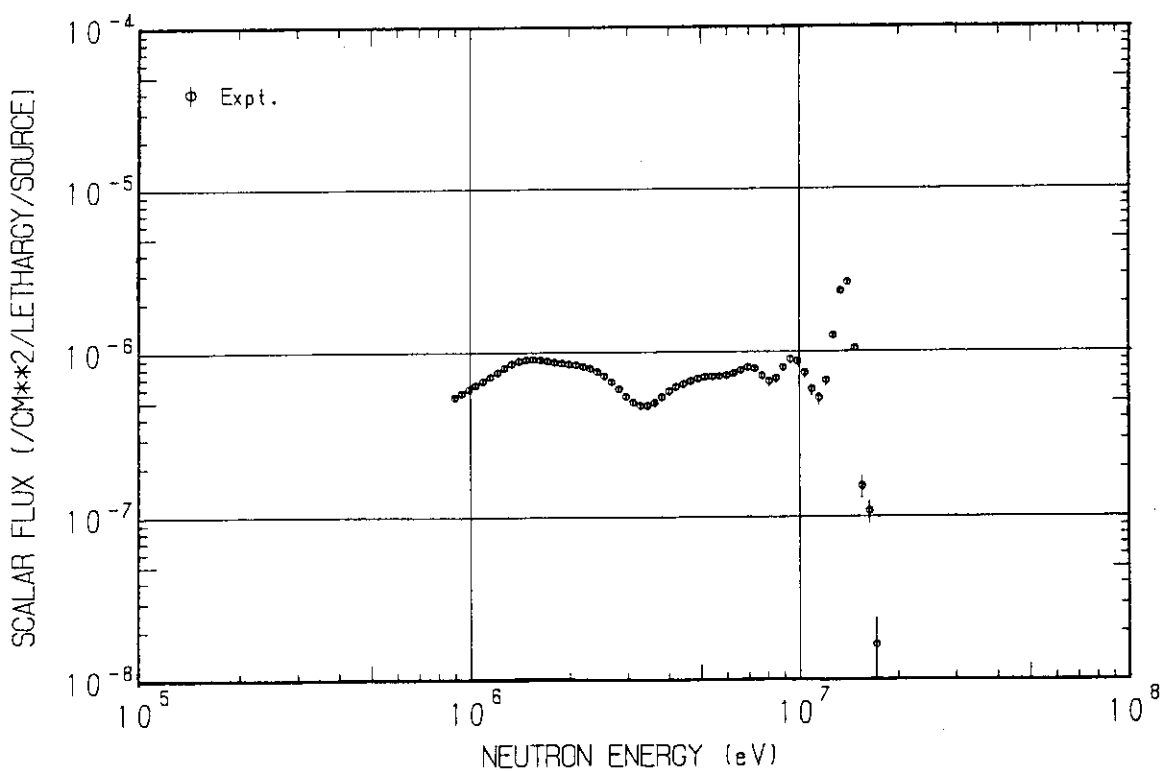


Fig. 5.8      Measured neutron scalar spectrum in the graphite assembly ( $z = 77.2$  cm).

## 6. Response Distribution of Thermoluminescence Dosimeters

In preparation for the experimental study of nuclear heating in a simulated fusion blanket assembly, response distributions of thermoluminescence dosimeters (TLD) were measured in the Li<sub>2</sub>O slab assembly. Types of TLDs are summarized in Table 6.1. The TLD powder was sealed in an Pyrex glass ampoule of 2 mm dia. × 12 mm length.

Five or seven TLDs of each type were placed in the spaces between the special-sized Li<sub>2</sub>O blocks. These blocks were loaded in the drawer and inserted in the experimental channel. Some TLDs were also placed on the front and the back surfaces. Ten or fifteen TLDs of each type were used for the determination of background. Deuteron beam current, irradiation time and total neutron yield at the target were 150 μA, 1300 sec and 1.99<sub>0</sub> × 10<sup>13</sup>, respectively.

A TLD reader of type UD-502B (Matsushita Electric Industrial Co., Ltd.) was used for measurement of the absorbed dose. The observed data are summarized in Table 6.2. The errors in the table were estimated from the standard deviation of the observation and the uncertainty in the neutron yield (See Table 6.1.). Measured response-rate distributions are shown in Figs. 6.1, 6.2 and 6.3.

Table 6.1 Type of TLDs and neutron yield during irradiation.

Run No.	Sample	TLD material	Neutron yield
1	TLD-100*1	${}^{\text{N}}\text{LiF}(\text{Mg})$	$2.09_4 \times 10^{13}$ (2.4%)
2	TLD-600*1	${}^6\text{LiF}(\text{Mg})$	$2.09_6 \times 10^{13}$ (2.4%)
3	TLD-700*1	${}^7\text{LiF}(\text{Mg})$	$2.09_9 \times 10^{13}$ (2.4%)
4	UD-110S*2	$\text{CaSO}_4(\text{Tm})$	$2.09_4 \times 10^{13}$ (2.4%)
5	UD-136N*2	${}^6\text{LiF} + \text{CaSO}_4(\text{Tm})$	$2.09_7 \times 10^{13}$ (2.4%)
6	UD-137N*2	${}^7\text{LiF} + \text{CaSO}_4(\text{Tm})$	$2.09_3 \times 10^{13}$ (2.4%)
7	{ MSO-S*3 SSO-S*3	$\text{Mg}_2\text{SiO}_4(\text{Tb})$ $\text{Sr}_2\text{SiO}_4(\text{Tb})$	$3.15_0 \times 10^{13}$ (2.4%) *4
8	BSO-S*3	$\text{Ba}_2\text{SiO}_4(\text{Tb})$	$6.8_1 \times 10^{12}$ (6.4%)

\*1 TLD powders were manufactured by Harshaw Chemical Co.

\*2 Manufactured by Matsushita Electric Industrial Co., Ltd.

\*3 Manufactured by Kasei Optonix Ltd.

\*4 Neutron yield was estimated from the recorder chart of rate meter for the  $\alpha$ -monitor.

Table 6.2 Response rates of TLDs in the graphite assembly.

(a) TLD-100, TLD-600, TLD-700

Z <sup>*1</sup> [cm]	TLD response [ R( <sup>60</sup> Co equivalence) / source ]		
	TLD-100	TLD-600	TLD-700
20.0	1.46 <sub>1</sub> -14 (12.2%)	4.24 -14 (13.3%)	2.01 -14 ( 9.7%)
25.1	1.49 <sub>8</sub> -14 ( 9.3%)	7.34 -14 (10.4%)	1.46 <sub>4</sub> -14 (13.0%)
30.1	1.72 <sub>5</sub> -14 ( 4.4%)	1.10 <sub>9</sub> -13 (15.1%)	9.39 -15 (12.6%)
35.2	1.87 <sub>4</sub> -14 ( 7.6%)	1.36 <sub>4</sub> -13 ( 8.4%)	7.62 -15 ( 8.4%)
40.2	2.11 -14 ( 6.7%)	1.40 <sub>3</sub> -13 (14.2%)	6.89 -15 (14.9%)
45.3	1.98 <sub>9</sub> -14 ( 8.1%)	1.49 <sub>9</sub> -13 (14.0%)	6.49 -15 (24.9%)
50.4	1.86 <sub>0</sub> -14 (10.7%)	1.37 <sub>2</sub> -13 (12.6%)	4.44 -15 (13.5%)
55.4	1.70 <sub>9</sub> -14 ( 6.0%)	1.13 <sub>5</sub> -13 ( 9.9%)	4.13 -15 (38.2%)
60.5	1.40 <sub>1</sub> -14 ( 8.8%)	9.31 -14 (17.5%)	3.24 -15 (14.6%)
65.5	1.09 <sub>1</sub> -14 (11.5%)	7.94 -14 (13.1%)	2.50 -15 ( 8.8%)
70.6	8.08 -15 ( 9.4%)	5.03 -14 ( 9.5%)	2.06 -15 (27.8%)
75.7	4.58 -15 (10.6%)	2.83 -14 ( 7.4%)	1.24 <sub>4</sub> -15 (18.1%)
80.7	1.25 <sub>6</sub> -15 ( 8.4%)	9.04 -15 (31.0%)	4.03 -16 (12.0%)

\*1 Distance from the target and along the central axis.

\*2 Read as  $1.46_1 \times 10^{-14}$ .

\*3 Experimental error.

Table 6.2 (continued).

(b) UD-110S, UD-136N, UD-137N

Z [cm]	TLD response [ R( $^{60}\text{Co}$ equivalence) / source ]		
	UD-110S	UD-136N	UD-137N
20.0	6.52 -13 ( 7.1%)	3.47 -13 ( 4.8%)	2.36 -13 (17.9%)
25.1	3.99 -13 ( 5.4%)	3.49 -13 (11.8%)	1.45 <sub>2</sub> -13 (14.7%)
30.1	2.59 -13 ( 5.2%)	3.98 -13 (16.5%)	9.87 -14 ( 6.9%)
35.2	1.61 <sub>1</sub> -13 ( 5.3%)	4.44 -13 ( 8.2%)	6.06 -14 ( 7.4%)
40.2	1.15 <sub>1</sub> -13 ( 6.8%)	4.66 -13 (10.9%)	4.40 -14 (16.6%)
45.3	7.74 -14 ( 5.2%)	4.64 -13 (15.8%)	2.92 -14 (15.8%)
50.4	5.40 -14 ( 5.4%)	3.99 -13 (11.0%)	1.96 <sub>4</sub> -14 (13.5%)
55.4	3.68 -14 ( 6.1%)	3.66 -13 (11.5%)	1.35 <sub>3</sub> -14 ( 4.5%)
60.5	2.67 -14 ( 7.8%)	2.82 -13 (11.5%)	1.00 <sub>0</sub> -14 ( 6.9%)
65.5	1.88 <sub>5</sub> -14 ( 4.4%)	2.30 -13 (13.0%)	7.82 -15 ( 9.7%)
70.6	1.26 <sub>9</sub> -14 ( 6.6%)	1.62 <sub>6</sub> -13 (19.1%)	5.03 -15 (10.5%)
75.7	8.78 -15 ( 7.0%)	8.78 -14 ( 8.4%)	3.16 -15 ( 9.6%)
80.7	4.77 -15 ( 6.4%)	2.54 -14 (23.7%)	1.80 <sub>0</sub> -15 (15.6%)

Table 6.2 (continued).

(c) MSO-S, SSO-S, BSO-S

Z [cm]	Response [ R( $^{60}\text{Co}$ equivalence) / source ]		
	MSO-S	SSO-S	BSO-S
25.1	1.60 <sub>0</sub> -13 ( 7.3%)	2.24 -13 ( 9.8%)	3.41 -13 (14.9%)
30.1	1.03 <sub>8</sub> -13 (20.9%)	1.78 <sub>8</sub> -13 ( 6.7%)	2.97 -13 (25.3%)
35.2	5.91 -14 ( 8.3%)	1.32 <sub>4</sub> -13 ( 7.0%)	2.33 -13 (31.1%)
40.2	4.40 -14 (21.1%)	9.52 -14 (11.0%)	1.49 <sub>0</sub> -13 (19.9%)
45.3	2.76 -14 ( 7.1%)	6.86 -14 ( 6.6%)	1.25 <sub>9</sub> -13 (28.9%)
50.4	1.89 <sub>8</sub> -14 (18.6%)	5.11 -14 ( 9.0%)	7.94 <sub>8</sub> -14 (26.5%)
55.4	1.33 <sub>3</sub> -14 (17.3%)	3.52 -14 ( 6.4%)	6.23 -14 (37.8%)
60.5	9.12 -15 (16.8%)	2.62 -14 ( 6.8%)	3.55 -14 (46.7%)
65.5	6.29 -15 (18.7%)	1.73 <sub>8</sub> -14 (17.2%)	2.37 -14 (65.7%)
70.6	4.41 -15 (31.2%)	1.23 <sub>8</sub> -14 (12.2%)	1.78 <sub>2</sub> -14 (74.1%)
75.7	2.64 -15 (58.5%)	8.30 -15 (12.7%)	1.25 <sub>1</sub> -14 (128 %)

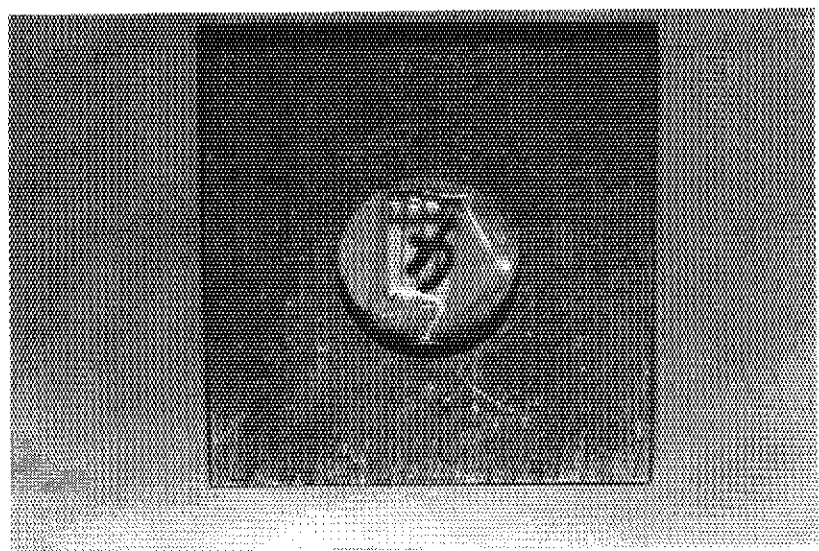
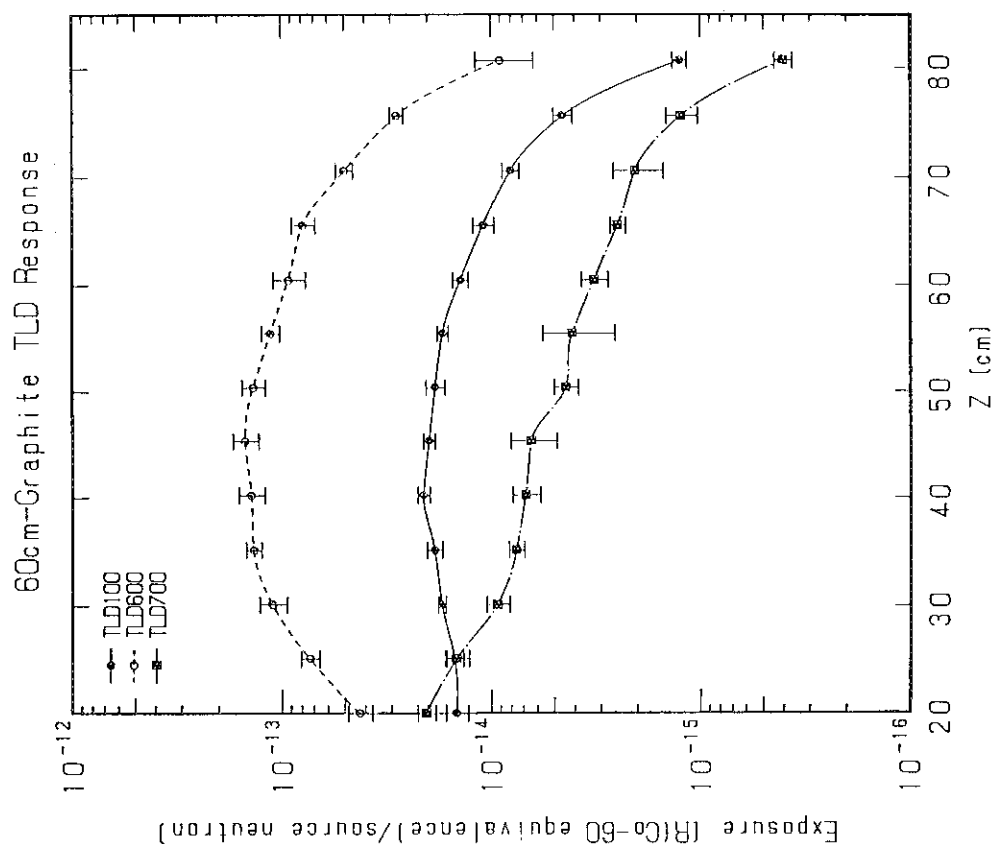


Fig. 6.1 TLDs in a hole of thin graphite plate.

Fig. 6.2 Response distributions of TLD-600, TLD-700 and TLD-100 in the graphite assembly.

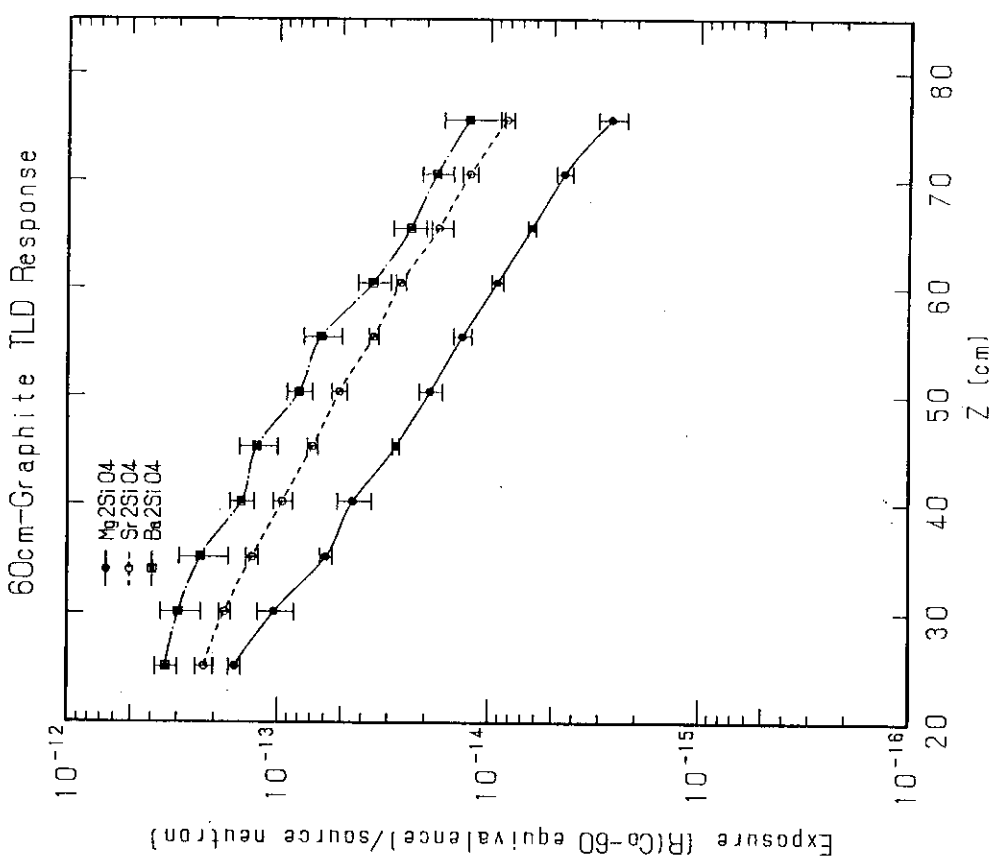


Fig. 6.3 Response distributions of UD-110S, UD-136N and UD-137N TLDs in the graphite assembly.

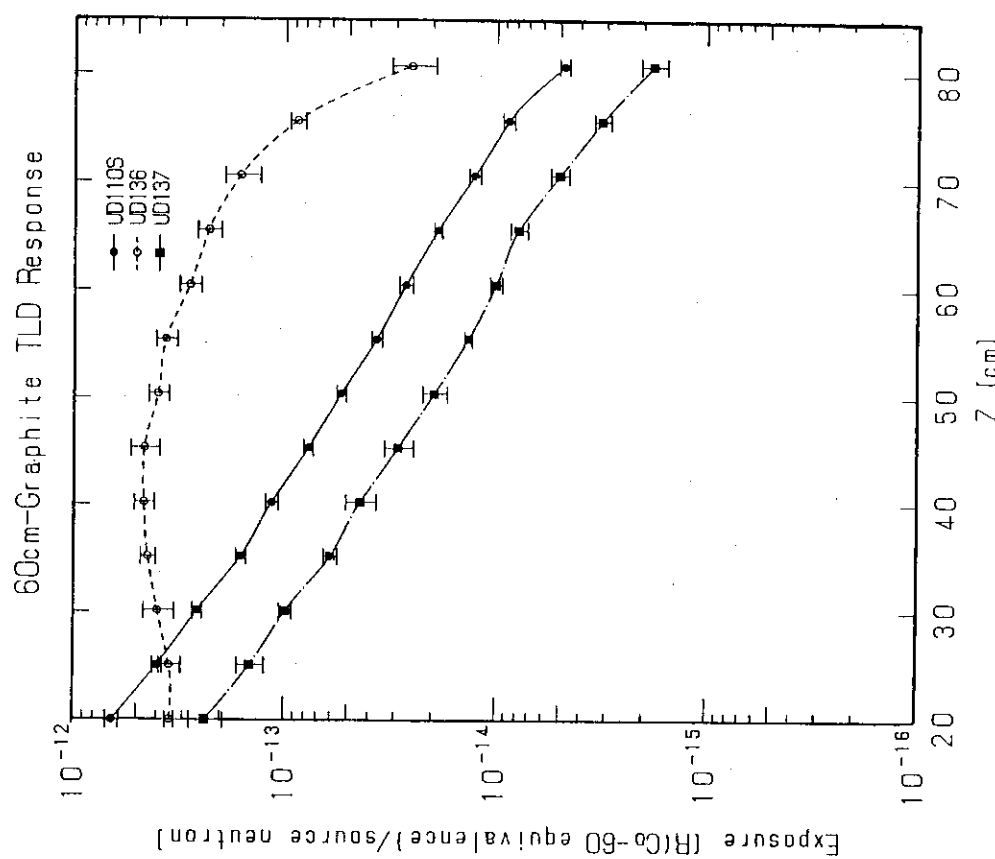


Fig. 6.4 Response distributions of MSO-S, SS0-S and BS0-S TLDs in the graphite assembly.

Fig. 6.4 Response distributions of MSO-S, SS0-S and BS0-S TLDs in the graphite assembly.

## 7. Discussion and Concluding Remarks

To confirm the reliability of measured data, they were intercompared by the assistance of calculated values, that is, the ratio of calculated to experimental values (C/E). Because it is a good method to compare the measurements of different type. First, the C/E distribution of U-238 fission rate measured by the micro-fission chamber was compared with the reaction rate of  $^{58}\text{Ni}(n,p)^{58}\text{Co}$  and the integrated flux over above 5.03 MeV measured by the NE213 spectrometer. This comparison is shown in Fig. 7.1. The sensitivities of  $^{238}\text{U}(n,f)$  and  $^{58}\text{Ni}(n,p)^{57}\text{Ni}$  cover almost the same energy range. Figure 7.1 indicates that, though data were measured independently by quite different methods, they show similar tendency and agree well within experimental errors.

Second comparison was performed between the high threshold reaction of  $^{58}\text{Ni}(n,2n)^{57}\text{Ni}$  and the integrated flux over above 11.2 MeV measured by the NE213 spectrometer. The C/E distributions are shown in Fig. 7.2. These measured values agree also well within the experimental errors.

Above comparisons support the view that the reliability of the measured data is adequate for use in benchmark verification of calculational methods and nuclear data. Therefore, these data have been applied to the integral test of JENDL-3PR1 and -3PR2 (Preliminary versions of JENDL-3). One should note that the accurate reaction cross sections are used for the calculation of reaction rates. In addition, the reaction of  $^{197}\text{Au}(n,\gamma)^{198}\text{Au}$  has a sharp resonance at 5 eV. Though very thin gold foils of 0.001 mm thick were used in the experiment, there was some self-shielding effect. As the measured reaction rates of  $^{197}\text{Au}(n,\gamma)^{198}\text{Au}$  shown in Table 4.2 are not corrected for the self-shielding effect, special attention should be paid to calculate the reaction rate of  $^{197}\text{Au}(n,\gamma)^{198}\text{Au}$ .

A sample calculational procedure is provided in Appendix A.3. It is clear from Fig. A.3.3 that the  $^{27}\text{Al}(n,\alpha)^{24}\text{Na}$  reaction-rate prediction based on JENDL-3PR2 is in good agreement with measured values. The calculated results mentioned above were obtained by the same procedure based on JENDL-3PR2.

The next experiments in this series of benchmark measurements, using a 40-cm long Li<sub>2</sub>O cylinder with 20-cm long graphite reflector and a Be-sandwiched Li<sub>2</sub>O cylinder (5-cm long Li<sub>2</sub>O, 5-cm long Be and 50-cm long Li<sub>2</sub>O), have been completed ; results will be reported in the near future.

### Concluding Remarks

- (1) Integral experiments on a 60 cm-thick graphite cylindrical assembly have been carried out using the FNS facility. Measured data are very reliable and can be used for testing method and data as the benchmark data.
- (2) Preliminary versions of the JENDL-3 nuclear data file and the newly developed transport codes BERMUDA and MORSE-DD, are being evaluated using present benchmark data. They are also useful for tests of not only the JENDL-3 file but the other files such as the ENDF/B-VI, JEF (Joint European File), EFF (European Fusion File) and BROND.

### Acknowledgement

The authors are deeply indebted to Messrs. J. Kusano, C. Kutsukake and S. Tanaka for their operation of the FNS accelerator.

### References

- (1) Maekawa H., et al. : "Fusion Blanket Benchmark Experiments on a 60 cm-Thick Lithium-Oxide Cylindrical Assembly," JAERI-M 86-182 (1986).
- (2) Rhoades W. A., Mynatt F. R.: "The DOT-III Two Dimensional Discrete Ordinates Transport Code," ORNL/TM-4280 (1979).
- (3) Seki M., et al.: J. Nucl. Sci. Technol., 16, 838 (1979).

The next experiments in this series of benchmark measurements, using a 40-cm long Li<sub>2</sub>O cylinder with 20-cm long graphite reflector and a Be-sandwiched Li<sub>2</sub>O cylinder (5-cm long Li<sub>2</sub>O, 5-cm long Be and 50-cm long Li<sub>2</sub>O), have been completed ; results will be reported in the near future.

### Concluding Remarks

- (1) Integral experiments on a 60 cm-thick graphite cylindrical assembly have been carried out using the FNS facility. Measured data are very reliable and can be used for testing method and data as the benchmark data.
- (2) Preliminary versions of the JENDL-3 nuclear data file and the newly developed transport codes BERMUDA and MORSE-DD, are being evaluated using present benchmark data. They are also useful for tests of not only the JENDL-3 file but the other files such as the ENDF/B-VI, JEF (Joint European File), EFF (European Fusion File) and BROND.

### Acknowledgement

The authors are deeply indebted to Messrs. J. Kusano, C. Kutsukake and S. Tanaka for their operation of the FNS accelerator.

### References

- (1) Maekawa H., et al. : "Fusion Blanket Benchmark Experiments on a 60 cm-Thick Lithium-Oxide Cylindrical Assembly," JAERI-M 86-182 (1986).
- (2) Rhoades W. A., Mynatt F. R.: "The DOT-III Two Dimensional Discrete Ordinates Transport Code," ORNL/TM-4280 (1979).
- (3) Seki M., et al.: J. Nucl. Sci. Technol., 16, 838 (1979).

The next experiments in this series of benchmark measurements, using a 40-cm long Li<sub>2</sub>O cylinder with 20-cm long graphite reflector and a Be-sandwiched Li<sub>2</sub>O cylinder (5-cm long Li<sub>2</sub>O, 5-cm long Be and 50-cm long Li<sub>2</sub>O), have been completed ; results will be reported in the near future.

### Concluding Remarks

- (1) Integral experiments on a 60 cm-thick graphite cylindrical assembly have been carried out using the FNS facility. Measured data are very reliable and can be used for testing method and data as the benchmark data.
- (2) Preliminary versions of the JENDL-3 nuclear data file and the newly developed transport codes BERMUDA and MORSE-DD, are being evaluated using present benchmark data. They are also useful for tests of not only the JENDL-3 file but the other files such as the ENDF/B-VI, JEF (Joint European File), EFF (European Fusion File) and BROND.

### Acknowledgement

The authors are deeply indebted to Messrs. J. Kusano, C. Kutsukake and S. Tanaka for their operation of the FNS accelerator.

### References

- (1) Maekawa H., et al. : "Fusion Blanket Benchmark Experiments on a 60 cm-Thick Lithium-Oxide Cylindrical Assembly," JAERI-M 86-182 (1986).
- (2) Rhoades W. A., Mynatt F. R.: "The DOT-III Two Dimensional Discrete Ordinates Transport Code," ORNL/TM-4280 (1979).
- (3) Seki M., et al.: J. Nucl. Sci. Technol., 16, 838 (1979).

- (4) Maekawa H., et al.: "Neutron Yield Monitors for the Fusion Neutronics Source (FNS) --- For 80° Beam Line ---," JAERI-M 83-219 (1983).
- (5) Ikeda Y., et al: To be published in JAERI-M report.
- (6) Oyama Y., Maekawa H.: Nucl. Instr. Meth. A245, 173 (1986).
- (7) Oyama Y., et al.: "Development of a Spherical NE213 Spectrometer with 14 mm Diameter," JAERI-M84-124 (in Japanese) (1984); Nucl. Instr. Meth. A256, 333 (1987).
- (8) Seki Y., et al.: J. Nucl. Sci. Technol., 20, 686 (1983).
- (9) Maekawa H., Seki Y.: J. Nucl. Sci. Technol. 14, 97 (1977).
- (10) Baba H.: "Usage of the BOB7-Series Programs for the Analysis of Ge(Li) Gamma-ray Spectra," JAERI-M 7017 (1977).
- (11) Lederer C. M., Shirley V. S. (edited): "Table of Isotopes," Seventh Edition, John Wiley and Sons, Inc., New York (1978).
- (12) Kinbara S., Kumahara T.: Nucl. Instr. Meth., 70, 173 (1969).
- (13) "FORIST Spectra Unfolding Code," Radiation Shielding Information Center, Oak Ridge National Laboratory, PSR-92 (1975).
- (14) Narita M., et al.: "Some Applications of Solid State Nuclear Track Detectors to Fast Reactor Physics Experiments [1]," Bull. of Faculty of Engineering, Hokaido University, No 103, pp. 27-39 (1981) (in Japanese).
- (15) Seki Y., Muir D. W., Maekawa H.: J. Nucl. Sci. Technol. 14 [9] 680-681 (1977).
- (16) Maekawa H., et al.: ibid., 16 [5] 377-379 (1979).
- (17) Seki Y., et al.: "Calculation of Absolute Fission-Rate Distributions measured in Graphite-Reflected Lithium Oxide Blanket Assembly," JAERI-M 83-061 (1983).
- (18) Ikeda Y., et al.: To be submitted to Nucl. Instr. Meth.
- (19) Kosako K., et al.: "Neutron Cross-Section Sets of 125-group for Fusion Neutronics Calculations," JAERI-M 86-125, pp157-159 (1986); Further report is under preparing for publication.
- (20) Hasegawa A.: To be published in JAERI report.
- (21) Nakagawa M., Mori T.: "MORSE-DD, A MonteCarlo Code Using Multi-Group Double Differential Form Cross Sections," JAERI-M 84-126 (1984).
- (22) Kosako K.: To be published.
- (23) Mori T., Nakagawa M.: Private communication.

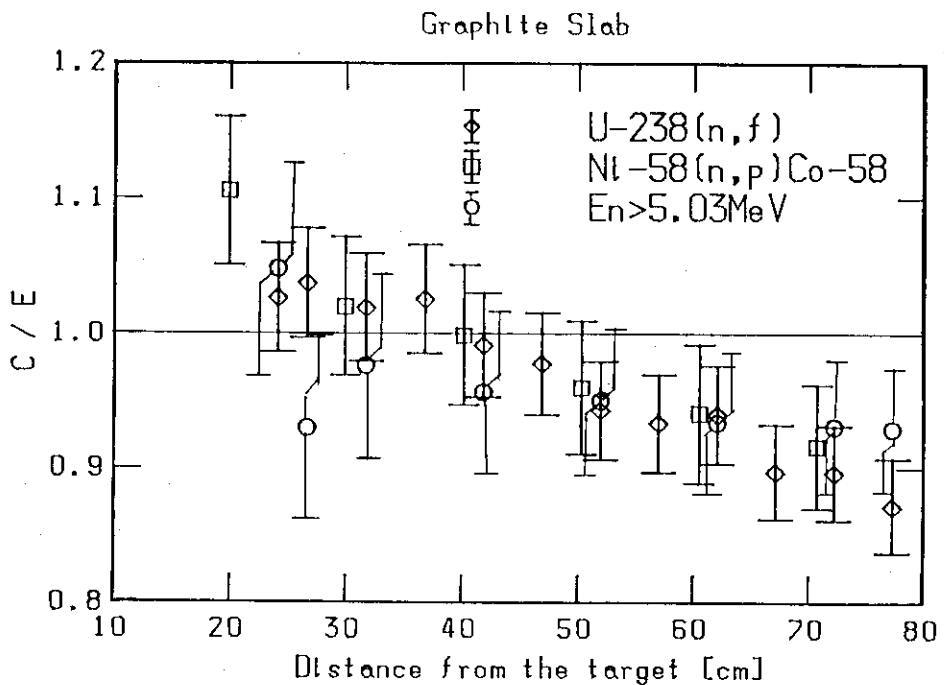


Fig. 7.1 Comparison among measured  $U-238$  fission rates,  $^{58}Ni(n,p)$   $^{58}Co$  reaction rates and integrated scalar flux above 5.03 MeV.

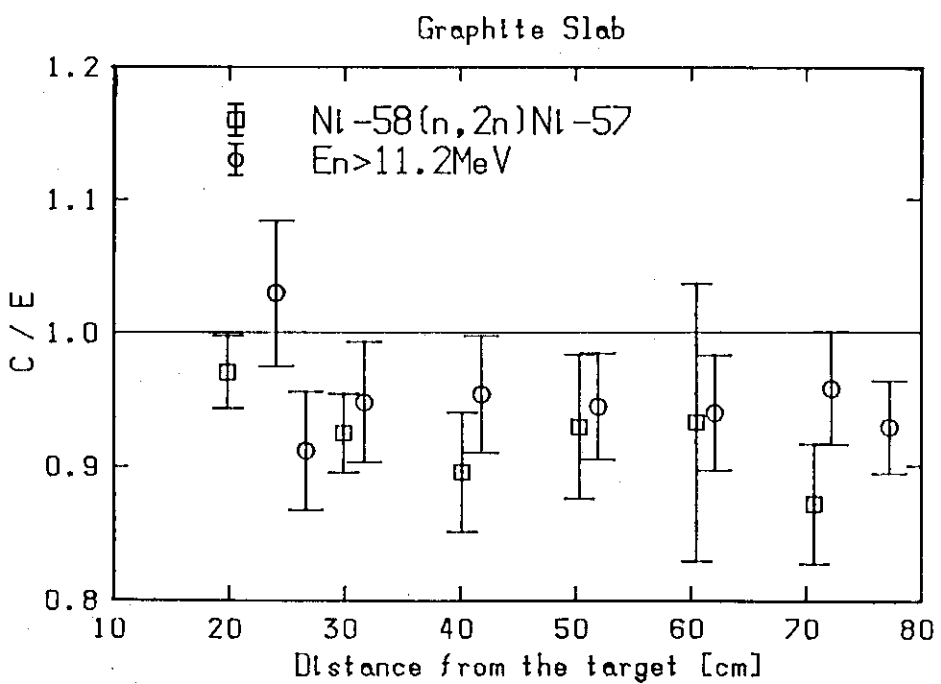


Fig. 7.2 Comparison between  $^{58}Ni(n,2n)^{57}Ni$  reaction rates and integrated scalar flux above 11.2 MeV.

## Appendix 1 Fission-Rate Distributions Measured by Fission Track Recorders (FTD)

Solid state track recorders (SSTR) were used to measure fission rates in an effort to examine their applicability to fusion neutronics experiments, where the SSTRs were coupled with fission foils to form fission track detector (FTD). This study is a result of collaboration with Hokkaido University, where considerable research has been done on the SSTR technique. In contrast to the micro-fission chambers, FTDs have an advantage of being small, thus affording good spatial resolution and little perturbation to the environment. Polycarbonate film (Takiron PC-1600) of 30 mm × 20 mm and 0.5 mm thickness was used as the solid state track recorder, with fission foils of both thorium depleted uranium and enriched-uranium/aluminum alloy. The foils were standard diameter, and were mounted at the center of the polycarbonate films.

Detectors were inserted into gaps between the graphite blocks loaded in the central experimental drawer. A stepwise irradiation was performed to keep track densities as uniform as practicable throughout the drawer. The required source intensities and irradiation times were evaluated by pre-experiment analysis. The track densities thus obtained ranged from 10000 to 30000 per square centimeter.

Irradiated films were treated for etched in 30 w/o KOH bath for 30 minutes at 60°C, washed in water, rinsed and dried.

Etch-pit tracks were measured by a semi-automatic image processing apparatus, LUZEX 450 (Toyo Ink Co.), with an optical field of 150 μm × 150 μm. The track size spectrum was measured, affording discrimination against small-sized pits due to recoil protons. One to two thousands tracks were accumulated by scanning a number of fields.<sup>14)</sup> Details of the chemical processing and reported elsewhere.

The calibration of FTD was performed by directly irradiating different detectors of the same type in a 15 MeV neutron beam. The neutron flux in this case was determined by the absolute yield monitor, an associated α-particle detector, while the neutron spectrum was calculated by 3-D Monte Carlo analysis<sup>8)</sup> and confirmed by time-of-flight experiments. The prime sensitivity for the each type

of FTD was determined by taking the effective fission cross section at the source field. Table A.1.1 gives the prime sensitivity that was used in the present experiment.

Measured values with experimental errors are summarized in Table A.1.2. The error includes the statistical error and errors of neutron yield (2.4 %) and prime sensitivity (1.7, 1.8 and 4.2 % for Th-232, U-238 and U-235, respectively). The fission rates distributions in the graphite assembly are shown in Fig. A.1.1 with those of micro-fission chambers (MFC). In the case of U-235, the data of FTD agree well with those of MFC within the experimental errors. In the case of U-238, the distribution shape of FTD data is simular to that of MFC, however, the value of FTD are systematically lower than those of MFC by about 10 %. The data of FTD for TH-232 are also systematically lower than those of MFC by about 15 % for  $z < 40$  cm and the deviation increases with the distance. The distribution shapes of FTD for U-238 and Th-232 are seemed to be reasonable. The large deviation might be attributed to the fissile impurity, which has the sensitivity for low energy neutrons, in the Th-232 MFC. The same fact was observed in the integral experiments on Li-C and Li<sub>2</sub>O-C spherical assemblies.<sup>15,16,17)</sup>

Table A.1.1 Measured prime sensitivity.

Radiator	Fissionable material	Prime sensitivity $k [cm^{-2}]$
Th	Th-232	$(1.04 \pm 0.02) \times 10^{19}$
DU	U-238	$(7.39 \pm 0.13) \times 10^{18}$
	U-235	$(2.79 \pm 0.05) \times 10^{15}$
EU-A1	U-238	$(6.46 \pm 0.27) \times 10^{16}$
	U-235	$(5.72 \pm 0.24) \times 10^{17}$

Table A.1.2 Absolute fission rate in Graphite assembly measured by FTD method.

Position* <sup>1</sup> [cm]	Absolute fission rate [fissions/atom/source neutron]		
	U-235	U-238	Th-232
19.90	1.50, <sup>2</sup> -27 (5.9%)	2.65 -28 (4.0%)	6.38 -29 (4.5%)
24.85	_____	_____	4.51 -29 (3.9%)
27.35	5.08 -27 (5.7%)	_____	_____
27.40	_____	1.24 <sub>5</sub> -28 (4.1%)	_____
29.93	_____	_____	2.94 -29 (4.3%)
35.00	7.49 -27 (5.8%)	5.46 -29 (4.1%)	1.45 <sub>3</sub> -29 (3.9%)
40.10	8.39 -27 (5.7%)	3.35 -29 (4.8%)	9.88 -30 (4.3%)
45.15	9.23 -27 (5.6%)	2.28 -29 (4.0%)	5.91 -30 (3.9%)
50.20	8.75 -27 (5.6%)	1.31 <sub>1</sub> -29 (4.8%)	3.96 -30 (4.4%)
55.30	_____	8.68 -30 (5.7%)	2.36 -30 (3.9%)
57.80	6.85 -27 (5.8%)	_____	_____
60.40	_____	6.22 -30 (6.7%)	1.46, <sub>7</sub> -30 (4.5%)
65.40	4.69 -27 (5.7%)	_____	_____
65.45	_____	3.93 -30 (5.4%)	9.54 -31 (5.1%)
70.55	_____	2.76 -30 (8.2%)	_____
73.00	2.92 -27 (5.7%)	_____	_____

\*1 Distance from the target and along the central axis.

\*2 Read as  $1.50, \times 10^{-27}$ .

\*3 Experimental error. The error includes statistical error and errors of neutron yield (2.4 %) and prime sensitivity (1.7, 1.8 and 4.2 % for Th-232, U-238 and U-235, respectively). There is some unknown error such as the error in a chemical processing.

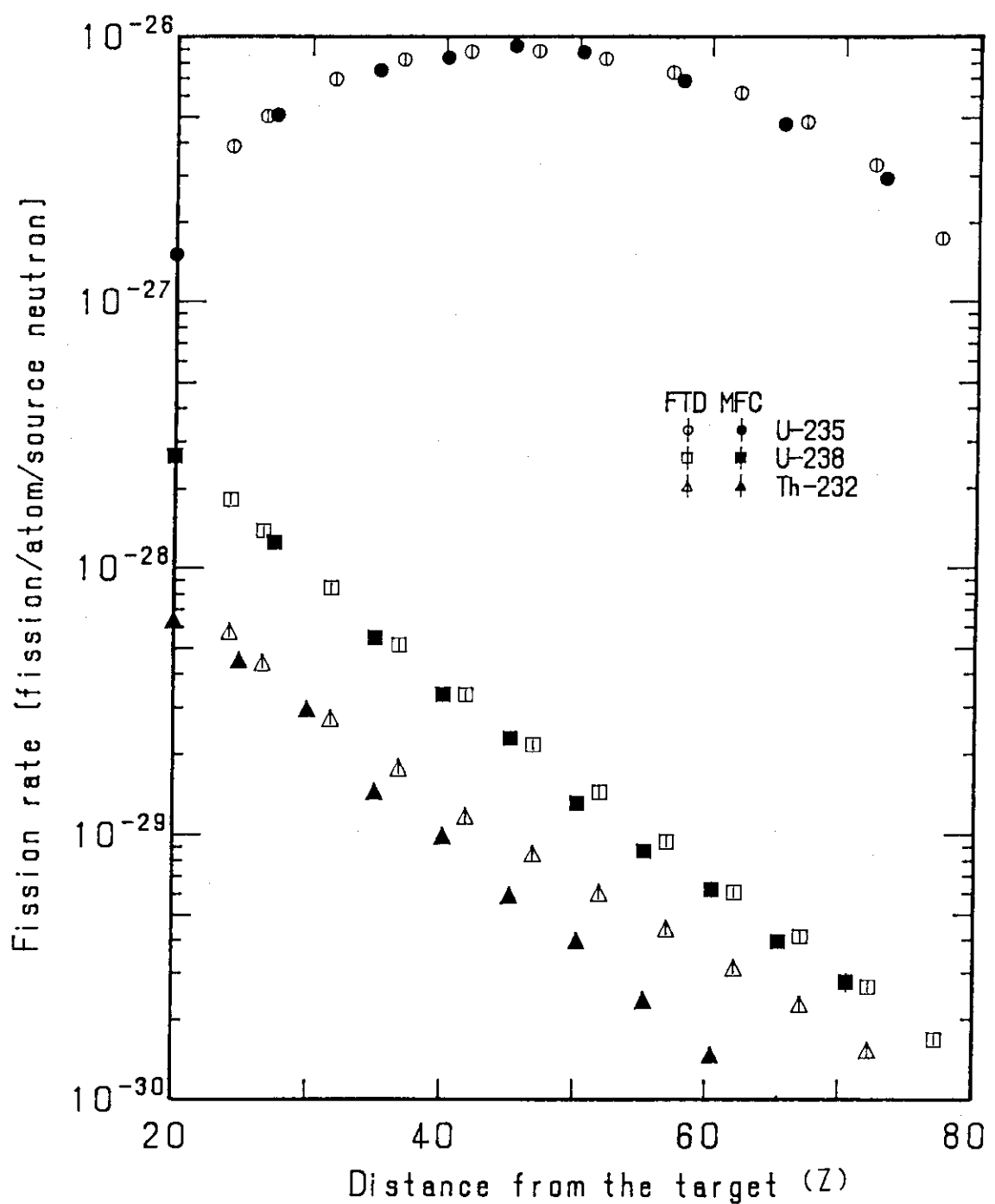


Fig. A.1.1 Fission-rate distributions in the graphite assembly measured by FTD and those by micro-fission chambers.

## Appendix 2 Response Distribution of PIN Diode

A PIN diode measurement was carried out along the central axis of the graphite assembly in addition to the fission rates and reaction rates measurements. With a low threshold energy of 0.2 MeV, the PIN diode is suitable to measure the intermediate energy neutron flux.

The PIN diodes, Studsvik Type 5430, were set in the space between the graphite blocks in the same manner as the reaction-rate measurement. Total neutron yield at the target was  $9.14 \times 10^{14}$  during the irradiation. After the irradiation, the forward voltage drop of the PIN diode was measured by a Studsvik Type 3809A reader at a constant current of 25 mA. The voltage drop difference between before and after irradiation is proportional to the neutron fluence.

The results of the PIN diode measurement are shown in Table A.2.1 and Fig. A.2.1. The value is in unit of Volt $\cdot$ cm $^2$ /source neutron. The response function of the PIN diode was experimentally determined; it will be published elsewhere.<sup>18)</sup>

Table A.2.1 Measured response rate of PIN diode  
in the graphite assembly.

Position <sup>*1</sup> [cm]	PIN diode response <sup>*2</sup> [V $\cdot$ cm $^2$ /source neutron]	Error <sup>*4</sup> [ $\pm$ %]
19.9	3.31 -15 <sup>*3</sup>	3.3
29.9	1.27 -15	3.0
40.2	4.87 -16	2.0
50.3	1.96 -16	3.0
60.5	8.41 -17	3.0
70.7	3.61 -17	3.1
80.9	1.20 -17	9.1

\*1 Distance from the target and along the central axis.

\*2 The PIN diodes were measured at one day after  
the irradiation.

\*3 Read as  $3.31 \times 10^{-15}$ .

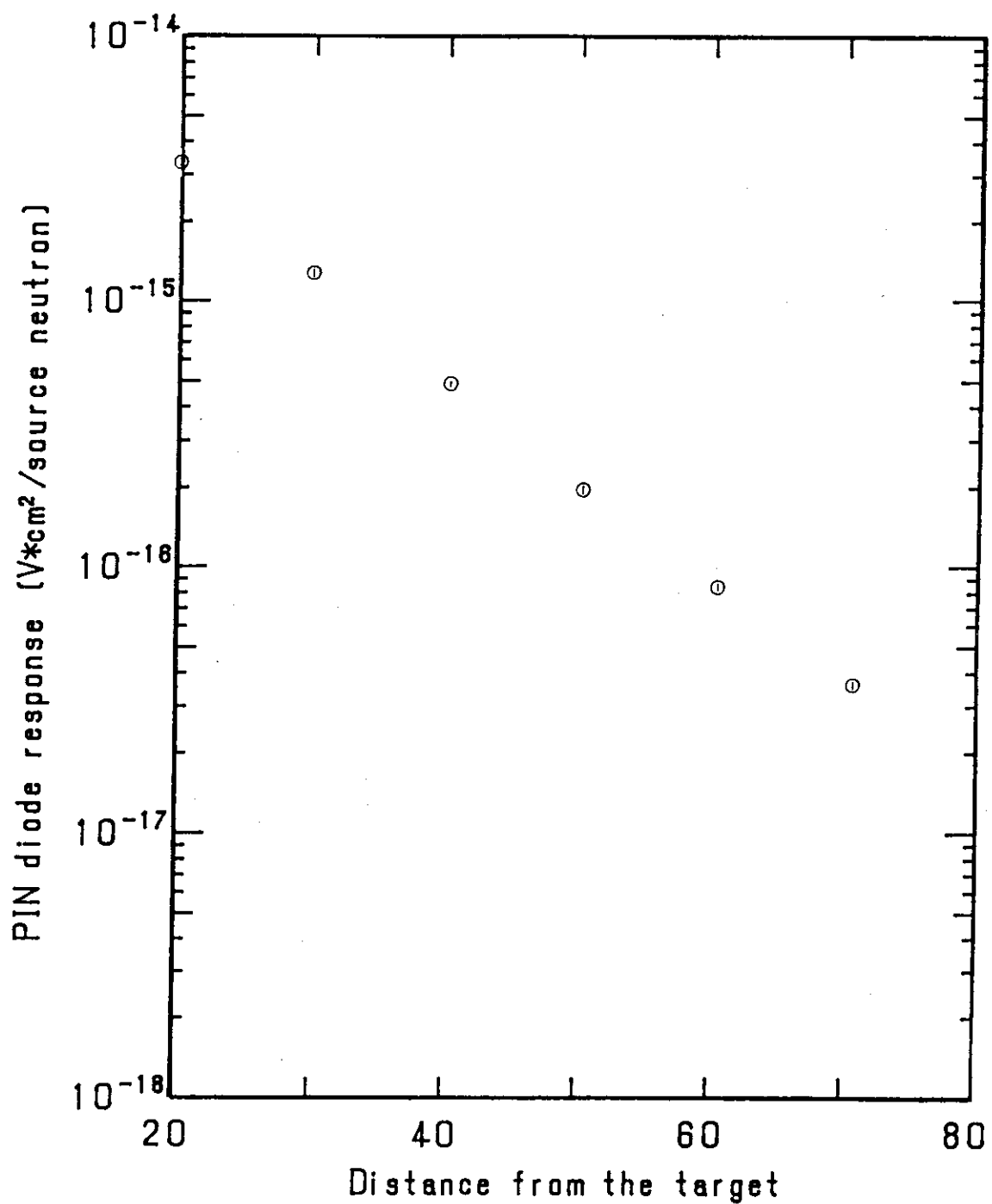


Fig. A.2.1 Response distribution of PIN diode in the graphite assembly.

### Appendix 3 Sample Calculation

In order to make clear how the calculational model is used for analysis, a sample calculation using the DOT3.5<sup>2)</sup> is described in this Appendix.

A two-dimensional R-Z model was adopted in this calculation. The equivalent radius was 31.4 cm. The calculational model is shown in Fig. A.3.1. The zero-degree source neutron spectrum, calculated by a Monte Carlo program<sup>8)</sup>, was used as a isotropic input spectrum. All experimental data were normalized to one source neutron generated at the target. It is noticeable that the integrated flux of input source neutron spectrum is not unity but 1.173 because of its anisotropy.

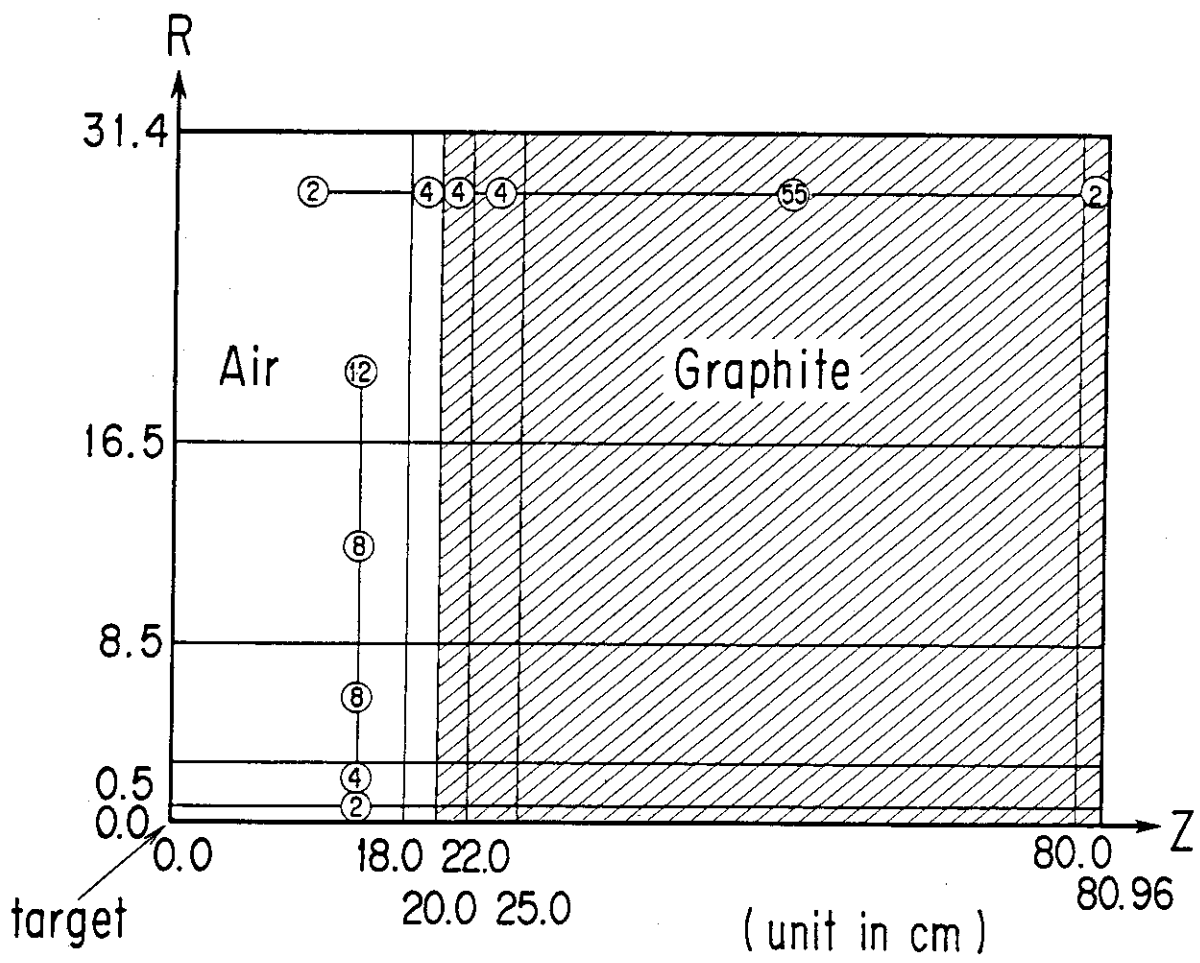
The GRTUNCL code was used to calculate the first collision source in order to eliminate the "ray effect". The number of Legendre polynomials was 5 ; the number of angular quadratures was 16. The mesh width was 9 cm in air and about 1 cm in the graphite region except near the front surface of assembly. A sample of input data for the GRTUNCL and the DOT3.5 is shown in Fig. A.3.2. The cross section set JACKAS<sup>19)</sup> is taken from the JENDL-3PR1 using the PROF-GROUCH-G/B<sup>20)</sup> process code. The group structure is just the same as used in MORSE-DD.<sup>21)</sup> The source neutron spectrum data of 3\* in Fig. A.3.2 (a) were interpolated from the result of a Monte Carlo calculation.<sup>8)</sup> In this sample calculation, air was assumed to be made of Oxygen and Al frame region was ommitted. After calculation of the neutron flux distribution in the assembly, the INTERF code<sup>22)</sup> was used for calculating the reaction-rate distributions. As a typical example, the calculated-to-experimental ratios (C/E) for the  $^{27}\text{Al}(n,\alpha)^{24}\text{Na}$  reaction rate were shown in Fig. A.3.3.

Additional points of information are as follows:

- 1) Aluminum support
  - homogenized nuclide density :  $1.234 \times 10^{22}$
  - effective outer radius : 56.7 cm
  - \* A pre-analysis showed that the effect of the aluminum support was very small.
- 2) Anisotropy of source neutrons
  - The effect of this anisotropy may be small but we will consider it in further analysis.

## 3) Room return effect

A layout of the target vicinity is shown in Fig. A.3.4. Room-return effect on a  $\text{Li}_2\text{O}$  cylindrical assembly<sup>1)</sup> was calculated by the MORSE-DD code. The results showed that the room-return neutrons had some effect on the reaction rates that were sensitive to low energy neutrons<sup>23)</sup>.



\* Digit in a circle means mesh number for each region.

Fig. A.3.1 Calculational model.

FNS-GRTUNCL GRAPHITE ASSEMBLY #4 AIR(20)-C(60.96) JACKAS(J3PR2 E-FLAT) 00000100  
 0 .00000200  
 1\*\* .00000300  
 0 0 5 2 34 71 12500000400  
 4 5 129 72 0 15600000500  
 156 2 1 30000 10 000000600  
 1 0 18 0 0 1600000700  
 00000800  
 2\*\* 1.1767+00 0.0 0.0 00000900  
 T 00001000  
 1\*\* 00001100  
 F0.0 00001200  
 2\*\* 00001300  
 1I0.0 3I18.0 3I20.0 3I22.0 54I25.0 1I80.0 00001400  
 80.96 00001500  
 00001600  
 3\*\* 0.0 0.0 2.7828-03 1.7363-02 7.1310-02 2.3566-0100001700  
 2.8044-01 1.9088-01 8.8741-02 1.9619-02 4.7824-03 3.6889-0300001800  
 4.0824-03 3.0739-03 2.0627-03 1.5353-03 1.3058-03 1.0510-0300001900  
 9.1815-04 6.6341-04 4.9328-04 4.3340-04 3.5410-04 3.3956-0400002000  
 3.3951-04 4.7551-04 5.2166-04 5.4544-04 6.0839-04 5.8562-0400002100  
 5.9851-04 5.9892-04 2.3220-03 2.1711-03 1.9259-03 2.0821-0300002200  
 2.4699-03 2.3331-03 2.1203-03 2.3830-03 2.7193-03 2.5754-0300002300  
 2.5194-03 2.9628-03 3.5164-03 3.9704-03 4.3379-03 4.2412-0300002400  
 3.6099-03 3.3610-03 3.4485-03 3.7938-03 4.3795-03 4.7354-0300002500  
 5.0664-03 5.2928-03 5.3299-03 5.3383-03 5.3194-03 5.3179-0300002600  
 1.0130-02 9.9677-03 9.7640-03 9.6236-03 9.7275-03 9.9713-0300002700  
 9.7540-03 9.3421-03 8.6681-03 7.7929-03 6.8688-03 5.9791-0300002800  
 4.9397-03 3.8479-03 3.2890-03 2.8136-03 2.4317-03 2.1040-0300002900  
 1.8527-03 1.6141-03 1.4051-03 1.2219-03 9.1106-04 7.9663-0400003000  
 6.9762-04 6.1088-04 5.3606-04 4.7077-04 4.1340-04 3.6436-0400003100  
 3.2144-04 2.8444-04 2.5200-04 2.2407-04 2.0045-04 1.7891-0400003200  
 3.0516-04 2.4812-04 2.1369-04 1.9164-04 1.6038-04 1.3521-0400003300  
 1.1447-04 9.7598-05 8.3682-05 7.2417-05 6.3421-05 5.5907-0500003400  
 4.3479-05 00003500  
 F0.0 00003600  
 4\*\* 00003700  
 1I0.0 3I0.5 7I2.5 7I8.5 1II16.5 31.4 00003800  
 5\*\* 00003900  
 F1.0 00004000  
 6\*\* 00004100  
 1.0 00004200  
 7\*\* 00004300  
 1.0 00004400  
 8\*\* 00004500  
 34R1 5Q34 00004600  
 34R2 64Q34 00004700  
 9\*\* 00004800  
 -97 -103 00004900  
 10\*\* 00005000  
 4I97 102 1Q6 00005100  
 4I103 108 1Q6 00005200  
 46I109 156 00005300  
 00005400  
 11\*\* 6Z 4I31 36 00005500  
 6Z 4I91 96 00005600  
 48Z 00005700  
 12\*\* 00005800  
 6R0.0 6R4.9210-5 00005900  
 6R0.0 6R8.2322-2 00006000  
 48R0.0 00006100  
 13\*\* 00006200  
 -0.97753 -0.90676 -0.82999 -0.74536 -0.64979 -0.53748 00006300  
 -0.39441 -0.14907 1M8 00006400  
 14\*\* 00006500  
 F1.0 00006600  
 T 00006700

Fig. A.3.2 Input data for a sample calculation.

(a) Input data for GRTUNCL code.

FNS-DOT35 GRAPHITE ASSEMBLY #4 AIR(20)-C(60.96) JACKAS(J3PR2 E-FLAT) 00000100  
 0 00000200  
 61\*\* 00000300  
 0 12500000400  
 5 00000500  
 2 00000600  
 129 00000700  
 160 00000800  
 1 00000900  
 10 00001000  
 15 00001100  
 0 00001200  
 0 800001300  
 0 00001400  
 0 00001500  
 0 900001600  
 2 6000001700  
 3 00001800  
 11 00001900  
 156 00002000  
 1 00002100  
 0 00002200  
 0 00002300  
 0 00002400  
 T 00002500  
 7\*\* 00002600  
 -0.21082 -0.14907 1M1 00002700  
 -0.42164 -0.39441 -0.14907 1M2 00002800  
 -0.55777 -0.53748 -0.39441 -0.14907 1M3 00002900  
 -0.66667 -0.64979 -0.53748 -0.39441 -0.14907 1M4 00003000  
 -0.76012 -0.74536 -0.64979 -0.53748 -0.39441 -0.14907 00003100  
 1M5 -0.84327 -0.82999 -0.74536 -0.64979 -0.53748 -0.39441 00003200  
 -0.14907 1M6 -0.82999 -0.74536 -0.64979 -0.53748 00003300  
 -0.91894 -0.90676 1M7 -0.82999 -0.74536 -0.64979 -0.53748 00003400  
 -0.39441 -0.14907 1M8 -0.90676 -0.82999 -0.74536 -0.64979 00003500  
 -0.98883 -0.97753 -0.90676 -0.82999 -0.74536 -0.64979 00003600  
 -0.53748 -0.39441 -0.14907 1M8 00003700  
 1Q80 3R-0.97753 5R-0.90676 7R-0.82999 9R-0.74536 11R-0.64979 13R-0.53748 00003800  
 15R-0.39441 17R-0.14907 3R0.97753 5R0.90676 7R0.82999 9R0.74536 00003900  
 11R0.64979 13R0.53748 15R0.39441 17R0.14907 00004000  
 T 00004100  
 6\*\* 00004200  
 0.0 2R0.13586-1 0.0 4R0.97681-2 00004300  
 0.0 0.64738-2 0.50390-2 0.64738-2 1N3 00004400  
 0.0 0.64634-2 2R0.71124-2 0.64634-2 1N4 00004500  
 0.0 0.64634-2 0.14381-2 0.36342-2 0.14381-2 0.64634-200004600 00004600  
 1N5 00004700  
 0.0 0.64738-2 0.71124-2 0.36342-2 1N3 1Q6 00004800  
 0.0 0.97681-2 0.50390-2 0.71124-2 0.14381-2 0.71124-200004900 00004900  
 0.0 0.50390-2 0.97681-2 1N7 00005000  
 0.0 0.13586-1 0.97681-2 2R0.64738-2 1N4 1Q8 00005100  
 1Q80 00005200  
 T 00005300  
 3\*\* 00005400  
 F0.0 00005500  
 T 00005600  
 1\*\* 00005700  
 F0.0 00005800  
 2\*\* 00005900  
 110.0 3118.0 3120.0 3122.0 54125.0 1180.0 00006000  
 80.96 00006100  
 4\*\* 00006200  
 110.0 310.5 712.5 718.5 11116.5 31.4 00006300  
 5\*\* 00006400  
 99R1.0 8R1.0 18R0.0 00006500  
 8\*\* 00006600  
 34R1 5Q34 00006700  
 34R2 64Q34 00006800  
 9\*\* 00006900  
 -97 -103 00007000  
 10\*\* 00007100  
 4197 102 1Q6 00007200  
 41103 108 1Q6 00007300  
 461109 156 00007400  
 11\*\* 00007500  
 6Z 4131 36 00007600  
 6Z 4191 96 00007700  
 48Z 00007800  
 12\*\* 00007900  
 6R0.0 6R4.9210-5 00008000  
 6R0.0 6R8.2322-2 00008100  
 48R0.0 00008200  
 T 00008300

Fig. A.3.2 (b) Input data for DOT3.5 code.

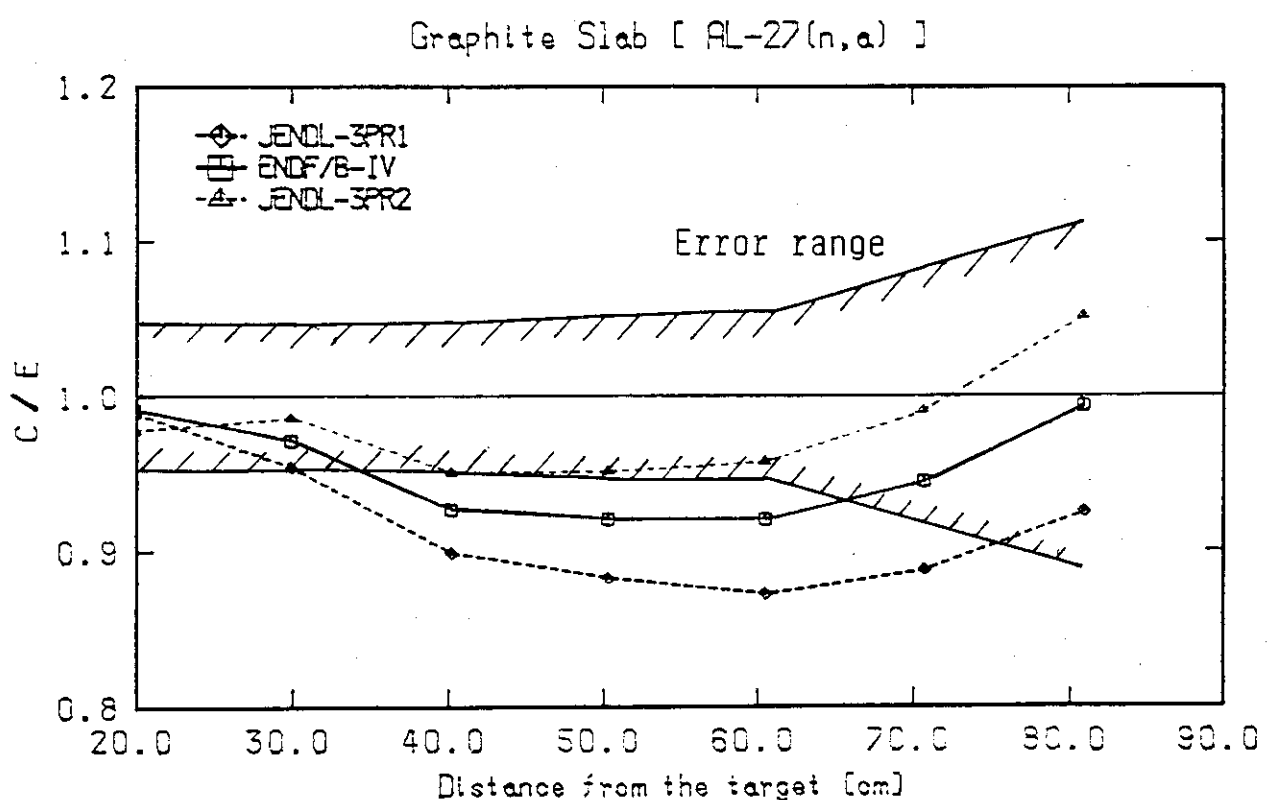


Fig. A.3.3 Comparison of C/E values for the  $^{27}\text{Al}(n,\alpha)^{24}\text{Na}$  reaction rate.

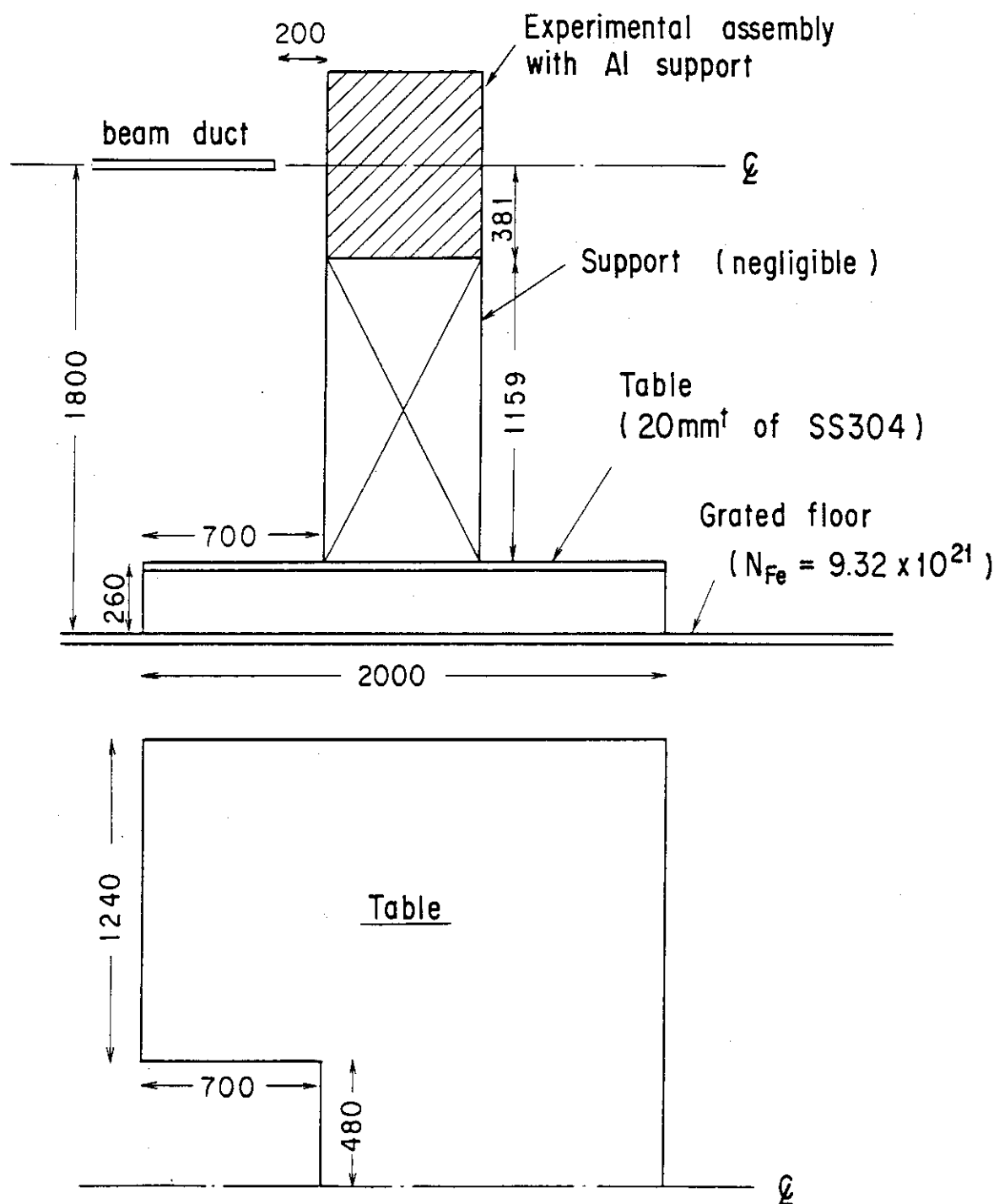


Fig. A.3.4 Configuration around the experimental assembly.